The functional and structural analysis of a mimetic peptide

of human hepatic lipase

by

Breanne M. Coady

A dissertation submitted to the

School of Graduate Studies

in partial fulfillment of the requirements for the degree of

Masters of Science in Biochemistry

Department of Biochemistry

Memorial University of Newfoundland

December 2015

St. John's   Newfoundland and Labrador

Abstract

Human hepatic lipase (hHL) is bound to the cell surface via heparan sulfate proteoglycans (HPSGs) and hydrolyzes triglycerides and phospholipids within circulating lipoproteins. High-density lipoprotein (HDL) transports excess extrahepatic cholesterol to the liver for excretion. However, small lipid-deficient HDL generated by hHL action has the ability to accept more cholesterol. I hypothesized that a peptide mimicking the cell surface associations of hHL will displace hHL from cell surfaces, increasing its activity in cell culture media. To test this hypothesis, I have recombinantly expressed and purified a tagged mimetic peptide, encompassing the major heparin-binding domain of hHL. Results from *in vitro* lipase displacement assays showed that the peptide has an ability to displace active HPSG associated lipases. Data from proton nuclear magnetic resonance experiments showed that structural changes occur in the peptide in the presence of heparin. Overall, these data provide a foundation to use mimetic peptides for the displacement of cell surface associated lipases.

.

Acknowledgements

Most importantly, I would like to thank both my supervisors, Dr. Booth and Dr. Brown for all of their guidance, attention, support and patience throughout this process. I truly appreciate everything you both have done for me. Secondly, I would like to thank my committee member, Dr. Paterno for all of his time and constructive feedback on this project and thesis. I would also like to thank Yanbo Yang, Madeline Fitzpatrick, Narmadaa Thyagarajan, and Emily Courage for all of their help, both in the lab and with this thesis. I could have never asked for a more supportive environment to work in. For the lab technicians, Donna Jackman and Danielle Gardiner, thank you for all of your help and advice. I would also like to thank Dr. Fairbridge for his time and help in the writing of this thesis. Lastly, I would also like to thank my family for all of their love and support throughout this, especially David Young for always understanding.

Table of Contents

List of Figures

List of Tables

List of Abbreviations

1D	One-dimensional
2D	Two-dimensional
6xhis	Hexahistidine
A/A	Antibiotic/antimycotic
ABCA1	Adenosine-triphosphate binding cassette transporter A1
ABCG1	Adenosine-triphosphate binding cassette transporter G1
Apo	Apolipoprotein
ApoA-I	Apolipoprotein A-I
ApoA-II	Apolipoprotein A-II
APP	Amyloid precursor protein
BSA	Bovine serum albumin
C-	Carboxyl terminal
CD	Circular dichroism
CE	Cholesteryl ester
CETP	Cholesteryl ester transfer protein
CM	Chylomicron
CV	Column volume
CVD	Cardiovascular disease
D_2O	Deuterium oxide
dH_2O	Deionized water

DMEM	Dulbecco's Modified Eagle Medium
DSS	4,4-Dimethyl-4-silapentane-1-sulfonic acid
E. coli	*Escherichia coli*
FBS	Fetal bovine serum
HBD	Heparin binding domain
HDL	High-density lipoprotein
HDL-C	High-density lipoprotein cholesterol
HEK-293T	Human embryonic kidney cell line-293T
hEL	Human endothelial lipase
hHL	Human hepatic lipase
HL	Hepatic lipase
hLPL	Human lipoprotein lipase
hPL	Human pancreatic lipase
HSPG	Heparan sulfate proteoglycan
HSQC	Heteronuclear single-quantum correlation
HT	High tension
IDL	Intermediate-density lipoprotein
IPTG	Isopropyl-β-D-1-thiogalactopyranoside
LB	Lysogeny Broth
LCAT	Lecithin-cholesterol acyltransferase
LDL	Low-density lipoprotein
LRP1	LDL receptor-related protein 1

LXR	Liver-X-receptor
mHL	Mouse hepatic lipase
MWCO	Molecular weight cut off
N-	Amino terminal
NMR	Nuclear magnetic resonance
NOESY	Nuclear Overhauser effect spectroscopy
OD	Optical density
OPTI-MEM	Optimal Minimal Essential Medium
oxLDL	Oxidized low-density lipoprotein
PBS	Phosphate buffered saline
PBS-T	Phosphate buffered saline-tween 20
PCR	Polymerase chain reaction
PL	Phospholipid
RCT	Reverse cholesterol transport
rHL	Rat hepatic lipase
RPMI	Roswell Park Memorial Institute
RT	Room temperature
SDS-PAGE	Sodium dodecyl sulfate polyacrylamide gel electrophoresis
sn	Stereospecifically numbered
SR-BI	Scavenger receptor B type I
TBS	Tris-buffered saline
TFE	Trifluoroethanol

TG	Triglyceride
TGS	Tris/glycine/sodium dodecyl sulfate
TOCSY	Total correlated spectroscopy
Trx	Thioredoxin
U	Unit
VLDL	Very low-density lipoprotein
Xaa	Any amino acid

Chapter 1: Introduction

1.1 Overview

By definition, cardiovascular disease (CVD) is any disease or injury that affects the heart and/or circulation; this includes coronary heart disease, stroke, and coronary artery disease (or atherosclerosis). CVD has the highest mortality for any non-communicable disease worldwide, accounting for 17.5 million deaths in 2008.[1] In Canada, CVD accounted for 74,255 deaths in 2003, accompanied with an economic burden of 18.5 billion dollars.[2,3] In 2005, it was estimated that Canada spent 96 million dollars towards funding CVD research.[4] The general causes of CVD are correctable lifestyle choices that include tobacco use, physical inactivity, diet, and excess alcohol use. However, lifestyle habits are not the whole story. Hereditary elements can also contribute greatly to the development of CVD and especially premature death of individuals suffering with the disease. Considering the huge socioeconomic impact CVD has world wide, current research is focused on developing new approaches to treat and prevent CVD. Since one of the risk factors of CVD is the imbalance of cholesterol within the body, understanding how cholesterol is synthesized, metabolized, stored, and removed from the body is important for developing new treatments. The removal of excess cholesterol from peripheral tissues for bile excretion is achieved by a multi-step process known as reverse cholesterol transport (RCT).[5-7] This anti-atherogenic process is accomplished with the help of numerous proteins, some which are also important in lipoprotein metabolism.

1.1.1 Atherosclerosis

Atherosclerosis is one of the major underlying causes of severe health problems, such as coronary heart disease and stroke. It is defined by the hardening of the arteries due to cholesterol accumulation within the intima of the artery.[8] The progression of atherosclerosis results from the interplay of various molecular events that usually go undetected until a clinical event occurs, such as a myocardial infarction. Both researchers and physicians have been interested in understanding the clinical and molecular factors that contribute to the development of atherosclerosis. Considering that cholesterol accumulation plays an integral part in the progression of atherosclerosis, researchers have been particularly motivated to fully understand the role that cholesterol metabolism plays in atherosclerosis. Research thus far has been able to chronologically elucidate the events of atherosclerosis, however, the progression of some of these events still remains unclear.

One of the first events of arterial thickening is the appearance of fatty streaks on the inner surface of the artery. They are inert and do not impede blood flow. Fatty streaks appear yellow-white in colour due to the accumulation of cholesterol-loaded macrophages. These cholesterol-loaded macrophages have a foamy appearance and are aptly referred to as foam cells. The cholesterol that accumulates within foam cells is carried by low-density lipoproteins (LDL), which is commonly termed "bad cholesterol". LDL is given this name because it functions to carry cholesterol from the liver to peripheral tissues. This is why elevated LDL is considered a risk factor for CVD.[9] Increased LDL within the circulation increases the chances of LDL penetrating into the artery intima and developing into a fatty streak. How these fatty streaks mature into

2

atherosclerotic plaques remains to be fully elucidated. Maturation is believed to involve a complex interplay between oxidative stress, pro-inflammatory cytokines, and the infiltration of oxidized LDL (oxLDL). Theories suggest that in order for LDL to penetrate the intima of the artery, a process known as endothelial activation must occur.[8] During this process, LDL penetrates the endothelium and is retained within the intima of the artery where it can be oxidized. The oxLDL initiates the expression of adhesion molecules on the surface of the artery, allowing circulating monocytes to adhere, penetrate the endothelium, and enter the intima. Once inside the intima, the intruding monocytes differentiate into macrophages and start to accumulate oxLDL. The increased accumulation of oxLDL within macrophages positively fuels the process for more monocytes to enter the intima. When the macrophage accumulates oxLDL, it is then termed a foam cell. This differentiation is an essential step for the progression of atherosclerosis.[10] It is the build up of lipid-laden foam cells that start to form fatty streaks and eventually mature into atherosclerotic plaques. The progression from fatty streak to plaque is believed to occur when smooth muscle cells penetrate the endothelium and accumulate within the intima.[8] Once the plaque has grown beyond the capacity of the intima, it encroaches on the arterial lumen and affects blood flow. Often a growing plaque is fragile, increasing its chance of rupture. If a plaque ruptures, the contents come into contact with blood coagulation factors, creating a thrombus that obstructs blood flow (Figure 1). This increases the risk of serious health problems such as myocardial infarction or stroke.

Figure 1: Schematic depiction of the progression of atherosclerosis
Increased LDL within the circulation increases the incidence of LDL penetrate the vascular endothelium and entry to the intima. Once inside the intima, the LDL can be oxidized, forming oxLDL. The oxLDL increases the expression of adhesion molecules on the endothelium, attracting circulating monocytes. The monocytes can enter the intima where they can accumulate oxLDL, thus differentiating the monocytes into macrophages and eventually foam cells. As the foam cells start to accumulate and expand within the intima, the lamina is weakened, allowing smooth muscle cells to infiltrate the intima and increase plaque growth. When the plaque outgrows the limitations of the intima it ruptures, resulting in thrombosis, leading to a cardiac event.

Figure 1

LDL

Monocytes

Plaque rupture/
thrombosis

Plaque formation

Endothelium

Adhesion
molecule

oxLDL

Lamina

Smooth muscle
cell migration

Foam cell

Intima
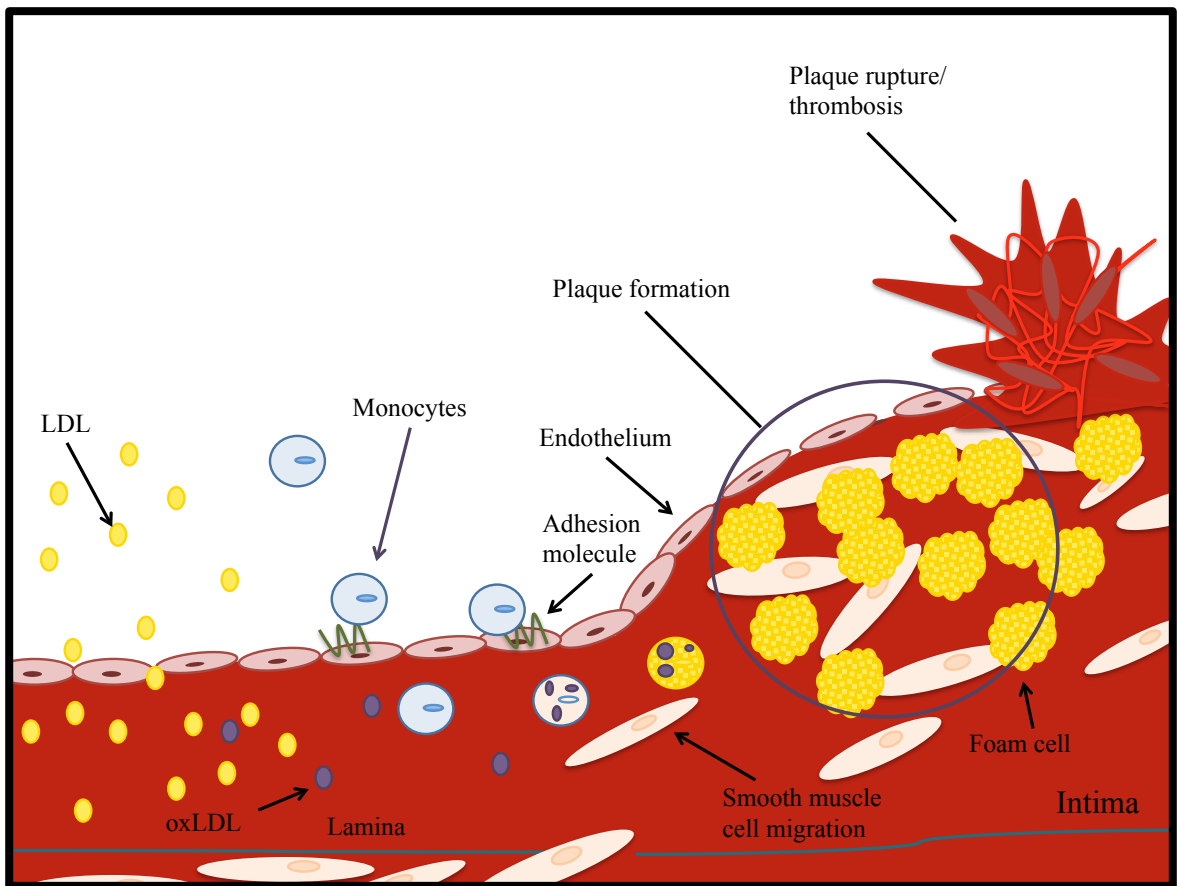
1.1.2 Lipoproteins: structure, function, and metabolism

Considering cholesterol is a major player in the progression of atherosclerosis, it is very important to study and understand its means of transportation throughout the body. Cholesterol is amphipathic, meaning it has both "water loving" and "water hating" properties and is not completely soluble in the aqueous environment of the blood stream. The body deals with this problem by packing cholesterol within lipoprotein molecules, shielding the "water hating" portion of cholesterol from the hydrophilic environment of the circulation.[11] However, cholesterol is not the only molecule that is packed and transported by lipoproteins. Hydrophobic lipids, such as triglycerides (TG), are completely "water hating" and are entirely insoluble within the bloodstream; this is why lipids require a special means of transport within the circulation. Lipoproteins contain both lipid and protein moieties, with their function being dependent upon both. Lipoproteins are also classified by their densities (Figure 2). The protein moieties associated with a lipoprotein can aid in the scaffolding of the lipoprotein molecule, act as cofactors for enzymes, and act as ligands for cell surface receptors.

All lipoproteins have the same basic structure: a hydrophobic core containing TG and cholesteryl esters (CE) that is surrounded by an amphipathic monolayer of phospholipids (PL) with embedded apolipoproteins and cholesterol. Lipoproteins require apolipoproteins for two crucial functions in the lipidation and catabolism of lipoprotein molecules. The first major function is to act as a structural scaffold, which shapes and holds the lipoprotein together, thus shielding the hydrophobic core from the bloodstream.

Figure 2: The classes of lipoproteins

There are 5 classes of lipoproteins that are characterized by their density obtained by density gradient ultracentrifugation analysis.[12] The classes are high-density lipoprotein (HDL), intermediate-density lipoprotein (IDL), low-density lipoprotein (LDL), very-low density lipoprotein (VLDL) and the least dense called chylomicron. The diameters of lipoproteins are inversely proportional to their densities. For example, chylomicrons have the largest diameter but have the lowest density. The density range for each lipoprotein class is given next to the diagram for each. The percentage of total lipid and protein associated with each class are also indicated. (Figure reproduced from reference 12 with permission).

Figure 2
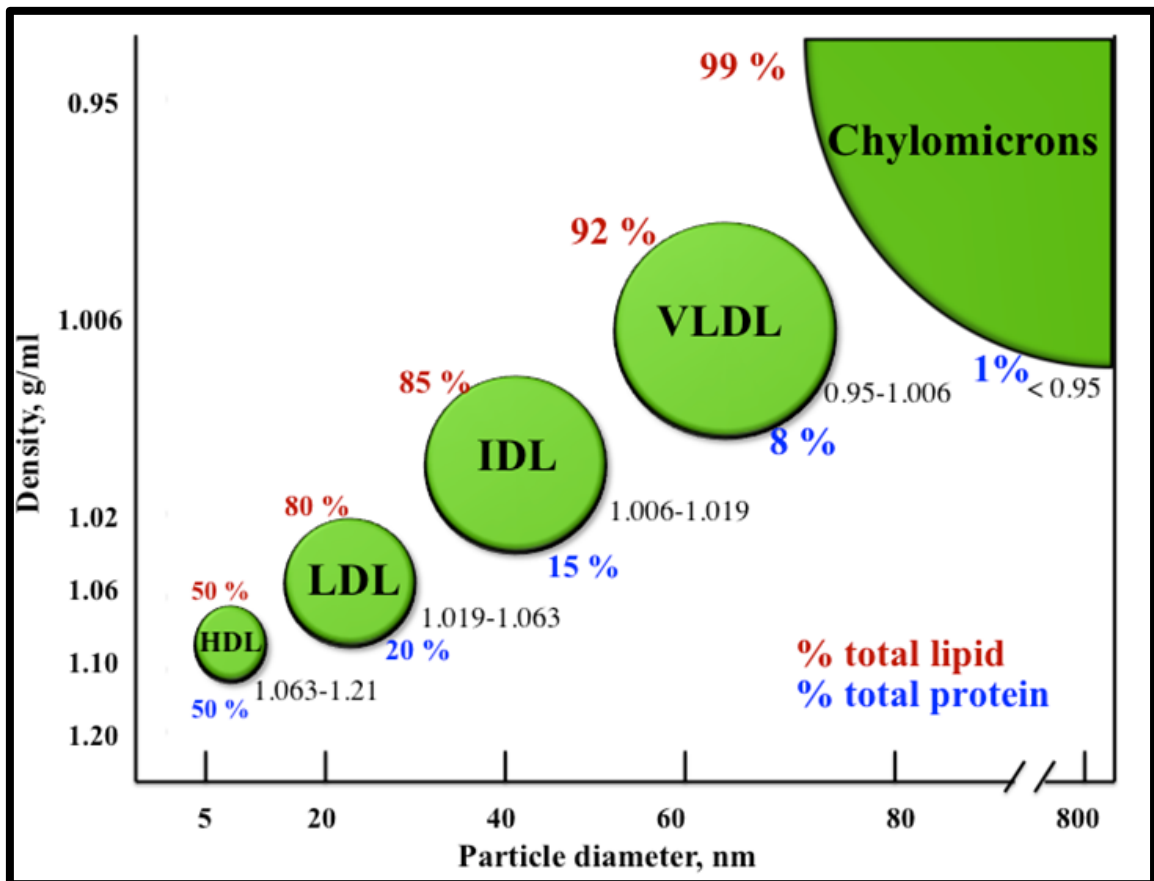
The second major function is to act as a receptor for lipoprotein uptake via receptor-mediated endocytosis in various tissues. The apolipoproteins associated with lipoproteins differ among the lipoprotein classes. For example, apolipoprotein (apo) A-I and apoA-II are primarily found embedded on the monolayer of high-density lipoprotein (HDL) molecules, while apoB is primarily found on very-low density lipoproteins (VLDL) and LDL.

When a meal is ingested, the dietary TG and PL pass through the stomach and enter the small intestine where they are hydrolyzed by human pancreatic lipase (hPL), generating free fatty acids. The free fatty acids cross the brush border membrane of the intestine and enter the enterocytes.[13,14] Once inside, the free fatty acids are trafficked through the endoplasmic reticulum.[15] These are then combined with CE and apoB-48 to form chylomicrons (CM). The CMs pass through the lymphatic capillaries and enter the vascular circulation via the thoracic duct. Once within the circulation, the CMs transport TGs to various tissues to be used for lipid storage or oxidation. The TG components of CMs are hydrolyzed by human lipoprotein lipase (hLPL), creating smaller, more dense CMs, termed CM remnants.[16] These CM remnants are taken up by the liver, allowing for its protein and lipid cargo to be used for intracellular functions, such as VLDL synthesis.[16] The liver synthesizes and secretes VLDL, which functions similarly to CM to transport endogenous lipids within the circulation. As VLDL travels throughout the circulation, it encounters hLPL on epithelial cell surfaces, which acts to cleave the acyl esters of the TG components of VLDL. This hydrolysis results in the de-lipidation of the molecule, creating a more dense VLDL particle that is classified as intermediate-density

9

lipoprotein (IDL). IDL molecules can have two fates: they can either continue to circulate within the bloodstream, or they can be taken up by the liver via receptor-mediated endocytosis. If IDL continues to circulate within the bloodstream, it can be further hydrolyzed to produce the cholesterol-rich lipoprotein LDL. LDL functions to transport cholesterol to peripheral tissues where the cholesterol is either metabolized or stored. Considering this function of LDL, it is well accepted to be pro-atherogenic in nature, as it transports cholesterol from the liver and deposits it in the peripheral tissues. In an attempt to keep the cholesterol levels in balance, HDL functions to transport cholesterol from peripheral tissues back to the liver, where it can be excreted in bile. HDL is synthesized both by the liver and the intestines to contribute to the HDL pool within the bloodstream.[17,18] HDL is considered anti-atherogenic due to the role it plays in the process of RCT by moving cholesterol from the peripheral tissues to the liver for excretion.[6]

HDL can be classified into α and preβ molecules, based upon their electrophoretic mobility on an agarose gel.[16] This classification is due to variations in the lipid and apolipoprotein content of HDL. Preβ-HDL molecules are lipid deficient and α-HDL are lipid rich.[19] Due to the low amount of lipid and the high amount of apoA-I, preβ-HDL is a very potent cholesterol acceptor.[20] HDL can carry anywhere from one to four apoA-I molecules, accounting for roughly 65% of the protein mass in HDL.[21,22] ApoA-I has a structure which consists of a single polypeptide chain with stretches of amphipathic α-helices.[23] The hydrophobic face of the polypeptide is embedded into the lipid surface of the lipoprotein. ApoA-I is secreted from both the liver and intestines as a lipid-deficient

10

protein with a squat and oblate spheroid structure. The squat structure matures into a more open extended conformation as the apoA-I moiety is covalently lipidated.[23] However, the intestines and liver are not the only source of lipid deficient apoA-I, as it can also be liberated from lipoproteins as they are hydrolyzed in the bloodstream, producing lipid-deficient preβ-HDL.[24] Lipids are loaded onto apoA-I by the adenosine-triphosphate binding cassette transporter A1 (ABCA1).[25] ABCA1 is a transmembrane protein and it functions to control the traffic of cholesterol and PL from inside a cell to a cholesterol acceptor, located outside the cell, such as apoA-I.

ApoA-I has also been observed to have some beneficial anti-inflammatory properties, which may be effective for reducing inflammation associated with atherosclerosis.[26] Rabbits with collar induced atherosclerosis and that were treated with HDL, had an increased ratio of smooth muscle cells to macrophages compared to untreated rabbits.[27] A reduction in atherosclerotic plaque size was also observed in cholesterol-fed, atherosclerotic rabbits when they were treated with HDL.[28] This study also observed that the reduction in plaque size was comparable to animals treated with a common statin, atorvastatin. This provides further evidence that raising preβ-HDL within the circulation could be an effective therapy against atherosclerosis.

1.1.3 Reverse cholesterol transport

Human hepatic lipase (hHL) is an extracellular enzyme that cleaves the *sn*-1 acyl esters of TGs and PLs within circulating lipoprotein molecules.[29] The hydrolysis of TG

11

and PL in HDL by hHL produces smaller, lipid deficient HDL molecules.[30] It has been proposed that HDL promotes the transfer of cholesterol from peripheral tissues back to the liver for excretion.[31] As HDL molecules are metabolized within the circulation, the density of HDL increases and their lipid composition is altered. (See *section 1.1.4* for more about cholesteryl ester transfer protein (CETP)). A form of HDL known as preβ-HDL can be generated during HDL metabolism via the displacement of its major protein component, apoA-I.[32] It is the most dense form of HDL and it is the most lipid deficient. Considering preβ-HDL's lipid deficiency, it has the capacity to accept more cholesterol than its lipid-laden HDL counterparts *in vitro*.[33] This may allow preβ-HDL molecules to transport more cholesterol back to the liver for excretion in the bile.[34] Due to its cholesterol accepting nature, increasing the concentration of preβ-HDL molecules within the circulation is an appealing treatment strategy to combat CVD. One way to increase preβ-HDL molecules within the circulation is to increase the hydrolysis function of hHL, thus generating more cholesterol accepting preβ-HDL molecules. An increase of hHL activity within the circulation could provide a promising anti-atherogenic therapy for reducing the risk of CVD, through the increased generation of preβ-HDL molecules and excretion of excess cholesterol via RCT (Figure 3).

There are two ways in which cholesterol can be transported in the bloodstream: forward transport and reverse transport. Forward transport describes the movement of cholesterol from the liver to peripheral tissues. This is usually carried out by TG rich lipoproteins and is a process that is recognized as pro-atherogenic. Reverse transport of cholesterol is the movement of cholesterol from the peripheral tissues to the liver where it

Figure 3: Schematic of reverse cholesterol transport

Preβ-HDL, a lipid deficient molecule, has the propensity to accept cholesterol from extra-hepatic tissues through the process of cholesterol efflux. As preβ-HDL travels through the bloodstream, it can accumulate more cholesterol, TG and PL, and consequently develops into a mature HDL molecule. Cell surface associated hHL will cleave the acyl esters of the TG and PL at the site of the liver. The liver will selectively uptake the cholesteryl esters (CE) and ultimately excrete the cholesterol through the bile. To complete the process of reverse cholesterol transport, the apoA-I moiety of the HDL molecule can be recycled back to preβ-HDL, thus continuing the process of removing cholesterol from the peripheral tissues and taking it back to the liver for excretion.

Figure 3
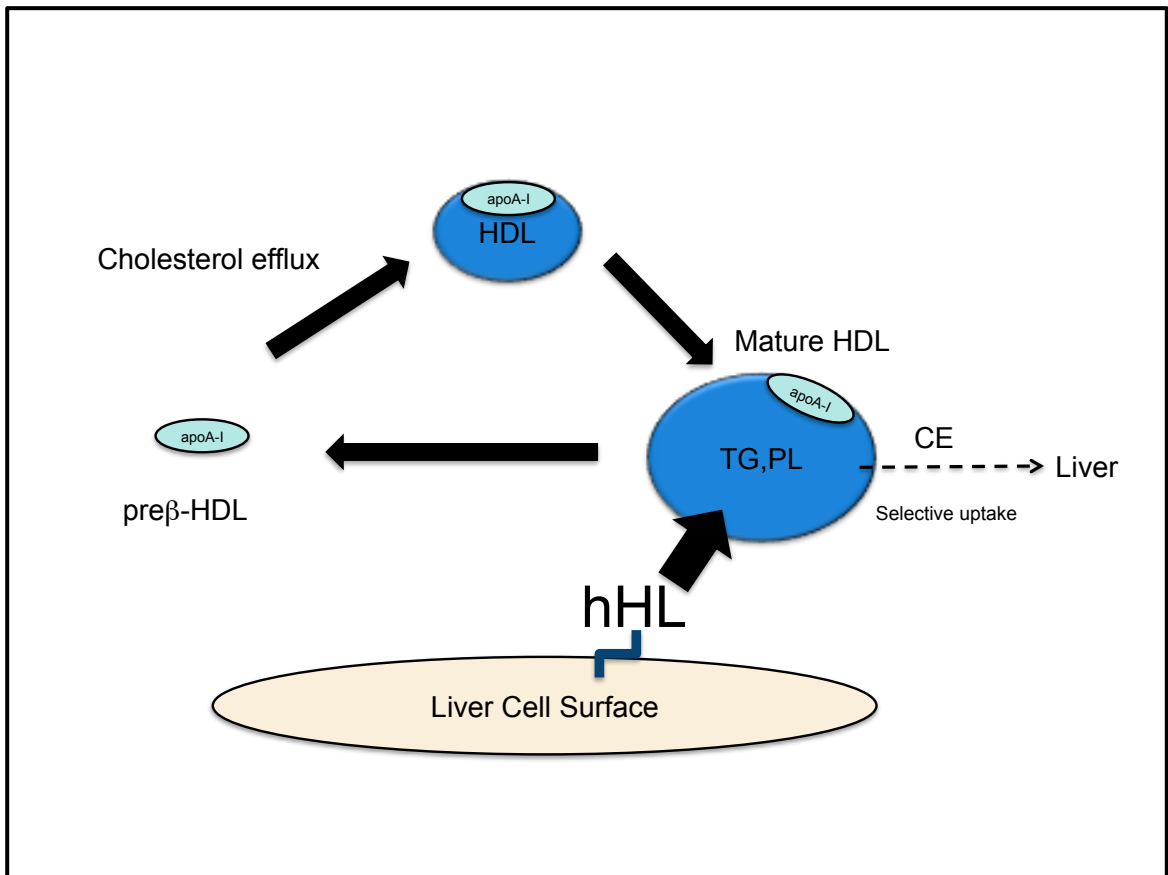
can ultimately be excreted. The pioneers of RCT, Glomset and Wright, have defined RCT as the overall flux of cholesterol from the entire periphery to the liver and then finally being excreted.[5] They have also proposed that the esterification of cholesterol in lipoproteins would drive the net efflux of cholesterol and "trap" the HDL bound cholesterol, preventing the exchange of the cholesterol from HDL back to the cells.

The complex process of RCT can be broken down into four critical steps: 1) free cholesterol is effluxed to HDL from the extra hepatic cells;[35] 2) free cholesterol is esterified by the enzyme lecithin-cholesterol acyltransferase (LCAT);[5] 3) the cholesterol is receptor-mediated endocytosed by the liver via the scavenger receptor B type I (SR-BI);[36] and 4) HDL is remodelled by hHL,[30] and the apoA-I moiety may reinitiate the process of continuing to remove cholesterol from the peripheral tissues.[37] The first step in RCT is to efflux the cholesterol to the cholesterol acceptor, apoA-I, via ABCA1. The binding also decreases the degradation of apoA-I.[38] These studies also suggest that increasing preβ-HDL within the circulation could potentially increase cholesterol efflux.

As cholesterol and PL are effluxed to the circulating apoA-I molecule, it becomes more enriched in lipid and continues to accumulate more PL and cholesterol. As it continues to circulate through the bloodstream collecting more PL and cholesterol, preβ-HDL is converted into a mature α-HDL molecule. The free cholesterol is converted by LCAT to the less toxic esterified cholesterol that is then stored within the hydrophobic core of HDL.[36] When the mature HDL reaches the liver, the surface-bound hHL hydrolyzes the TG and PL, thus altering the lipid content of HDL.[39] This alteration of the lipid content promotes the dissociation of apoA-I from the HDL molecule, allowing it to

15

reinitiate the process of RCT. The liver takes up the lipids released from HDL via SR-BI. The CEs are converted back into cholesterol and ultimately excreted with the bile.[36]

Another important cholesterol transporter is adenosine-triphosphate cassette binding transporter G1 (ABCG1). It is similar to ABCA1, however, it preferentially effluxes cholesterol to mature α-HDL particles. ABCG1 increases the unesterified cholesterol in the plasma membrane where it can be readily effluxed to the HDL particles.[40] Both ABCA1 and ABCG1 are under the transcriptional control of the liver-X-receptor (LXR).[41,42] *In vivo*, LXR is activated by oxidized cholesterol within cholesterol loaded foam cells,[43] which increases the expression of transporters in the plasma membrane that will in turn increase the efflux of cholesterol to apoA-I or preβ-HDL.[38,40] Double-knockout studies of ABCA1 and ABCG1 transporters in macrophages have shown a reduction in the efflux of cholesterol and lipid accumulation within macrophages.[44] These findings provided evidence of the importance of these transporters in cholesterol efflux and the overall process of RCT.

1.1.4 HDL functionality

Researchers and physicians have understood for quite some time that the risk for CVD is inversely proportional to the circulating levels of HDL cholesterol (HDL-C).[45] This is due to the anti-atherogenic function of HDL: raising your levels of HDL would increase RCT and reduce your risk of CVD. However, over the past few years this understanding has been changing. Many studies have investigated whether increasing

HDL within the circulation will result in an increase of RCT; however, the results show that it is not the amount of HDL-C, but actually the functionality of the HDL molecule itself that is of importance in CVD protection.[46]

Studies were performed to increase the expression of ABCA1 and ABCG1 by using an agonist for the upstream regulator LXR to potentially increase the amount of cholesterol that is effluxed to HDL, thereby increasing RCT.[47] These studies reported increased HDL levels in agonist-treated LDL receptor knockout mice, along with increased cholesterol efflux to the HDL molecules.

The elevation of HDL-C within the circulation with a potent HDL-raising drug, niacin, initially showed great promise. Niacin has been shown in small clinical trials to increase HDL-C levels up to 25%.[48] However, when niacin was tested in larger and longer clinical trials, there was an absence of improved CVD outcomes despite elevated HDL-C, thus the studies were subsequently terminated.[49]

Another therapeutic strategy to raise HDL was through the use of CETP inhibitors that function to retain cholesterol in HDL and prevent the transfer of cholesterol to pro-atherogenic lipoproteins. The use of CETP inhibitors stem from the observation that the transgenic expression of the *CETP* gene stimulated the development of severe atherosclerosis in mice.[50] Clinical trials with torcetrapib, a CETP inhibitor, showed an increased incidence of CVD events with a 1.25 hazard ratio, despite an increase of HDL-C by 72% and the lowering of LDL cholesterol by 25%.[51] Thus, the inhibition of CETP raised concerns about the ability to produce functional HDL molecules. These studies

provide further evidence of the importance of the functionality of the HDL molecule and not just the arbitrary raising of HDL-C amount.

What does show more promise than raising HDL-C levels is to instead raise apoA-I levels via infusions of reconstituted apoA-I from human plasma.[52] In animal studies, increasing apoA-I, the protein component needed to synthesize preβ-HDL, increases RCT.[53] In addition to studies with full-length apoA-I, apoA-I mimetic peptides have been tested and shown to also to increase in the amount of cholesterol that is also effluxed.[54] These studies suggest that cholesterol efflux is dependent on the functionality of the HDL molecule and its ability to accept cholesterol.

1.1.5 Human hepatic lipase and its role in atherosclerosis

hHL is an extracellular enzyme bound to the cell surface via heparan sulfate proteoglycans (HSPG).[55] It functions to hydrolyze the *sn*-1 acyl esters of TG and PL within circulating lipoprotein molecules.[29] Considering its lipase function, hHL is very important in maintaining normal levels of lipoproteins within the circulation. However, its role in atherosclerosis is very controversial: there are arguments supporting that hHL play both a pro-atherogenic and an anti-atherogenic role.

Patients who are deficient in hHL exhibit increased TG content of VLDL and IDL.[56] Patients with hHL deficiency have also been observed to have higher levels of TG enriched HDL_2, a subfraction of HDL.[57] These studies indicate that hHL deficiency could result in an increased risk of an individual developing atherosclerosis. Animal studies also

have conflicting results on the role of HL in atherosclerosis. Barcat *et al.* had also confirmed that HL deficiency leads to development of atherosclerosis, using a mouse model lacking both HL and the LDL receptor.[58] The LDL receptor knockout model is a well-accepted atherosclerosis model.[59] Mice lacking both HL and the LDL receptor showed an increase in plasma TG rich lipoproteins with a reduction in liver uptake of remnants, as well as premature aortic lesions resulting in atherosclerosis.[58]

Other studies indicating that hHL is anti-atherogenic involve the increase in activity of hHL within the circulation. Fan *et al.* observed that rabbits overexpressing hHL have a 5-fold-decrease in plasma cholesterol with a reduction in the large TG-rich HDL particles, as well as IDL particles.[60] This indicates that hHL is important in the reduction of plasma cholesterol. Busch *et al.* observed similar findings: transgenic mice overexpressing hHL had a 34% decrease in HDL-C when compared to the control animals and a decrease in the size of the HDL particles.[61] They also observed a decrease in aortic cholesterol content in these mice. These studies provide evidence of the anti-atherogenic properties of hHL and the potential advantages to increasing its activity within the circulation.

Conversely, there are studies that provide evidence that hepatic lipase (HL) is pro-atherogenic.[62-64] Nong *et al.* studied two independent atherogenic mouse models, an apoE-deficient and a LCAT transgenic.[62] They observed that LCAT transgenic mice deficient in HL had increased plasma concentrations of apoB containing lipoproteins. However, despite this elevation in pro-atherogenic lipoproteins, the animals had a reduced risk of diet-induced atherosclerosis. Furthermore, in both the LCAT transgenic

and apoE-deficient models, they demonstrated that HL produced by macrophages increased aortic lesion formation and the absence of HL was observed to lower aortic lesion formation. This suggests that HL is involved in the progression of atherosclerosis in a manner that in independent of its role in lipoprotein metabolism. In support of these studies, a double knockout mouse model for apoE and HL exhibited increased plasma cholesterol accompanied with an unexpected reduction in atherosclerotic lesions.[65]

1.1.6 Human hepatic lipase structure

Secreted hHL is comprised of 476 amino acids with a molecular mass varying from 55-69 kDa, depending upon the degree of glycosylation on its four *N*-linked glycosylation sites.[66] Of the four glycosylation sites, asparagine-56 is crucial for the successful secretion and activity of hHL.[67] hHL is a member of the *sn*-1 specific subfamily of the lipase superfamily. This subfamily includes the closely related lipases hLPL, human endothelial lipase (hEL), and hPL. The percent identities between the members of the lipase family are listed in Table 1. To summarize, hLPL and hEL share 48.1% sequence identity, while hLPL and hHL share 45.7% sequence identity. However, hHL, hLPL, and hEL only share roughly 30% sequence identity with hPL. Considering their variations in conserved sequences, they still all share a characteristic catalytic triad (serine-aspartic acid-histidine) and a lipase consensus sequence (glycine-Xaa-serine-Xaa-glycine) which is conserved within the majority of lipases (Figure 4).[68] No portion of the hHL structure has been determined. However, sequence homology with the solved

Figure 4: Sequence alignment of the lipase family
The amino acid sequences of the human *sn*-1 lipase family are aligned. The alignment also includes mHL for comparison of the heparin binding domains with hHL. The amino acids are numbered according to the secreted protein sequence. The red box indicates the lipase consensus sequence. The blue box highlights a partial portion of the C-terminal that houses the major heparin-binding domain for hHL. When mHL and hHL C-termini are compared, there is a lack of conserved residues, specifically the 5 (KRKIR) basic residues of hHL, which accounts for the difference in cell surface binding between the two HL species. Highlighted in green within the distal N-terminal of hHL is another putative HBD (R310, K312, K314, R315).[74] The red line preceding the putative N-terminal HBD is the hinge region of hHL that dissects the N- and C-terminals.[72] Denoted by the black triangles are the 8 conserved cysteine residues. The *N*-linked glycosylation sites are highlighted in yellow, with asparagine-56 in orange. The lysine-aspartic acid-histidine catalytic triad is denoted with a pentagon overhead. The lid domain is denoted with a light blue box. The legend for the alignment is as follows: (*) fully conserved residue, (:) residues with strong similar properties, (.) residues with weak similar properties.

Figure 4

```
hPL     KEVCYERLGCFSDDSPWSGIT--ERPLHI--LPWSPKDVNTRFLLYTNENPNN--FQEVA   54
hHL     --------GQSLKPEPFGRRA------QAVETNKTLHEMKTRFLLF-GETN--QGCQIRI   43
mHL     --------GQGVGTEPFGRSL------GATEASKPLKKPETRFLLF-QDENDRLGCRLRP   45
hLPL    ----------------------------ADQRRDFIDIESKFALRTPEDTAEDTCHLIP   31
hEL     ----------AGSPVPFGPEGRLEDKLHKPKATQTEVKPSVRFNLRTSKDPEHEGCYLSV   50
                               .  .:* *   .

hPL     ADSSSISGSNFKTNRKTRFIIHGFIDKG-EENWLANVCKNLFKVE--SVNCICVDWKGGS   111
hHL     NHPDTLQECGFNSSLPLVMIIHGWSVDGVLENWIWQMVAALKSQPAQPVNVGLVDWITLA   103
mHL     QHPETLQECGFNSSQPLIMIIHGWSVDGLLENWIWKIVSALKSRQSQPVNVGLVDWISLA   105
hLPL    GVAESVATCHFNHSSKTFMVIHGWTVTGMYESWVPKLVAALYKREP-DSNVIVVDWLSRA    90
hEL     GHSQPLEDCSFNMTAKTFFIIHGWTMSGIFENWLHKLVSALHTREK-DANVVVVDWLPLA   109
                 . :  . *:. .    ::***:  *  *.*: ::   *.       *   ***   :

hPL     RTGYTQASQNIRIVGAEVAYFVEFLQSAFGYSPSNVHVIGHSLGAHAAGEAGRRTNG--T   169
hHL     HDHYTIAVRNTRLVGKEVAALLRWLEESVQLSRSHVHLIGYSLGAHVSGFAGSSIGGTHK   163
mHL     YQHYTIAVQNTRIVGQDVAALLLWLEESAKFSRSKVHLIGYSLGAHVSGFAGSSMDGKNK   165
hLPL    QEHYPVSAGYTKLVGQDVARFINWMEEEFNYPLDNVHLLGYSLGAHAAGIAGSLTNK--K   148
hEL     HQLYTDAVNNTRVVGHSIARMLDWLQEKDDFSLGNVHLIGYSLGAHVAGYAGNFVKG--T   167
              *  :     ::** .:* :: :::.      .**::*:*****.:* **        .

hPL     IGRITGLDPAEPCFQGTPELVRLDPSDAKFVDVIHTDGAPIVPNLGFGMSQVVGHLDFFP   229
hHL     IGRITGLDAAGPLFEGSAPSNRLSPDDANFVDAIHTFTRE-HMGLSVGIKQPIGHYDFYP   222
mHL     IGRITGLDPAGMFEGTSPNERLSPDDANFVDAIHTFTRE-HMGLSVGIKQPIAHYDFYP   224
hLPL    VNRITGLDPAGPNFEYAEAPSRLSPDDADFVDVLHTFTRG-SPGRSIGIQKPVGHVDIYP   207
hEL     VGRITGLDPAGPMFEGADIHKRLSPDDADFVDVLHTYTRS--FGLSIGIQMPVGHIDIYP   225
         : ****** * * *: :    **.*.**.***.:**       ..*:.  :.* *::*

hPL     NGGVEMPGCKKNILSQIVDIDGIWEGTRDFAACNHLRSYKYYTDSIVNPDG-FAGFPCAS   288
hHL     NGGSFQPGCHFLELYRHIAQHGF-NAITQTIKCSHERSVHLFIDSLLHAGTQSMAYPCGD   281
mHL     NGGSFQPGCHFLELYKHIAEHGL-NAITQTIKCAHERSVHLFIDSLQHSDLQSIGFQCSD   283
hLPL    NGGTFQPGCNIGEAIRVIAERGL-GDVDQLVKCSHERSIHLFIDSLLNEENPSKAYRCSS   266
hEL     NGGDFQPGCGLNDVLGSI---AY-GTITEVVKCEHERAVHLFVDSLVNQDKPSFAFQCTD   281
         ***  *** ***       :     .     :   * * *: : : **:.      .: * .

hPL     YNVFTANKCFPCPSGGCPQMGHYADRYPGKTNDVGQKFYLDTGDASNFARWRYKVSVTLS   348
hHL     MNSFSQGLCLSCKKGRCNTLGYHVRQEPRS---KSKRLFLVTRAQSPFKVYHYQFKIQFI   338
mHL     MGSFSQGLCLSCKKGRCNTLGYDIRKDRSG--KSKRLFLITRAQSPFKVYHYQFKIQFI   340
hLPL    KEAFEKGLCLSCRKNRCNNLGYEINKVRAK---RSSKMYLKTRSQMPYKVFHYQVKIHFS   323
hEL     SNRFKKGICLSCRKNRCNSIGYNAKKMRNK---RNSKMYLKTRAGMPFRVYHYQMKIHVF   338
              *    *:  * .  *  :*:  :     .:::* *       :  ::*:..: .

hPL     GKKVTGH----ILVSLFGNKGNSKQYEIFKGT-LKPDSTHSNEFDSDVDVGDLQMVKFIW   403
hHL     N-QTETPIQTTFTMSLLGTKEKMQKIPITLGKGIASNKTYSFLITLDVDIGELIMIKFKW   397
mHL     N-QIEKPVEPTFTMSLLGTKEEIKRIPITLGEGITSNKTYSFLITLDKDIGELILLKFKW   399
hLPL    GTESETHTNQAFEISLYGTVAESENIPFTLPE-VSTNKTYSFLIYTEVDIGELLMLKLKW   382
hEL     SYKNMGEIEPTFYVTLYGTNADSQTLPLEIVERIEQNATNTFLVYTEEDLGDLLKIQLTW   398
           :           : ::* *.  .:     :          : *  *  :  : *:*:* .  ::: *

hPL     YNNVI------------------NPTLPRVGASKIIVE-TNVGKQFNFCSPETVREEVL-   443
hHL     ENSA--VWANVWDTVQTIIPWSTGPRHSGLVLKTIRVKAGETQQRMTFCSENTDDLLLRP   455
mHL     ENSA--VWANVWNTVQTIMLWGIEPHHSGLILKTIWVKAGETQQRMTFCPENLDDLQLHP   457
hLPL    KSDSYFSWSDWWSS-----------PGFAIQKIRVKAGETQKKVIFCSREKVSHLQKG   429
hEL     EGASQ-SWYNLWKEFRSYLSQPRNP-GRELNIRRIRVKSGETQRKLTFCTEDPENTSISP   456
                                .  * *:  :. ::. ** :

hPL     ---LTLTPC----------------------   449
hHL     TQEKIFVKCEIKSKTSKRKIR----------   476
mHL     SQEKVFVNCEVKSKRLTESKEQMSQETHAKK   488
hLPL    KAPAVFVKCHDKSLNKKSG-----------   448
hEL     GRELWFRKCRDGWRMKNETSPTVELP-----   482
           : *
```

Table 1: Sequence similarity between members of the lipase family

	hPL	hHL	mHL	hLPL	hEL
hPL	100.00	31.85	31.24	31.48	31.93
hHL	31.85	100.00	75.63	45.70	42.49
mHL	31.24	75.63	100.00	46.17	43.76
hLPL	31.48	45.70	46.17	100.00	48.08
hEL	31.93	42.49	43.76	48.08	100.00

The amino acids sequences of the lipase family were aligned using Clustal Omega software[69] (Figure 4) with the following accession numbers: hHL: NP_000227.2, mHL: NP_032306.2, hPL: CAA4691.1, hLPL: NP_000228.1, hEL: NP_006024.1. The numbers in the table are represented of the percent homology between the different members of the *sn-1* lipase family.

structure of hPL provides some information about certain domains of hHL. hPL has been described as having a two-domain structure: the amino (N)-terminal domain has a globular structure and contains the active site, and the carboxyl (C)-terminal domain consists of β-sheets.[70] Like hPL, the active site for hHL is understood to be located in the N-terminal domain. The C-terminal domain of hHL has been characterized to hold the major heparin-binding site, as well as the main lipoprotein binding site.[71,72] This has been observed experimentally using peptide array assays to characterize the heparin binding ability of the C-terminal.[73,74] The heparin-binding domain (HBD) of hHL contains positively charged amino acids, which interact electrostatically with the negatively charged HSPG on the cell surface. The putative HBD of hHL was determined to reside within the last 70 amino acids of the hHL sequence, with the last five amino acids contributing greatly to heparin binding.[75] To provide further evidence of the location of the major HBD, when the sequences of mouse HL (mHL) and hHL are aligned, the mouse sequence is missing the last five (KRKIR) positively charged amino acids. This has been confirmed experimentally: mHL is observed to have a low affinity for heparin-sepharose, eluting with 0.4 M NaCl, when compared to full-length hHL, which elutes from heparin-sepharose with 0.7 M NaCl.[73] In agreement with the heparin-binding results, the activity of hHL within circulation increases 1,500 fold following its displacement from the cell surface HSPGs by heparin.[76]

hHL is thought to be catalytically active as a homodimer.[73] This is experimentally supported by the purification of hHL via size-exclusion chromatography. The eluted protein peak containing lipase activity has a calculated molecular mass of 107 kDa, in

agreement with the theoretical mass for an hHL dimer (106.8 kDa). To provide further evidence that active hHL exists as a dimer, when it is rendered inactive, the eluted protein fraction has a molecular mass is 63 kDa.[73]

1.1.7 Post-translational regulation of human hepatic lipase

The regulation of HL remains to be fully elucidated. It has been known for quite some time that the activity of hHL in the bloodstream increases after it is displaced from the cell surface via heparin.[76] It is proposed that there are two inactive pools of hHL: one is the HSPG bound enzyme and the other is the hHL bound to lipoproteins within the circulation.[77] In agreement with these proposals, Ramsamy *et al.* demonstrated that cell surface bound hHL is inactive.[78] However, there are studies which suggest that some lipases, specifically hLPL, is catalytically active when still bound to the cell surface via HSPG, and this association of hLPL with the HSPG actually enhances its activity.[79] Current findings suggest that the activity of hHL is dependent on its displacement from cell surfaces by its binding partner, HDL.[80,81] It has been known for some time that apoA-I and HDL are able to displace hHL from cell surface HSPG and that the association of hHL with these molecules modulates hHL activity.[78] These studies suggest that the activity of hHL is closely correlated with its ability to displace hHL from cell surface HSPGs. The liberation of hHL by HDL within the circulation enables hHL to gain access to its circulating substrates. HDL isolated from normolipidemic females has been shown to contain a significant amount of hHL mass compared to their male counterparts. This

may be responsible for the reduced magnitude of postprandial lipidemia, which is observed in women compared to men.[82] This may also increase the remodelling of HDL,[77] which could increase the RCT process. All of these studies suggest that increasing the displacement of hHL from cell surfaces is a promising approach to increasing the clearance of both cholesterol and TG from the bloodstream.

1.2 Objectives and Hypothesis

1.2.1 Objectives

The objective of this research is to investigate the HBD of hHL, and to use a mimetic peptide that is analogous to the C-terminal sequence of hHL to displace hHL from cell surfaces. This increase in activity will enhance the remodelling of HDL to create preβ-HDL: a more potent cholesterol acceptor that will increase the cholesterol efflux to these particles. This will potentially increase the overall process of RCT. The first part of this project deals with the functional analysis of the peptide and its ability to displace hHL from the cell surface. The second aspect of this project is to conduct a structural analysis of the peptide, $hHL_{442-476}$, to gain novel information about the structure of the HBD of hHL and to characterize the interaction between the peptide and heparin.

1.2.2 Hypothesis

I hypothesize that an hHL-derived peptide, which mimics the cell surface association of hHL, will be able to displace hHL from cell surfaces, in turn increasing free hHL activity upon displacement. This in turn will potentially increase cholesterol efflux to HDL and possibly increase the overall process of RCT.

1.3 Summary

CVD is the leading cause of mortality in the Western world.[1,83] Many therapies have attempted to reduce one's risk of CVD. However, many therapies have serious side effects or fail to reduce CVD in a large population. By conducting an investigation of a mimetic hHL peptide, we hope to provide a novel avenue in the world of cholesterol lowering agents. By carrying out both functional and structural studies, we hope to provide evidence using a mimetic peptide to displace hHL from cell surfaces. These studies will hopefully be the basis of a new peptide drug and therefore help combat the progression of atherosclerosis.

Chapter 2: Materials and Methods

2.1 Generation of the hHL$_{442-476}$ Peptide

2.1.1 Generation of the phHL$_{442-476}$ plasmid

The mimetic hHL protein construct was designed to be a thioredoxin (Trx) fusion protein containing a hexahistidine (6xhis)-tag for purification and immunoblot identification, an S-tag for immunoblot identification, and the hHL sequence containing the major HBD, specifically amino acids 442-476 (hHL$_{442-476}$)[75] (Figures 5 and S1). The last 26 amino acids within the 442-476 sequence of hHL contains clusters of positively charged amino acids that align with previously elucidated heparin binding motifs (Figure 5B). This HBD is absent in mHL, and is replaced with either neutral or negatively charged amino acids, resulting in mHL having a lower affinity for cell surface HSPGs compared to hHL.[75] The basic amino acids in hHL responsible for heparin binding are highlighted in red, while the analogous amino acids of mHL are highlighted in green. The basic amino acids within the HBD of hHL also align with previously elucidated heparin binding motifs.[84,85] The hHL$_{442-476}$ sequence also contains two cysteine residues and could form a putative disulfide bridge.

The nucleotide sequence corresponding to the 442-476 amino acid sequence was amplified by polymerase chain reaction (PCR) with primers that incorporated BamHI

**Figure 5: Schematic of the hHL$_{442-476}$-Trx protein**

A) Schematic of the hHL$_{442-476}$-Trx and the Trx protein constructs. Both constructs contain the Trx protein, plus 6xhis- and S-tags that are located within the region between the Trx protein and the hHL$_{442-476}$ sequence. There are also two cleavage sites: one for enterokinase (E) and one for thrombin (T), as indicated by the dashed lines. The constructs also contain a 7 amino acid linker region (AMADIGS), which links the hHL$_{442-476}$ sequence to the Trx protein. The Trx construct contains no hHL sequence and thus it was used as a vector control that produced a protein with a molecular mass of 21 kDa. The hHL$_{442-476}$-Trx construct contains the Trx protein linked to the hHL C-terminal sequence containing amino acids 442-476, having a molecular mass of 23 kDa. B) The hHL$_{442-476}$ sequence, aligned with the analogous sequence of mHL, shows the difference in the amino acid composition of the C-termini of the two proteins. The basic amino acids present in the hHL$_{442-476}$ sequence are arranged in patterns that align with previously elucidated heparin binding motifs.[84,85] B represents a basic amino acid and x is any amino acids. Also highlighted in blue is the putative disulfide bridge located within the hHL$_{442-476}$ sequence.

Figure 5

A.
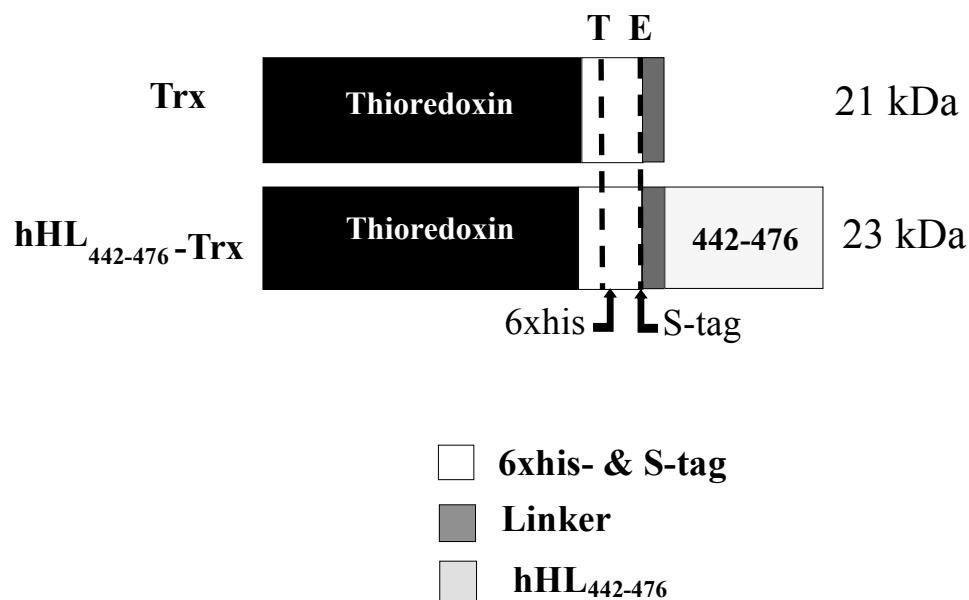
B.
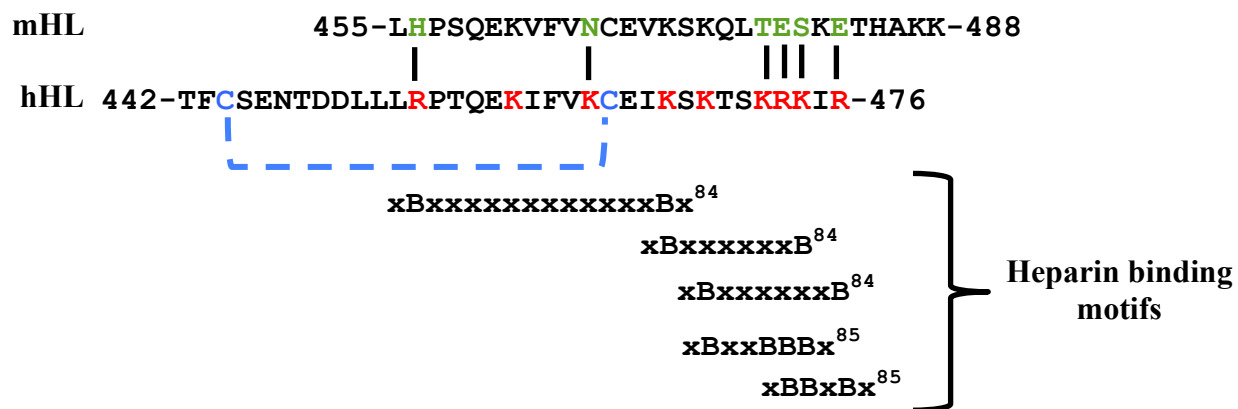
and HindIII restriction endonuclease sites into the PCR products (Table 2). The hHL cDNA (100 ng), 5 µL of both RB2 and RB3 primers (100 µM), and 25 µL of 2X PCR Master Mix (Promega, Madison, WI, USA) were mixed with ddH$_2$O for a total volume of 50 µL and treated to a series of repeated heat cycles. Cycle 1 consisted of denaturation of the DNA template at 95°C for 5 minutes. Cycle 2 continued the denaturation for 45 seconds, followed by an annealing step at 52°C for 1 minute, and an elongation step at 72°C for 2 minutes. Cycle 2 was repeated for 30 times. Cycle 3 consisted of a single step where the reaction temperature remained at 72°C for 5 minutes to ensure that any remaining single stranded DNA was fully extended. Once amplified, the product was digested with BamHI and HindIII and ligated into the pET32(+) vector (Novagen, Madison, WI, USA) (Figure 6) to create the plasmid to express the hHL$_{442-476}$ fusion protein (phHL$_{442-476}$-Trx). The plasmid was sequenced to verify its accuracy (data not shown). The phHL$_{442-476}$-Trx was transformed into the DH5α strain of *Escherichia coli* (Lucigen, Middleton, WI, USA). In brief, 50 µL of chemically competent DH5α cells in a 1.5 mL microfuge tube with a transformation efficiency of $\geq 1 \times 10^{10}$ colony forming units per µg DNA were incubated on ice with 10 ng of phHL$_{442-476}$-Trx for 30 minutes. The mixture was then heat shocked, using a heating block at 42°C for 90 seconds. The DH5α cell/plasmid mixture was cooled on ice for 10 minutes and 900 µL of Lysogeny Broth (LB) (Sigma, St. Louis, MO, USA) was added to the cells and incubated at 37°C, shaking at 175 rpm for 90 minutes. Then, 200 µL of cells was plated onto LB agar (Fisher Scientific, Ottawa, ON, Canada) plates containing 100 µg/mL sodium ampicillin (Sigma). The plates were incubated at 37°C upside down for 18 hours and subsequently stored at

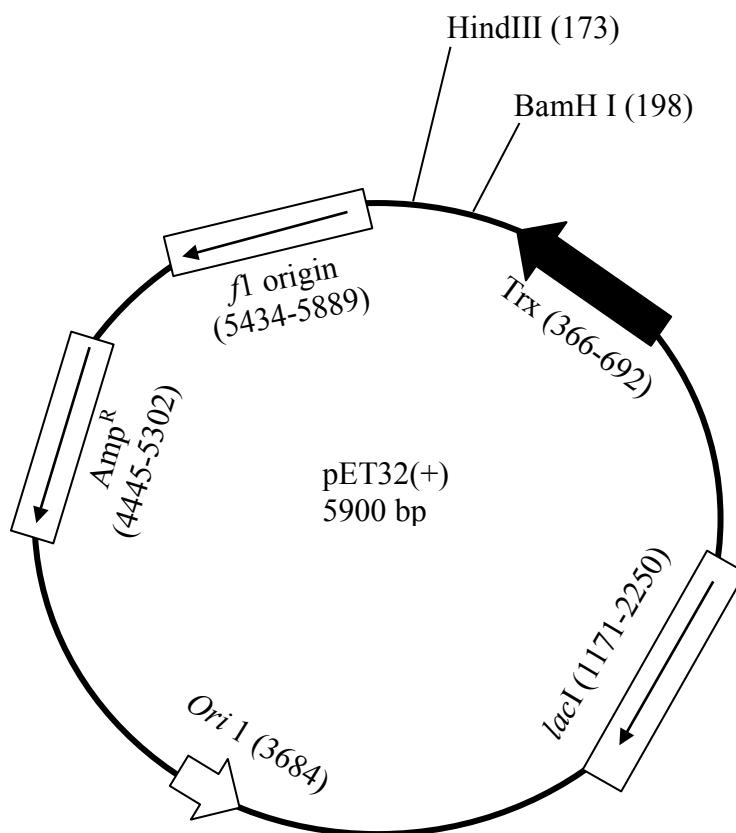**Table 2: PCR primer sequences used to create the hHL$_{442\text{-}476}$ peptide**.

Forward: RB2	5'-CAATA<u>GGATCC</u>ACATTTTGTTCAGAAAACACAGA-3'
	Template 1451…………………………………………………..………1470
Reverse: RB3	5'-CTGTT<u>AAGCTT</u>TCATCTGATCTTTTCGCTTTGATGAG-3'
	Template 1555……..………………………………………….………..1528

Primers were designed for *LIPC* gene (NM_000236). The restriction enzyme cut sites are underlined, RB2: BamHI and RB3: HindIII.

Figure 6: Schematic of pET32(+) vector used to construct phHL$_{442\text{-}476}$-Trx

The sequence encoding amino acids 442-476 of hHL was inserted into the pET32(+) vector between the HindIII and BamHI sites to create the phHL$_{442\text{-}476}$ plasmid. The vector contains an f1 origin to allow for single stranded replication to occur under specific conditions. The antibiotic resistance gene used for screening within this vector is ampicillin (Amp^r). To control the expression of the hHL$_{442\text{-}476}$-Trx protein, the vector contains the lac operator and the *lacI* gene is responsible for its regulation.

Figure 6

HindIII (173)

BamH I (198)

Trx (366-692)

*f*1 origin
(5434-5889)

Amp^R
(4445-5302)

pET32(+)
5900 bp

*lac*I (1171-2250)

Ori 1 (3684)

4°C until needed for the expression of the hHL$_{442-476}$ peptide.

2.1.2 Expression of hHL$_{442-476}$ peptide

To express the hHL$_{442-476}$-Trx protein in bulk, phHL$_{442-476}$-Trx was transformed into OverExpress™ C43(DE3) cells (Lucigen) using the protocol described in *section 2.1.1* for *E. coli* DH5α cells. Colonies (5-10) from the LB plates were grown in a 30 mL culture of LB containing 100 μg/mL of ampicillin at 37°C in a shaking incubator at 175 rpm for 18 hours. The culture was then evenly split (with a ratio of 15 mL of overnight culture into 1.5 L of fresh LB) and transferred to two flasks, each with 1.5 L of LB containing 100 μg/mL of ampicillin. The cultures were grown at 37°C in a shaking incubator at 175 rpm until the culture reached an optical density (OD) of 0.6 at 600 nm. Then, isopropyl-β-$_D$-1-thiogalactopyranoside (IPTG) (Gold Biotechnology, St. Louis, MO, USA) was added to a final concentration of 0.4 mM to allow the hHL$_{442-476}$-Trx protein to be expressed under control of the lac promoter. To allow for maximal protein expression, 3 L of bacterial culture at an OD$_{600 \, nm}$ of 0.6 was further incubated for 18 hours at 30°C in a shaking incubator at 175 rpm. Following the incubation, the culture was divided among four 1 L Nalgene bottles and centrifuged at 5,000 × *g* for 15 minutes to pellet the bacteria. The supernatants were discarded and the pellets were sequentially resuspended in 10 mL of 1X Tris-buffered saline (TBS: 6.06 g Tris, 8.76 g NaCl adjusted to pH 7.0 and a final volume of 1 L). The bacteria in TBS were lysed using a French press at 12,000 psi at 4°C; this step was repeated twice and followed by brief sonication using a

35

probe sonicator (Branson Sonifier 200, Wilmington, NC, USA) with a processor probe at setting 7 pulsing the bacteria 3 times for 15 seconds. The lysed bacteria were pelleted at 5,000 × g for 15 minutes at 4°C to separate the supernatant containing the fusion protein from the bacterial cell debris.

2.1.3 Purification of the hHL$_{442-476}$ peptide

In order to purify the fusion protein from the other bacterial proteins, the supernatant was added to a nickel-sepharose column (capacity of 40 mg/mL) (GE Healthcare, Baie d'Urfe, QC, Canada), with a 15 mL column volume (CV); the supernatant was incubated for 30 minutes to allow the 6xhis tag to bind to the nickel ions on the column. The column flow-through was collected by gravity in 1 mL fractions. Non-specific proteins were washed from the column using 3 CV of 40 mM imidazole (in 1X TBS). The column was further washed with 2 CV of 100 mM imidazole to elute any non-specific proteins with a modest affinity to the nickel ions. The hHL$_{442-476}$-Trx protein was eluted from the column using 2 CV of 300 mM imidazole. To determine the purity of the hHL$_{442-476}$-Trx protein, the column fractions were subjected to sodium dodecyl sulfate polyacrylamide gel electrophoresis (SDS-PAGE) (described in *section 2.2*). Fractions that contained the hHL$_{442-476}$-Trx protein with minimal bacterial protein contaminants were pooled and dialyzed using 6,000-8,000 molecular weight cut off (MWCO) tubing (Sigma) against 3 L of dialysis buffer (10 mM Tris-HCl, 100 mM NaCl at pH 7.0) at 4°C for 24 hours to remove the imidazole, exchanging the buffer after 12 hours with a fresh 3 L of

dialysis buffer. After dialysis, 30 mL of the fusion protein was incubated with 50 units (U) of thrombin (Sigma) at room temperature (RT) for 24 hours on a rocker (VWR, Edmonton, AB, Canada) at setting 5. (Five U of thrombin will cleave 1 mg of protein). This incubation was done in order to cleave the $hHL_{442-476}$ sequence from the Trx backbone. Specifically, thrombin recognizes the consensus sequence leucine-valine-proline-arginine-glycine-serine and cleaves between arginine and glycine.[86] This results in a 7.9 kDa cleaved $hHL_{442-476}$ peptide linked to both the 6xhis tag and S-tag. To verify that the cleavage reaction occurred, SDS-PAGE was performed on uncleaved (15.1 kDa) and cleaved (7.9 kDa) reaction samples. Once the correct molecular masses were verified from Coomassie Blue stained gels, the cleaved peptide was dialysed using 1,000 MWCO tubing (Sigma) against 2 L of 10 mM Na_2PO_4 at pH 7.0 for 24 hours at 4°C.

To separate the cleaved $hHL_{442-476}$ peptide from the Trx backbone and thrombin in the reaction mixture, the mixture was added to a Sephacryl S-100 size exclusion column having a column volume of 100 mL equilibrated with 1X phosphate buffered saline (PBS: 8.7 g NaCl, 2.3 g Na_2HPO_4, 0.5 g NaH_2PO_4 adjusted to pH 7.0 and a final volume of 1 L). One mL fractions of the column flow-through were collected for up to 100 mL. Fractions were assessed by SDS-PAGE using purchased Tris-tricine 16.5% gels (Bio-Rad, Mississauga, ON, Canada) to determine the purity of the cleaved $hHL_{442-476}$ peptide. Size exclusion chromatography was first employed to isolate the $hHL_{442-476}$ peptide; however, the method was determined not to be optimal due to the contaminants that co-eluted with the $hHL_{442-476}$ peptide.

To improve the isolation of the cleaved peptide from the Trx protein and thrombin, heparin-sepharose (GE Healthcare), was used in all subsequent hHL$_{442-476}$ peptide purifications. In brief, the thrombin reaction mixture was dialyzed against 2 L of 10 mM Na$_2$PO$_4$ at pH 7.0 at 4°C, using 1,000 MWCO dialysis tubing for 24 hours, with a change of fresh 2 L of buffer following 12 hours. The thrombin reaction mixture was then added to a 15 mL centrifuge tube containing 10 mL of heparin-sepharose (approximately 40 mg of heparin) in 10 mM Na$_2$PO$_4$ at pH 7.0. The mixture in heparin-sepharose was incubated at 4°C for 18 hours on a spinning wheel. Following the incubation, the slurry of resin was added to an empty 25 mL column and washed with 4 CV of 10 mM Na$_2$PO$_4$ at pH 7.0 to wash proteins not bound to the column; 1 mL fractions were collected by gravity. The cleaved hHL$_{442-476}$ peptide was eluted from the heparin-sepharose column with 2 CV of 1.0 M NaCl, (which disrupts the electrostatic interactions between the positively charged HBD of the hHL$_{442-476}$ peptide and the negatively charged heparin-sepharose). The fractions from the column were assessed using SDS-PAGE. Fractions containing the eluted hHL$_{442-476}$ peptide were pooled and dialyzed against 2 L of 1X PBS with 1,000 MWCO tubing at 4°C for 24 hours, with a change of the buffer after 12 hours. The concentration was determined using a NanoDrop 2000 spectrophotometer at the wavelength at 280 nm (extinction coefficient 125 M^{-1}cm^{-1}). The purified protein was divided into 1 mL aliquots and stored at 4°C until needed.

2.1.4 Generation of ^{15}N labeled hHL$_{442-476}$ peptide

For ^{15}N labeled peptide generation, M9 medium was prepared to culture bacteria transformed with the phHL$_{442-476}$-Trx. The medium contains minimal nutrients with a ^{15}N nitrogen source for the bacteria. The recipe for M9 medium is given nutrients per L as follows: 6 g Na$_2$PO$_4$ (Sigma), 3 g KH$_2$PO$_4$ (Sigma), 0.5 g NaCl (Fisher Scientific), and 1 g $^{15}NH_4Cl$ (Cambridge Isotopes, Tewksbury, MA, USA). The pH of the medium was adjusted to 7.4 and then autoclaved. Once autoclaved, the following minimal nutrients were filter sterilized using 0.22 μm filters (Fisher Scientific) and added to the autoclaved medium: 2 mM MgSO$_4$, 0.1 mM CaCl$_2$, 5 mL of 40% w/v glucose, 10 μM FeSO$_4$, 5 mg thiamine, and 100 mg ampicillin. Next, 2.5 mL of a stock solution of trace elements was added; the stock consisted of 2.7 g FeCl$_3$, 0.2 g ZnCl$_2$, 0.2 g CoCl$_2$, 0.2 g Na$_2$MoO$_4$, 0.1 g CaCl$_2$, 0.13 g CuCl$_2$, 0.05 g H$_3$BO$_3$, 10 mL of 10 N HCl, and 90 mL deionized H$_2$O (dH$_2$O). After the addition of the trace elements, 1 mL of a stock vitamin mixture was added to the medium; the stock consisted of 100 mg biotin, 50 mg choline, 50 mg folic acid, 100 mg myo-inositol, 50 mg nicotinamide, 50 mg pyridoxal, 5 mg riboflavin, 50 mg thiamine and 100 mL dH$_2$O.

An overnight culture of OverExpress™ C43(DE3) cells transformed with phHL$_{442-476}$-Trx was grown as described in *section 2.1.2*. Following the incubation, the 30 mL culture was centrifuged at 5,000 rpm for 15 minutes, the supernatant was discarded, and the bacterial pellet was used to inoculate 3 L of M9 medium. The inoculated medium was incubated at 37°C in a shaking incubator at 175 rpm until the OD$_{600}$ of the culture

reached 0.6. Once the OD was reached, IPTG was added to the culture to a final concentration of 0.4 mM; the culture was then incubated at 30°C in the shaker for 18 hours. Following the incubation, the hHL$_{442-476}$-Trx was purified and isolated as described in *section 2.1.3* to obtain the ^{15}N-labeled hHL$_{442-476}$ peptide. The peptide was subsequently analyzed via nuclear magnetic resonance (NMR).

2.2 Sodium Dodecyl Sulfate-Polyacrylamide Gel Electrophoresis (SDS-PAGE)

For SDS-PAGE preparation, samples were mixed with 4X lysis buffer (5.1 mL H$_2$O, 0.08% w/v SDS, 0.4% v/v glycerol, 5 μM bromophenol blue, 0.05% β-mercaptoethanol) (1:4 dilution for buffer to sample) and boiled for 2 minutes. Samples were separated using SDS-PAGE with 4% acrylamide (19:1 ratio) stacking (2 cm) and 12% acrylamide (19:1 ratio) separating (6 cm) gels for approximately 60 minutes at 200 V. The running buffer used was Tris/Glycine/SDS (TGS) (25 mM Tris, 192 mM glycine and 0.1% w/v SDS, pH 8.3) (Bio-Rad). After separation, the gels were either transferred to nitrocellulose membranes for immunoblot analysis or stained with 0.1% w/v Coomassie Blue (in 50% v/v methanol 40% v/v H$_2$O, 10% v/v glacial acetic acid) for approximately 2 hours on a rocking platform. After staining, the gel was destained using the staining solution without Coomassie Blue. However, if protein bands did not appear, the gel was subjected to silver stain (Bio-Rad). In brief, the gel was fixed in 15 mL of 10% ethanol/5% glacial acetic acid (v/v) for 30 minutes, and then washed 4 times (5 minutes per wash) with 15 mL of dH$_2$O. Once the washes were completed, the gel was

incubated with 15 mL silver stain reagent for 15 minutes. The staining reaction was stopped with 10% v/v glacial acetic acid.

2.2.1 Immunoblot analysis

For immunoblot analysis, samples were separated via SDS-PAGE and the gels were transferred to nitrocellulose membrane (Bio-Rad) for 2 hours at 350 mA at 4°C with a transfer buffer consisting of TGS with 20% v/v methanol (Fisher Scientific). The membranes were blocked with filtered blocking solution (5% bovine serum albumin (BSA) (Sigma), 0.05% v/v Tween-20 (Sigma), and 0.05% sodium azide (Fisher Scientific) in 1X PBS) for 2 hours at RT on a platform rocker. After blocking, membranes were incubated with the primary antibody for 3 hours at RT with a dilution of 1:1,000 in the 5% blocking solution. Primary antibodies used were: anti-hHL (xHL3-6) (Catalogue #sc21740, Santa Cruz Biotechnologies, Santa Cruz, CA, USA), anti-6xhis (H15) (Catalogue #sc-803, Santa Cruz Biotechnologies), anti-hLPL (H-53) (Catalogue #sc-32885, Santa Cruz Biotechnologies), anti-hLPL (F-1) (Catalogue #sc-373759, Santa Cruz Biotechnologies), anti-S-tag (Catalogue #8476s, Cell Signaling Technology, Danvers, MA, USA), anti-myc-tag (Catalogue #2272, Cell Signaling Technology). After the primary antibody incubation, membranes were washed 4 times for 5 minutes per wash with 1X PBS-T (1X PBS with 0.05% v/v Tween-20). The membranes were incubated for 2 hours at RT on a rocking platform with the secondary antibody (1:1,500) diluted in blocking solution not containing sodium azide. A donkey anti-rabbit secondary antibody

(Catalogue #SA1-100, Fisher Scientific) was used against the primary antibodies, anti-hLPL (H-53), anti-S-tag, anti-myc-tag and anti-6xhis. A donkey anti-mouse secondary antibody (Catalogue #SA1-200, Fisher Scientific) was used against the primary antibodies, anti-hHL and anti-LPL (F-1). The membranes were subsequently washed 4 times for 10 minutes each with 1X PBS. Membranes were subsequently developed with ECL Prime Western Blotting Detection Reagent Kit (GE Healthcare), according to the manufacturer's instructions. The membranes were imaged using the chemiluminescence setting on an ImageQuant 4000 gel imager (GE Healthcare).

2.3 Mammalian Cell Culture

2.3.1 HEK-293T cell culture and transfection

The HEK-293T human embryonic kidney cell line was donated by Dr. Sherri Christian (Department of Biochemistry, Memorial University of Newfoundland). The cells were maintained at 37°C in an atmosphere of 95% air and 5% CO_2 and cultured in T75 flasks (BD Biosciences, Mississauga, ON, Canada) at 80% confluency in Dulbecco's Modified Eagle Medium (DMEM) (Catalogue #SH30243.01, HyClone, South Logan, UT, USA), 10% v/v fetal bovine serum (FBS) (Catalogue #SH30088.03, HyClone), and 1% v/v antibiotic/antimycotic (A/A) (Catalogue #SV30079.01, HyClone). Cells were sub-cultured every 3-4 days. In brief, cells were washed with DMEM (without FBS and A/A) and detached from the flask surface using 2.5 mL of 0.25% w/v trypsin (Catalogue

#SV3003.01, HyClone). The adhered cells were rinsed with trypsin, then the trypsin was discarded; the cells were next incubated for approximately 2 minutes at 37°C in 5% v/v CO_2. The cells were then detached from the flask by re-suspending them using 10 mL of DMEM with 10% FBS and 1% A/A. Cells were divided into a new T75 flask using a 1:10 ratio of detached cells to DMEM (with 10% FBS and 1% A/A) and incubated at 37°C in 5% CO_2.

For the transfection of HEK-293T cells to express lipases, the cells were displaced from T75 flasks with trypsin and resuspended in 10 mL of DMEM (10% FBS, 1% A/A) but seeded in 100 mm plates (BD Biosciences) to 90% confluency. The cells were transfected with 5.85 μg of a pcDNA$_3$ mammalian expression plasmid containing the hHL,[87] hLPL,[87] or myc-tagged hLPL[88] cDNA using Optimal Minimal Essential Medium (OPTI-MEM) culture media (Invitrogen, Burlington, ON, Canada) and Lipofectamine[TM] (Invitrogen) according to the manufacturer's instructions. Of note, the myc-tag did not affect the hydrolytic activity of hLPL (Figure S2). After 5 hours, 5.8 mL of DMEM containing 20% FBS and 2% A/A was added to the plates without the removal of the plasmid-Lipofectamine™ mixture and incubated for an additional 19 hours. Following the 24 hour incubation, spent media was replaced with 5 mL of serum free DMEM containing 1% A/A and 10 U/mL heparin (Catalogue #C50430, Fresenius Kabi, Richmond Hill, ON, Canada). The plates were further incubated for 23.5 hours in 5% CO_2 at 37°C. To displace the lipase within the media, the heparin concentration was increased to 25 U/mL at 47.5 hours post-transfection. The media was collected in 15 mL centrifuge tubes and centrifuged at 750 rpm for 5 minutes to remove any cell debris. The

supernatant was divided into 500 μL aliquots and stored at -80°C until needed. The cells were washed with 5 mL of 1X PBS to remove any media still on the plates and then stored at -80°C.

For transfection in 6-well plates, each well received 2.5 μg of lipase plasmid and was incubated at 37°C at 5% CO_2 for 5 hours. Then, 1.5 mL of DMEM containing 20% v/v FBS and 2% v/v A/A was added to each well and plates were incubated for 24 hours at 37°C in 5% CO_2. The spent media was discarded and the cells were washed once with 1 mL of DMEM. Then, 1.5 mL of fresh DMEM was added to the cells and incubated for additional 24 hours at 37°C in 5% CO_2. Transfected cells were subsequently used for lipase displacement assays (see *section 2.4.2*).

2.4 Functional Analysis of the hHL$_{442-476}$ Peptide

2.4.1 Heparin-sepharose assay with NaCl step-wise gradient

The hHL$_{442-476}$ peptide was expressed and purified as described in *section 2.1.3*. Twenty μg of the hHL$_{442-476}$ peptide was added to 500 μL of heparin-sepharose in a 1.5 μL microfuge tube and mixed for 18 hours at 4°C on a spinning wheel. The tube was subsequently centrifuged at 2,000 rpm for 3 minutes to isolate the supernatant. The resin was then washed 6 times with 200 μL of 10 mM Na_2PO_4, pH 7.0 for 2 minutes per wash on the spinning wheel at 4°C. After each wash, the sample was centrifuged at 2,000 rpm for 3 minutes and the supernatant from all washes was collected. Following the washes,

44

the heparin-sepharose was incubated with 200 μL of a NaCl solution in a step-wise NaCl gradient, starting at 0.1 M NaCl and ending at 1.0 M NaCl, in increments of 0.1 M. Each incubation was for 15 minutes at 4°C on the spinning wheel. After each of the NaCl incubations, the slurry was centrifuged for 3 minutes at 2,000 rpm, and the supernatant was collected. All samples were subjected to SDS-PAGE analysis, as described in *section 2.2*.

2.4.2 Lipase displacement assay

HEK-293T cells were grown to 80% confluency and detached with trypsin (as described in *section 2.3.1*). Cells were resuspended in 20 mL of DMEM (with 10% FBS and 1% A/A). The cells were seeded into 6-well plates (Fisher Scientific) in a volume of 2.5 mL. Plates were incubated for 18 hours at 37°C in 5% CO_2. After 18 hours, the cells were transfected to express hHL, or hLPL, as described in *section 2.3.1*. On the 4th day post-transfection, HEK-293T cells were transferred to a 4°C cold room and washed 3 times with 1 mL of ice cold DMEM (without FBS and A/A). Following the washes, each plate of the cells was incubated for 1 hour at 4°C with 1 mL DMEM (without FBS and A/A) ± 200 μg/mL of the $hHL_{442-476}$ peptide. Prior to the addition of the $hHL_{442-476}$ peptide to the cells, the $hHL_{442-476}$ peptide was desalted and collected in plain DMEM using a PD-10 desalting column as per the manufacturer's instructions (GE Healthcare). After the 1 hour incubation without or with peptide, the treatment media was collected. The cells were washed with 3 times ice cold DMEM (without FBS and A/A). Next, three

45

wells were incubated with 1 mL of DMEM (without FBS and A/A), the remaining three

wells received 1 mL of DMEM (without FBS and A/A) containing 100 U of heparin and

incubated for 1 hour at 4°C. The media were collected and stored in microfuge tubes at

-80°C until needed. The cells were washed once with 1X PBS then the cells were stored

at -80°C. All of the samples (media and cells) were analyzed by immunoblot analysis, as

previously described in *section 2.2.1*. To lyse the cells, 1 mL of 4X lysis buffer was added

to each well and the cells were scraped using cell scrapers (Fisher Scientific). A 1:4

dilution with more 4X lysis buffer was done to analyze the cells via immunoblot. The cell

lysates were stored at -80°C until required again.

2.5 Lipase Activity

2.5.1 Resorufin ester assay

To evaluate the activity of the lipases from the media of transfected cells (as

described in *section 2.3.1*), an assay measuring the hydrolysis of a resorufin ester was

performed.[89] First, a stock solution for the substrate 1,2-*O*-dilauryl-*rac*-glycero-3-glutaric

acid-resorufin ester (Sigma) was prepared by dissolving 2 mg of the resorufin ester in 1

mL of dioxane (Sigma); the stock solution of substrate was stored at 4°C until needed.

For the assay, the stock solution was diluted to 0.3 mg/mL in the reaction buffer (20 mM

Tris, 1 mM EDTA, pH 8.0); 20 μL of the diluted substrate was used per reaction. To

assess lipase activity, 75 μL of the heparinized media from HEK-293T cells expressing

lipases was pipetted into the well of a 96-well microtitre plate (Fisher Scientific), followed by the addition of 105 μL of the reaction buffer and 20 μL of the diluted resorufin ester. The absorbance at 572 nm was read every 3 minutes for a 1 hour period at 25°C using a microtiter plate reader. A standard curve for determining resorufin concentration was created, using 0, 1, 2, 3, 4, 6, 10, 15, 20, 30, and 40 μM resorufin (Sigma), dissolved in the reaction buffer to a final volume of 200 μL.

2.6 Structural Analysis of Mimetic Peptide

2.6.1 Secondary structure: circular dichroism

Samples of the cleaved peptide for circular dichroism (CD) were prepared, as described above in *section 2.1.3*. The sample was lyophilized and 0.1 mg was dissolved in 1 mL of dH$_2$O and 160 μL was pipetted into a 0.5 mm CD cuvette for analysis in a Jasco J-810 CD spectrophotometer. The sample was initially subjected to 10 scans, while ensuring that the high tension (HT) voltage did not exceed 700 volts, which would indicate too much scatter from the sample and not enough light passing through the sample. If the HT voltage exceeds 700 volts, the spectrum obtained becomes noisy and unreliable. Once the scans were complete, either heparin or trifluoroethanol (TFE) was titrated into the sample within the cuvette. In the case of heparin, 100 U was titrated in and analyzed over 10 scans, followed by increasing the heparin concentration to 250 U for re-analysis over 10 scans. For the TFE titrations, 5, 10, 20, 30, and 40% v/v of TFE

was titrated into the sample and 10 scans were performed after each amount of TFE was added. Once the scans were finished, the raw data were plotted in Microsoft Excel (Mac 2010) to produce the CD spectra.

2.6.2 ^{1}H-NMR sample preparation

The cleaved peptide was expressed and purified as described in *section 2.1.3*. Following the heparin-sepharose purification, the peptide was dialyzed with 1,000 MWCO dialysis tubing against 2 L of low sodium phosphate buffer (1 L: 2.9 g NaCl, 2.3 g Na_2HPO_4, 0.5 g NaH_2PO_4, pH 7.0) for 24 hours at 4°C, with buffer exchange after 12 hours. Following dialysis, the protein solution was lyophilized. Specifically, the dialyzed sample was put in a beaker and placed in liquid nitrogen to freeze the sample to avoid any bumping out and loss of the sample once the vacuum of the freeze dryer was applied. The sample was applied to the freeze dryer and left for 48 hours. After the sample was lyophilized, the mass of the powder was determined and the powder was stored in a sealed vial at 4°C until needed. For ^{1}H-NMR, 1.5 mg of the lyophilized sample was dissolved in 1 mL of dH_2O. The pH was determined for each sample prior to analysis using pH indicator strips (Sigma). This was done to rule out any structural anomalies observed due to the pH of the sample. The total volume for the NMR sample was 600 µL, and it contained 90% H_2O, 10% v/v deuterium oxide (D_2O) (Sigma) and 0.4 mM 4,4-dimethyl-4-silapentane-1-sulfonic acid (DSS) (Cambridge Isotopes Laboratories, Inc., Tewsbury, MA, USA). The sample was pipetted into an NMR tube (New Era Enterprises,

Inc., Vineland, NJ, USA) and placed in the NMR machine, Bruker AVANCE II 600 (Bruker, Billerica, MA, USA) with a 600 MHz probe. ^{1}H-NMR of the samples was carried out either at 4°C or 25°C, in the absence or presence of either heparin or deuterated TFE (Cambridge Isotopes Laboratories, Inc.). Table 3 lists the experiments that were conducted in order. Experiment 1: 1 dimensional (1D) ^{1}H spectrum with water suppression was conducted to achieve a spectrum without the large signal that water produces. Experiment 3: 2 dimensional (2D) nuclear Overhauser effect spectroscopy (NOESY) with peptide was conducted to determine through-space interactions. Experiment 7: total correlation spectroscopy (TOCSY) was conducted to indicate through-bond correlations. After the initial set of NMR experiments was performed with the $hHL_{442-476}$ peptide, select NMR experiments were performed with heparin added to the samples. Specifically, 100 U of heparin was titrated into the sample and the experiments were conducted (experiment 4), then the heparin concentration was increased to 250 U and experiments 5-7 were carried out. Then, a new sample was prepared for experiments 8-16 and varying percentages of TFE (5, 10, 20, and 30% v/v) were titrated in and experiments were run after each percentage of TFE was added. The same sample used in experiments 5-7 was used for experiment 17. For experiments 19 and 20, a ^{15}N labeled $hHL_{442-476}$ peptide was generated as described in *section 2.1.4*. Once experiments were finished, the spectra were analyzed using iNMR software.

Table 3: List of NMR experiments conducted with the hHL$_{442-476}$ peptide

NMR Experiment	Parameters	Filename
1. 1D-^{1}H water suppression with peptide	25°C, recycle delay 2s, scans 224, receiver gain 1150	A2 peptide/2
2. 1D-^{1}H water suppression with peptide	5°C	A2 peptide/3
3. 2D-^{1}H NOESY with peptide	25°C, 112 scans, number of points 1024 by 386	A2 peptide/4
4. 1D-^{1}H water suppression with peptide and 100 U heparin	25°C	A2 peptide/5
5. 1D-^{1}H water suppression with peptide and 250 U heparin	25°C	A2 peptide/6
6. 2D -^{1}H NOESY with peptide and 250 U heparin	25°C, 122 scans, number of points 1024 by 400	A2 peptide/7
7. 2D-^{1}H TOCSY with peptide and 250 U heparin	25°C, 136 scans, number of points 1024 by 5 mixing time 60 μs	A2 peptide/8
8. 1D-^{1}H water suppression 5% TFE and peptide	25°C	A2 peptide/10
9. 1D-^{1}H water suppression 5% TFE and peptide	5°C	A2 peptide/11
10. 1D-^{1}H water suppression 10% TFE and peptide	5°C	A2 peptide/12
11. 1D-^{1}H water suppression 10% TFE and peptide	25°C	A2 peptide/13
13. 2D-^{1}H NOESY 10% TFE and peptide	25°C, 112 scans, number of points 1024 by 364 mixing time 300 μs	A2 peptide/14
14. 1D-^{1}H water suppression 20% TFE and peptide	25°C	A2 peptide/15
15. 1D-^{1}H water suppression 20% TFE and peptide	5°C	A2 peptide/16
16. 1D-^{1}H water suppression 30% TFE and peptide	5°C	A2 peptide/17
^{1}H- ^{15}N-NMR Experiments		
19. ^{1}H-^{15}N HSQC (heteronuclear single quantum coherence) with peptide	5°C, scans 409, number of points 1024 by 109, receiver gain 1030, relaxation delay 1s	A2 conc. Aug 4 / 3
20. ^{1}H-^{15}N HSQC with peptide and 250 U heparin	5°C scans 409, number of points 1024 by 109, receiver gain 1030, relaxation delay 1s	A2 conc.+250 U Heparin Aug 4 / 3

2.7 Statistical Analysis

The p-values presented in figures were determined using a one-way ANOVA with a Tukey's test for multiple comparisons, calculated using Excel; a p-value of less than 0.05 was taken to be significant. The error bars were generated by using the standard deviation of the mean.

Chapter 3: Results

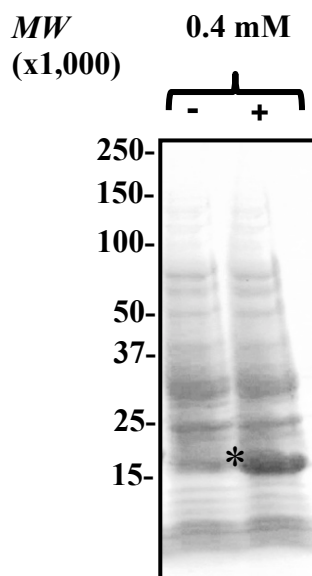## 3.1 Expression and Isolation of the hHL$_{442-476}$ Peptide

The phHL$_{442-476}$-Trx plasmid was transformed into the OverExpress™ C43(DE3) strain of *E. coli* and the expression of hHL$_{442-476}$-Trx protein was achieved at 30°C in the presence of 0.4 mM IPTG (Figure 7A). Figure 7A also shows that the hHL$_{442-476}$-Trx oligopeptide was not expressed in the absence of IPTG. To isolate the hHL$_{442-476}$-Trx protein from the supernatant of pelleted OverExpress™ C43(DE3) cell lysates, the supernatant was subjected to nickel-sepharose chromatography. The elution of the hHL$_{442-476}$-Trx protein was achieved with 300 mM imidazole (Figure 7B). Following isolation by nickel-sepharose chromatography, the hHL$_{442-476}$-Trx protein was incubated with thrombin to cleave the hHL$_{442-476}$ sequence from Trx, yielding the hHL$_{442-476}$ peptide with a theoretical molecular mass of 7.9 kDa (Figure 7C). However, the hHL$_{442-476}$ peptide has an experimental molecular weight of approximately 12 k. The discrepancy between the two values is a consequence of the hHL$_{442-476}$ peptide having numerous positively charged amino acids (lysines and arginines) that allows it to migrate slower in SDS-PAGE due to a reduction in the charge-to-mass ratio.[90] The 12 k band was confirmed to be the hHL$_{442-476}$ peptide by immunoblot analysis using the S-tag antibody (data not shown). Also observed in Figure 7C is thrombin at approximately 29 kDa. This is representative of the B chain of thrombin (31 kDa); the A chain (6 kDa) is joined by a disulfide bridge and under reducing conditions is not observed. The Trx protein (15.1 kDa) is not observed. These results show that the hHL$_{442-476}$-Trx protein can be expressed

Figure 7: Expression and isolation of hHL$_{442\text{-}476}$ peptide from *E. coli* C43(DE3)
A) OverExpress™ C43(DE3) cells were transformed with the phHL$_{442\text{-}476}$-Trx plasmid. Cells were inoculated in 15 mL of LB broth and grown to mid-log phase at 37°C, followed by an incubation for 18 hours at 30°C with (+) or without (-) 0.4 mM ITPG. The presence of the hHL$_{442\text{-}476}$-Trx protein is observed as a distinct band at 25 kDa on a Coomassie Blue stained 12% acrylamide gel (indicated with "*"). B) hHL$_{442\text{-}476}$-Trx protein was isolated using nickel-sepharose chromatography. The supernatant (S) was applied to the column and the flow-through (FT) was passed through by gravity. The column was then washed 3X with 1X TBS (pH 7.0) containing 40 mM imidazole (W1-3). The column was washed twice with 1X TBS (pH 7.0) containing 100 mM imidazole (W4-5). Finally, the 23 kDa hHL$_{442\text{-}476}$-Trx protein was eluted from the nickel-sepharose column with 1X TBS (pH 7.0) containing 300 mM imidazole. The proteins from the nickel-sepharose column were separated by SDS-PAGE with 12% acrylamide and stained with Coomassie Blue. C) The nickel-sepharose eluent containing the hHL$_{442\text{-}476}$-Trx protein was pooled (30 mL) and incubated with 50 U of thrombin for 18 hours at room temperature on a shaker. Following the incubation, samples were analyzed by SDS-PAGE with 12% acrylamide and stained with Coomassie Blue. FP = fusion hHL$_{442\text{-}476}$-Trx protein, CP= cleaved hHL$_{442\text{-}476}$ peptide

Figure 7

A.

MW
(x1,000)

0.4 mM

- +

250-
150-
100-

50-
37-

25-

15- *

B.

MW
(x1,000)

S   FT   W1   W2   W3   W4   W5   hHL$_{442-476}$
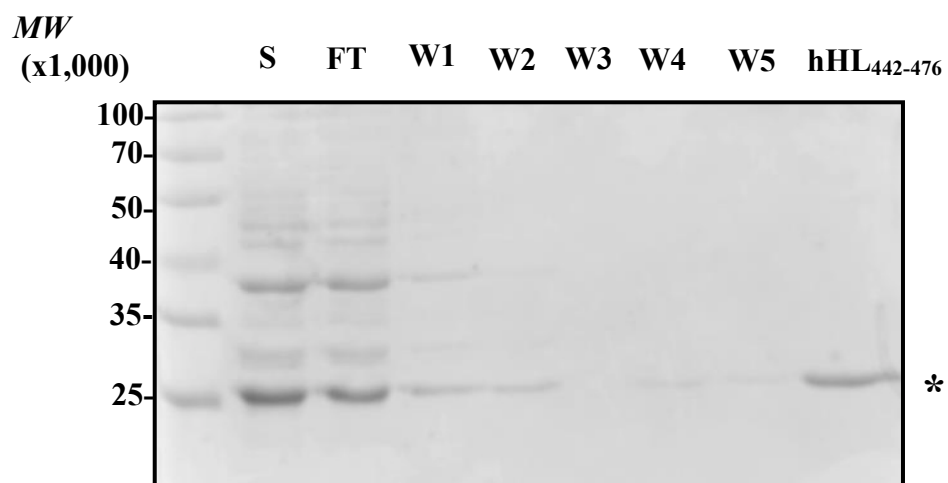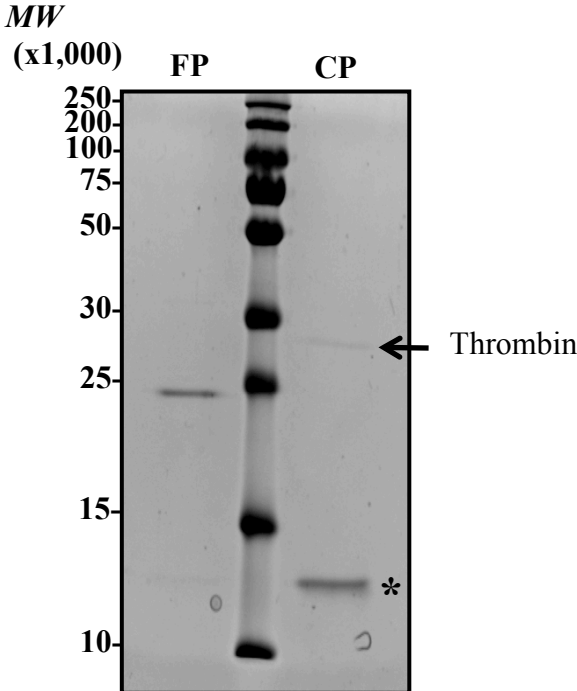
100-
70-

50-

40-

35-

25- *

Figure 7 (cont.)

C.

and that the $hHL_{442-476}$ peptide can be subsequently cleaved from the $hHL_{442-476}$-Trx protein.

To isolate the $hHL_{442-476}$ peptide from the 15.1 kDa Trx protein and the 37 kDa thrombin enzyme, a Sephacryl S-100 size-exclusion column was used. Figure 8 indicates that the fractionation of the $hHL_{442-476}$ peptide did not successfully purify the $hHL_{442-476}$ peptide from Trx and thrombin. There are also other bacterial protein contaminants with higher molecular masses that are present in fractions 40 and 45. Since the size-exclusion chromatography was unsuccessful in the isolation of the $hHL_{442-476}$ peptide, heparin-sepharose chromatography was then tried. Heparin-sepharose is a resin that mimics HSPGs that are present at the cell surface; proteins with affinity to heparin-sepharose are released by buffers with a high ionic strength. Figure 9 shows the elution of the $hHL_{442-476}$ peptide with 1.0 M NaCl, as seen by a single band. These results demonstrate that the $hHL_{442-476}$ peptide can be successfully cleaved from Trx and subsequently purified by heparin-sepharose chromatography.

3.2 Optimal Heparin-Sepharose Association of the $hHL_{442-476}$ Peptide

Having shown that the $hHL_{442-476}$ peptide can be eluted from heparin-sepharose with a high 1.0 M NaCl concentration, a step-wise NaCl gradient was used to determine the optimal amount of NaCl required to dissociate the $hHL_{442-476}$ peptide from heparin-sepharose. As shown in Figure 10A, the $hHL_{442-476}$ peptide elutes from heparin-sepharose once the NaCl gradient begins (starting at 0.1 M), with the peak of elution at 0.3 M NaCl

Figure 8: Isolation of hHL$_{442-476}$ peptide from thioredoxin protein by size-exclusion chromatography

Approximately 30 mL of pooled fractions from the nickel-sepharose column containing the hHL$_{442-476}$ peptide, Trx protein and thrombin were lyophilized, resuspended in 2 mL of 1X PBS (pH 7.0), and loaded onto a size exclusion Sephacryl S-100 column that was pre-equilibrated with 1X PBS (pH 7.0). One mL fractions were collected from the column and the presence of the hHL$_{442-476}$ peptide was analyzed by SDS-PAGE with 0.05% β-mercaptoethanol using a Tris-tricine gradient gel (4-16%) stained with Coomassie Blue. The hHL$_{442-476}$ peptide was observed in fractions (F) 40-55, denoted by "*".

Figure 8

MW
(x1,000)

F40   **F45**   **F50**   **F55**   **F60**

8.5-

3.5-

*

58
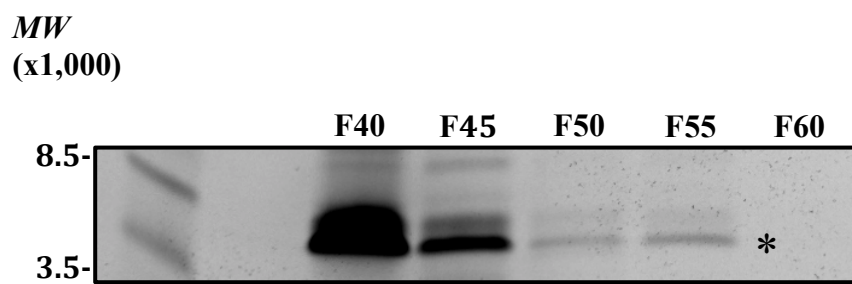
Figure 9: Isolation of hHL$_{442-476}$ peptide from thioredoxin protein by heparin-sepharose chromatography

The cleavage reaction containing the hHL$_{442-476}$ peptide, Trx and thrombin was dialyzed against 10 mM sodium phosphate (pH 7.0) then incubated with heparin-sepharose resin, as described in *section 2.1.3*. Following incubation, the resin was packed into a PD-10 column and the flow-through (FT) was collected by gravity. The column was washed with 4 CV (10 mL) of 10 mM sodium phosphate (pH 7.0) (W1-4). Following the washes, the hHL$_{442-476}$ peptide was eluted with 1.0 M NaCl. The 1 ml fractions were collected from the column and 20 µL were analyzed for the presence of the hHL$_{442-476}$ peptide by 12% SDS-PAGE and stained with Coomassie Blue. The elution of the hHL$_{442-476}$ peptide is denoted by "*".
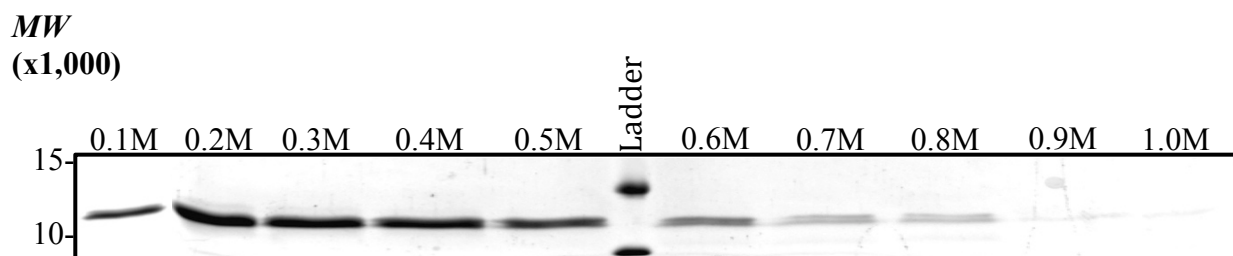
Figure 9
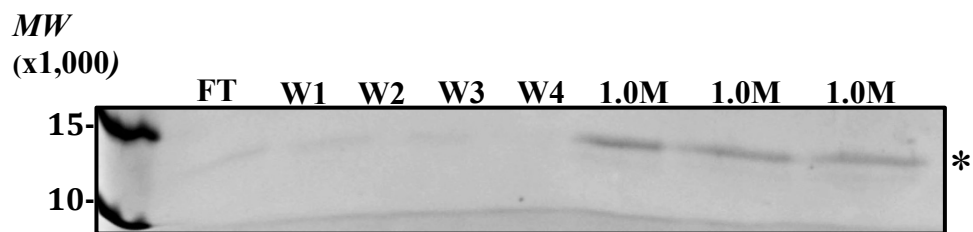
Figure 10: Optimal elution of the hHL$_{442\text{-}476}$ peptide from heparin-sepharose under reducing and non-reducing conditions

The hHL$_{442\text{-}476}$ peptide (20 μg) was incubated with 200 μL of heparin-sepharose at 4°C for 18 hours either in the absence (panels A and B) or presence (panels C and D) of 0.5% v/v β-mercaptoethanol. Following the 18 hour incubation, the heparin-sepharose beads were pelleted and the supernatant was collected, then the heparin-sepharose was treated with a step-wise NaCl gradient as described in *section 2.4.1*. Fractions were analyzed by 12% SDS-PAGE and stained with Coomassie Blue. A) Elution of hHL$_{442\text{-}476}$ peptide from heparin-sepharose under non-reducing conditions. B) Band intensities were quantified from A using ImageJ software. Individual band intensities are represented as a percentage of the total individual band intensities. C) Elution of hHL$_{442\text{-}476}$ peptide from heparin-sepharose under reducing conditions. D) Band intensities were quantified using ImageJ software. Individual band intensities are represented as a percentage of the total individual band intensities.

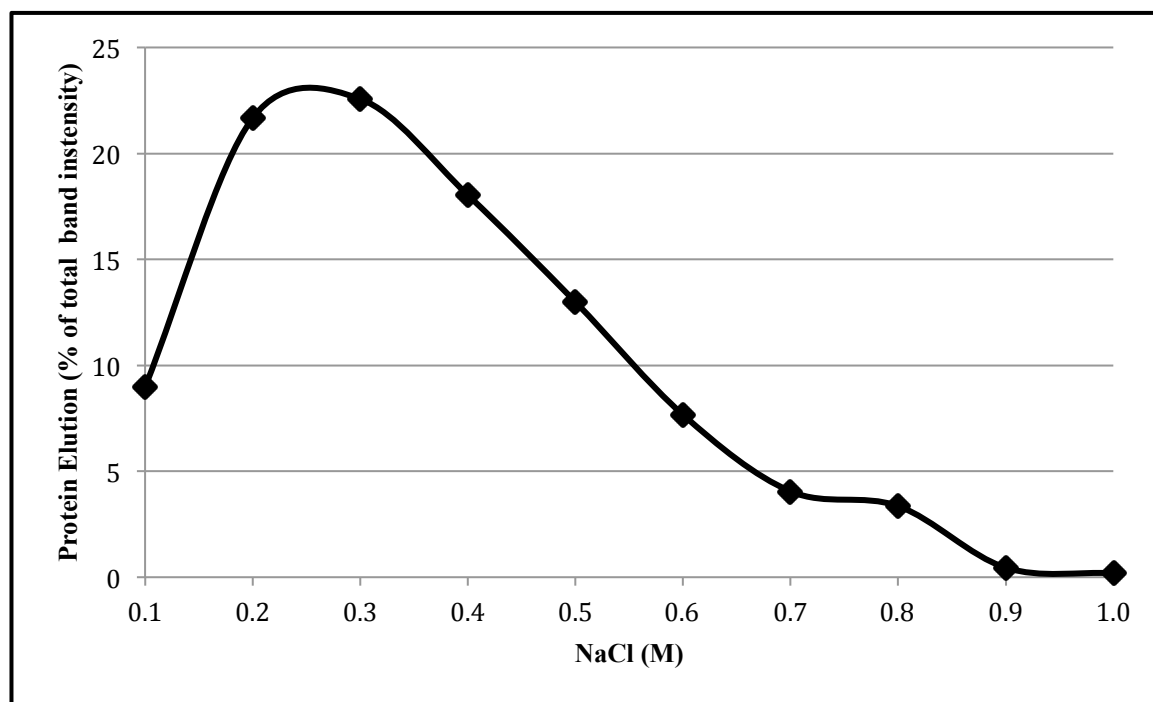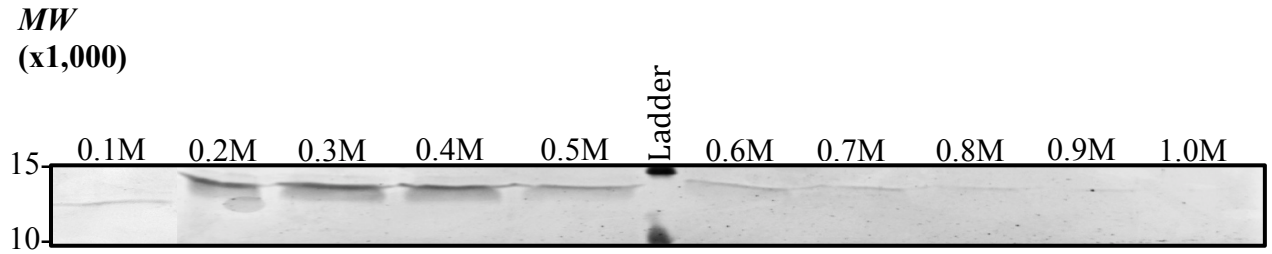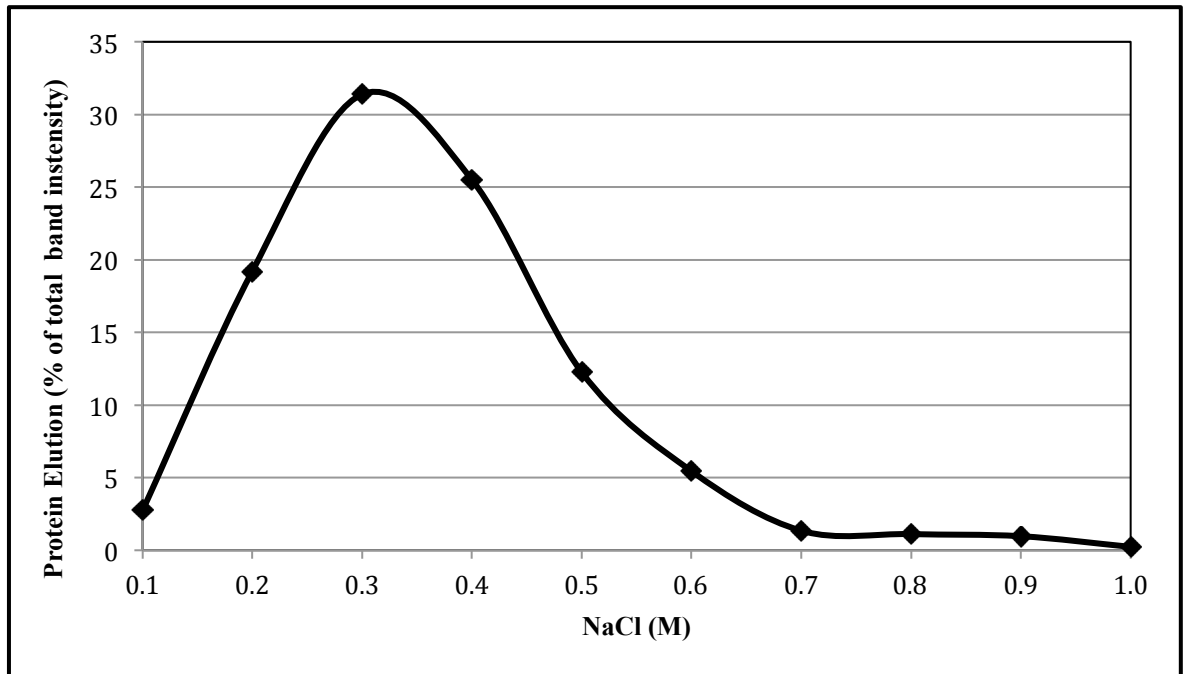**Figure 10**

A. **(–) β-mercaptoethanol**

B.

Figure 10 (cont.)

C. (+) β-mercaptoethanol

MW
(x1,000)

| 0.1M | 0.2M | 0.3M | 0.4M | 0.5M | Ladder | 0.6M | 0.7M | 0.8M | 0.9M | 1.0M |

15—

10—

D.

(Figure 10A & B). To investigate whether the two cysteine residues within the $hHL_{442-476}$ peptide form a disulfide bridge that influences the heparin-sepharose association, the assay was also conducted under reducing conditions. The data from Figure 10C & D strongly suggest that the putative disulfide bridge is not required for the optimal association of the $hHL_{442-476}$ peptide to heparin-sepharose, as indicated by the very similar elution profiles of the $hHL_{442-476}$ peptide under both reducing and non-reducing conditions.

3.3 Displacement of Cell Surface Associated Lipases by the $hHL_{442-476}$ Peptide
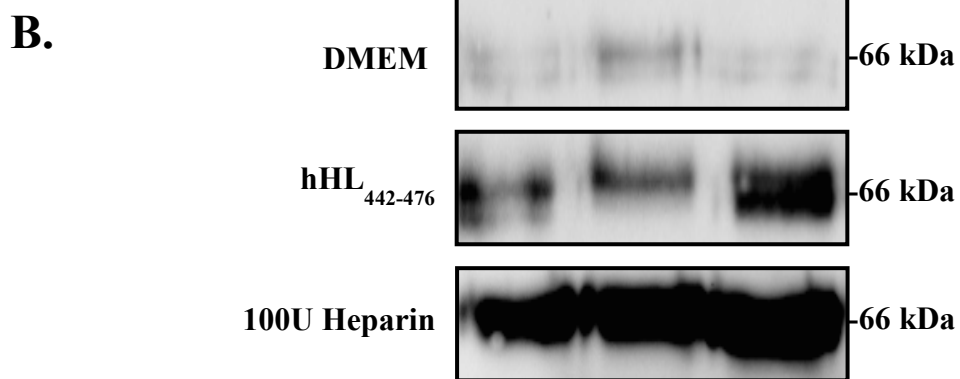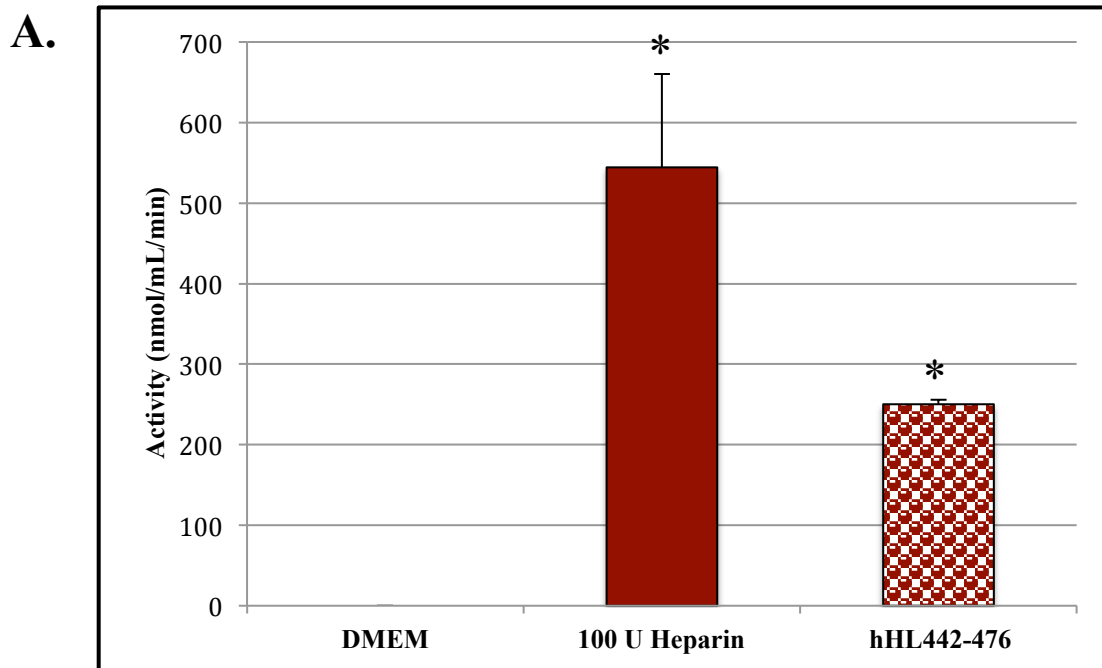
To investigate if the $hHL_{442-476}$ peptide has the ability to displace cell surface associated hHL, 200 µg/mL of $hHL_{442-476}$ peptide was incubated with HEK-293T cells overexpressing hHL at 4°C. The media were analyzed for displaced hHL lipase activity using a resorufin ester hydrolysis assay and qualitatively by immunoblot analysis. The lipase activity data for hHL in Figure 11A indicates that the $hHL_{442-476}$ peptide does displace active hHL from cell surfaces compared to the DMEM control. However, the $hHL_{442-476}$ peptide displaces less hHL from cell surfaces compared to the 100 U/ml heparin control. An immunoblot confirms the activity data, the $hHL_{442-476}$ peptide does not displace as much hHL from cell surfaces, as the 100 U/ml heparin control (Figure 11B).

In order to assess if the $hHL_{442-476}$ peptide is specific and only displaces hHL from cell surfaces, the $hHL_{442-476}$ peptide was also tested against another cell surface associated

64

Figure 11: Displacement of hepatic lipase by the hHL$_{442-476}$ peptide
Six well plates containing transfected HEK-293T cells expressing hHL were incubated for 1 hour at 4°C with plain DMEM (negative control), DMEM containing 200 µg/mL hHL$_{442-476}$ peptide, or DMEM containing 100 U/mL heparin (positive control). Following the incubation, the media and cells were collected. A) The media were analyzed for lipase activity using a resorufin ester substrate. Data are presented as the µM resorufin released per minute. n=3. *, $p<0.005$ versus DMEM control. B) Immunoblot analyses of media, using the primary anti-hHL antibody XHL3-6. Proteins from triplicate experiments were separated – one experimental sample per lane.

Figure 11

A.

B.

lipase. hLPL was chosen as a control for the $hHL_{442-476}$ peptide due to the pro-atherogenic properties hLPL possesses.[91-93] Considering the pro-atherogenic properties of hLPL,displacing active hLPL from cell surfaces with the $hHL_{442-476}$ peptide could potentially increase the risk of atherosclerosis. This is why testing the ability of the $hHL_{442-476}$ peptide to displace cell surface associated hLPL *in vitro* is necessary. When 200 µg/mL of the $hHL_{442-476}$ peptide was incubated with HEK-293T cells overexpressing myc-tagged hLPL, the activity data from the cells indicates that the $hHL_{442-476}$ peptide does displace hLPL (Figure 12). However, the hLPL activity detected by the cells treated with the $hHL_{442-476}$ does have less detectable activity when compared to the 100 U/mL heparin control.

An immunoblot of the hLPL displaced by the $hHL_{442-476}$ peptide was not obtained. The polyclonal hLPL antibody (H-53) produced immunoblots with a lot of non-specific binding to the membrane, creating unreliable immunoblots (Figure S3). A monoclonal hLPL antibody (F-1) was then tried to detect the presence of the hLPL in the media and the cells of transfected cells compared to the mock control (Figure S4). The immunoblot shown in Figure S4 indicates that the monoclonal hLPL antibody was also non-specific. Considering the difficulty encountered with obtaining an immunoblot for both the hLPL and hLPL-myc displacements, it is speculated that the amount of hLPL displaced into the media at 4°C is not enough to detect by immunoblot.

Figure 12: Displacement of lipoprotein lipase by the hHL$_{442\text{-}476}$ peptide
Six well plates containing transfected HEK-293T cells expressing myc tagged human LPL were incubated for 1 hour at 4°C with plain DMEM (negative control), DMEM containing 200 µg/mL hHL$_{442\text{-}476}$ peptide, or DMEM containing 100 U/mL heparin (positive control). Following the incubation, the media were analyzed for lipase activity using a resorufin ester substrate. Data are presented as the µM resorufin released per minute. n=3. *, p<0.005 versus DMEM control.

Figure 12
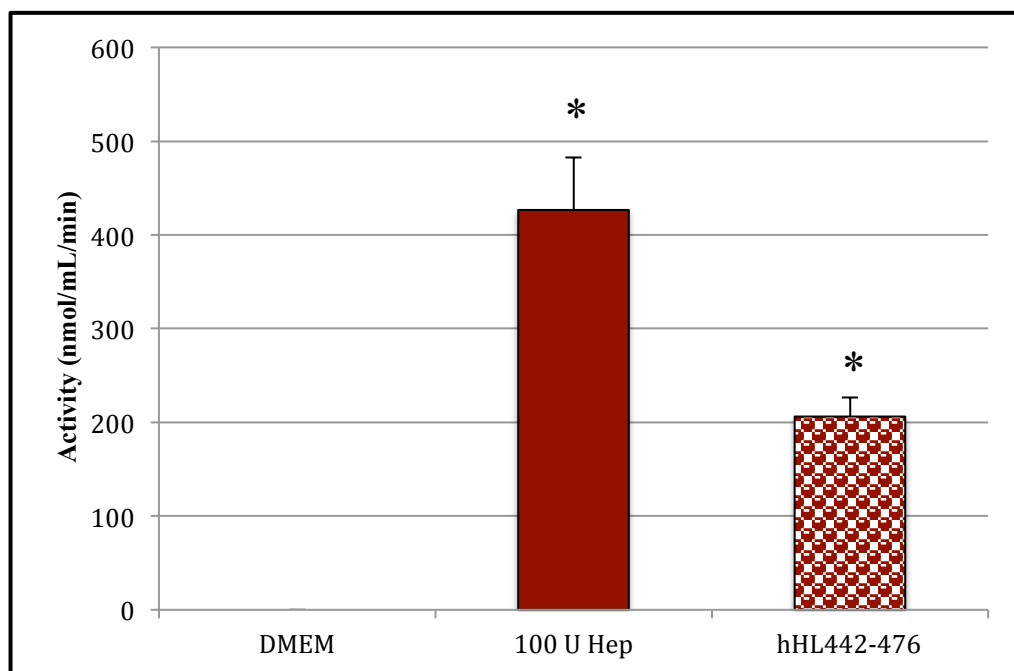
3.4 Structural Analysis of the hHL$_{442-476}$ Peptide

In an attempt to identify the structural elements of the C-terminal amino acids of hHL that account for the cell surface binding, the hHL$_{442-476}$ peptide was subjected to CD and NMR analyses. CD spectra for the hHL$_{442-476}$ peptide indicate that the peptide does not have the characteristic secondary structure of an α-helix or a β-sheet, but rather that it is relatively unstructured. As shown in Figure 13, the hHL$_{442-476}$ peptide has a single minimum at 200 nm, which is consistent with the spectrum of a peptide with a random coil secondary structure.[94] The observed lack of secondary structure in the hHL$_{442-476}$ peptide was also apparent in the presence of 250 U of heparin (Figure 13). The secondary structure of the hHL$_{442-476}$ peptide was further assessed in the presence of the structure inducing agent TFE (Figure 14). The CD spectra of the hHL$_{442-476}$ peptide in increasing concentrations of TFE show that the peptide adopts a more α-helical structure, as indicated by the minimum at 200 nm shifting towards 210 nm and resembling a double minima that are characteristic of an α–helical secondary structure.[94] Overall, the CD experiments indicate that the hHL$_{442-476}$ peptide is mostly unstructured but it does have the ability to adopt a more α-helical ordered structure.

In order to gain information about the tertiary structure of the hHL$_{442-476}$ peptide, ^{1}H-NMR was used. At 25°C, almost no peaks could be observed for the hHL$_{442-476}$ peptide within the H-N region (approximately 6.0 ppm to 10.0 ppm) (Figure 15). In an attempt to observe more peaks, the temperature was lowered to 5°C. The ^{1}H-NMR spectrum obtained resembles the spectrum for the hHL$_{442-476}$ peptide at 25°C, thus

Figure 13: Determining secondary structure of the hHL$_{442-476}$ peptide using circular dichroism in the presence and absence of heparin

The hHL$_{442-476}$ peptide (0.1 mg/mL, pH 6.5) was added to a 0.5 mm CD cuvette and analyzed with 10 scans by the CD spectrophotometer. Following the 10 scans, 250 U heparin was titrated into the hHL$_{442-476}$ peptide sample and subjected to additional 10 scans.

Figure 13
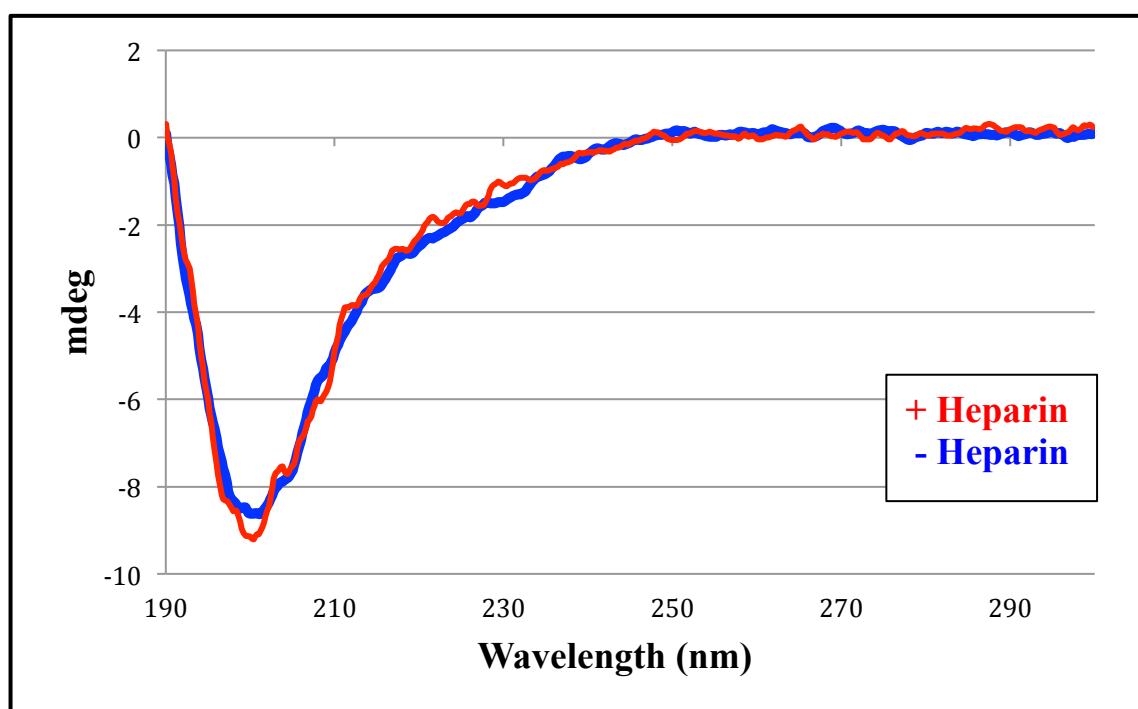
Figure 14: Analyzing the secondary structure of hHL$_{442\text{-}476}$ peptide using circular dichroism by titrating in trifluoroethanol (TFE)

The hHL$_{442\text{-}476}$ peptide (0.1 mg/mL, pH 6.5) in 5% v/v TFE was added to a 0.5 mm CD cuvette. The sample was analyzed with 10 scans of the CD spectrometer. Following the 10 scans, the TFE percentage was increased to 10% v/v and another 10 scans were recorded. This procedure was repeated as indicated until the percentage of TFE was 40% v/v.

Figure 14
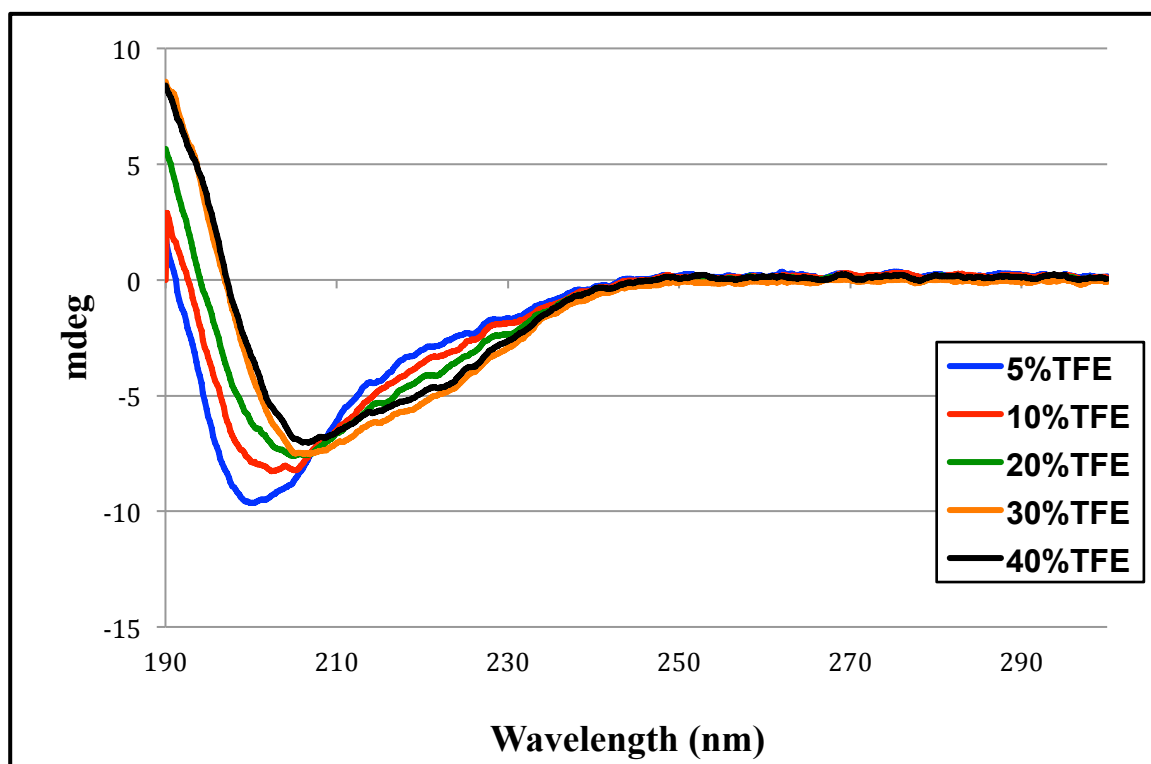
Figure 15: Determining structural components of the hHL$_{442-476}$ peptide using ^{1}H-NMR with varying temperatures

The hHL$_{442-476}$ peptide (1.5 mg) was reconstituted in 1 mL of 90% dH$_2$O and 10% D$_2$O, and analyzed at A) 25°C and B) 5°C, both with 1D water suppression (250 scans). The spectra were Fourier transformed and phase corrected. The box highlights the H-N region.

Figure 15

A.

Figure 15 (cont)

B.

indicating that the peptide does not become more structured when the temperature is decreased. To further investigate the structural components of the $hHL_{442-476}$ peptide, the structure inducing effect of TFE was assessed with the next set of ^{1}H-NMR experiments. The spectra in Figure 16A and 16B indicate th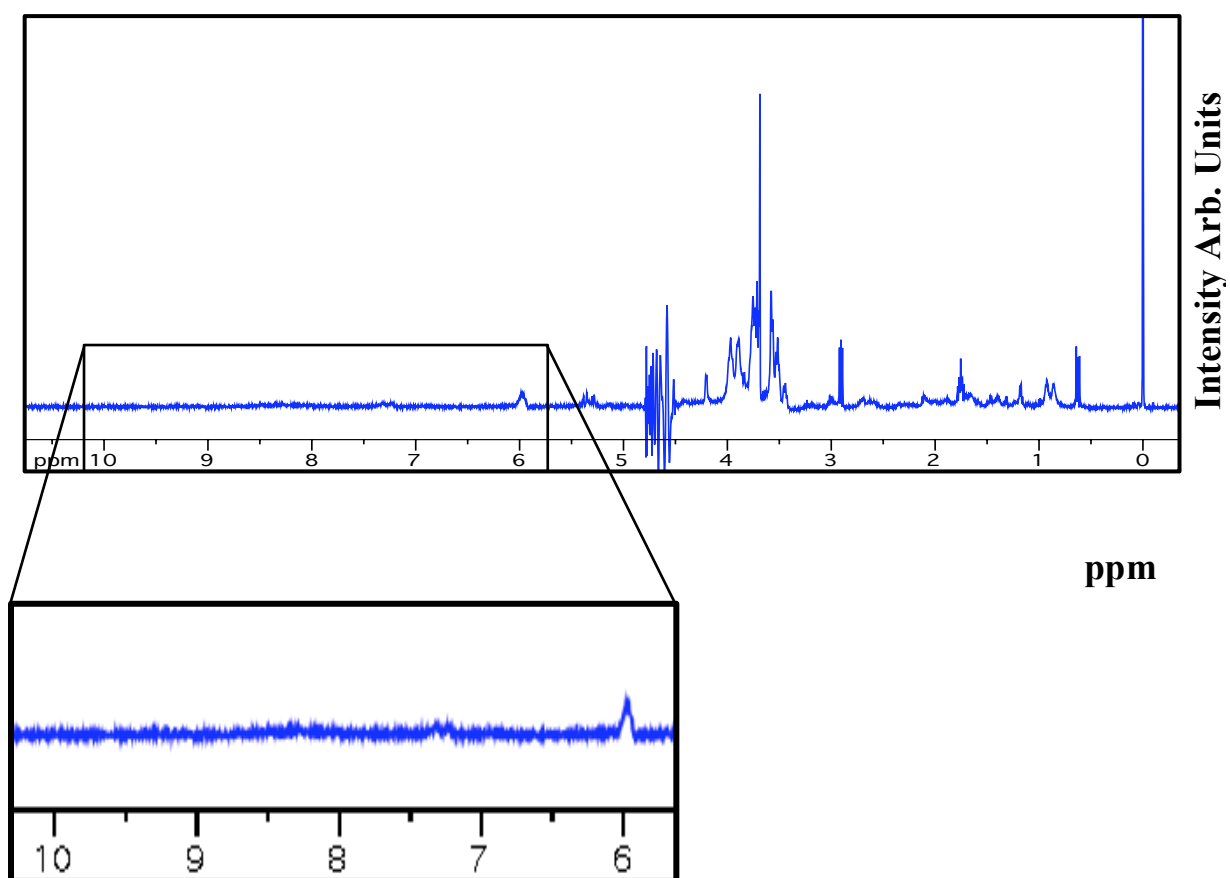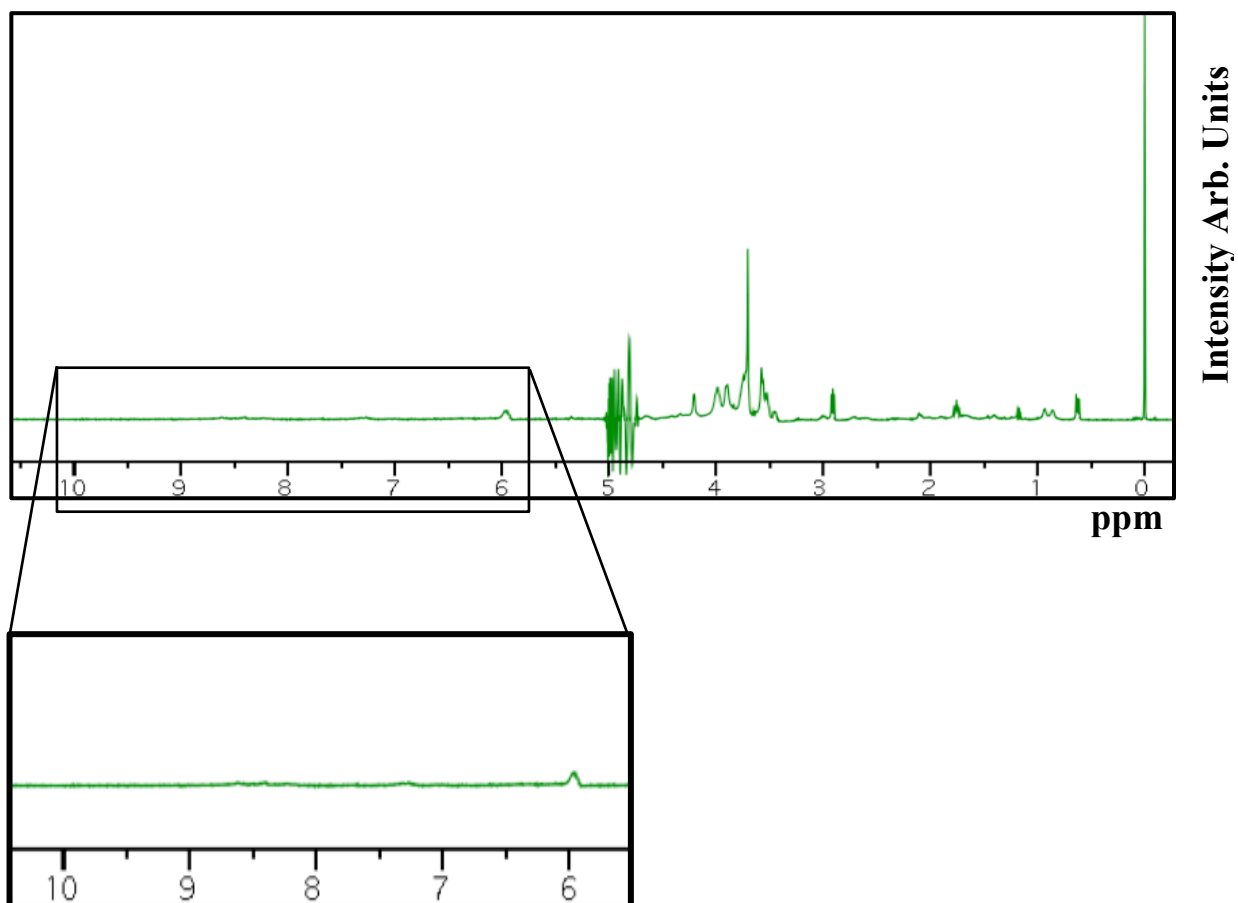at TFE (5% and 30% v/v) does not have any effect on the tertiary structure of the $hHL_{442-476}$ peptide. Figure 16C also indicates that lowering the temperature to 5°C does not have any effect on its tertiary structure. The lack of peaks in the H-N region of the spectrum is consistent with a peptide that is neither completely structured nor completely unstructured. Instead, the $hHL_{442-476}$ peptide appears to be in an intermediate state where it is interconverting between different conformations and exchanging between these different conformations on an intermediate timescale.

The addition of 250 U of heparin did induce some changes in the structural preferences of the $hHL_{442-476}$ peptide at 25°C (Figure 17). This is indicated by the increased intensity of the peaks within the H-N region, specifically at 6.00, 7.25 and 8.40 ppm (Table 4). Based on their chemical shifts, as well as their line widths, that are greater than would be expected from small molecule contaminants, the new peaks are most likely from the $hHL_{442-476}$ peptide. Their appearance indicates that heparin induces a change in the structural preferences of the $hHL_{442-476}$ peptide, thus heparin induces a greater level of defined structure in the peptide than is apparent in its absence. The two prominent peaks at 7.0 and 8.0 ppm are most likely from the heparin molecule itself.

Two-dimensional TOCSY-NMR was next used to gain information about the $hHL_{442-476}$ peptide via bond correlations, Figure 18. The crosspeaks (i.e., the peaks not on

78

Figure 16: Determining structural components of the hHL$_{442-476}$ peptide using ^{1}H-NMR with varying concentrations of TFE

The hHL$_{442-476}$ peptide (1.5 mg) was reconstituted in 1 mL of 90% dH$_2$O and 10% D$_2$O, in the presence of A) 5% v/v TFE at 25°C and B) 30% v/v TFE at 25°C. C) 30% v/v TFE at 5°C. 1D water suppressions were run for 250 scans. The resulting spectra were Fourier transformed and phase corrected. The box highlights the H-N region.

Figure 16

A.
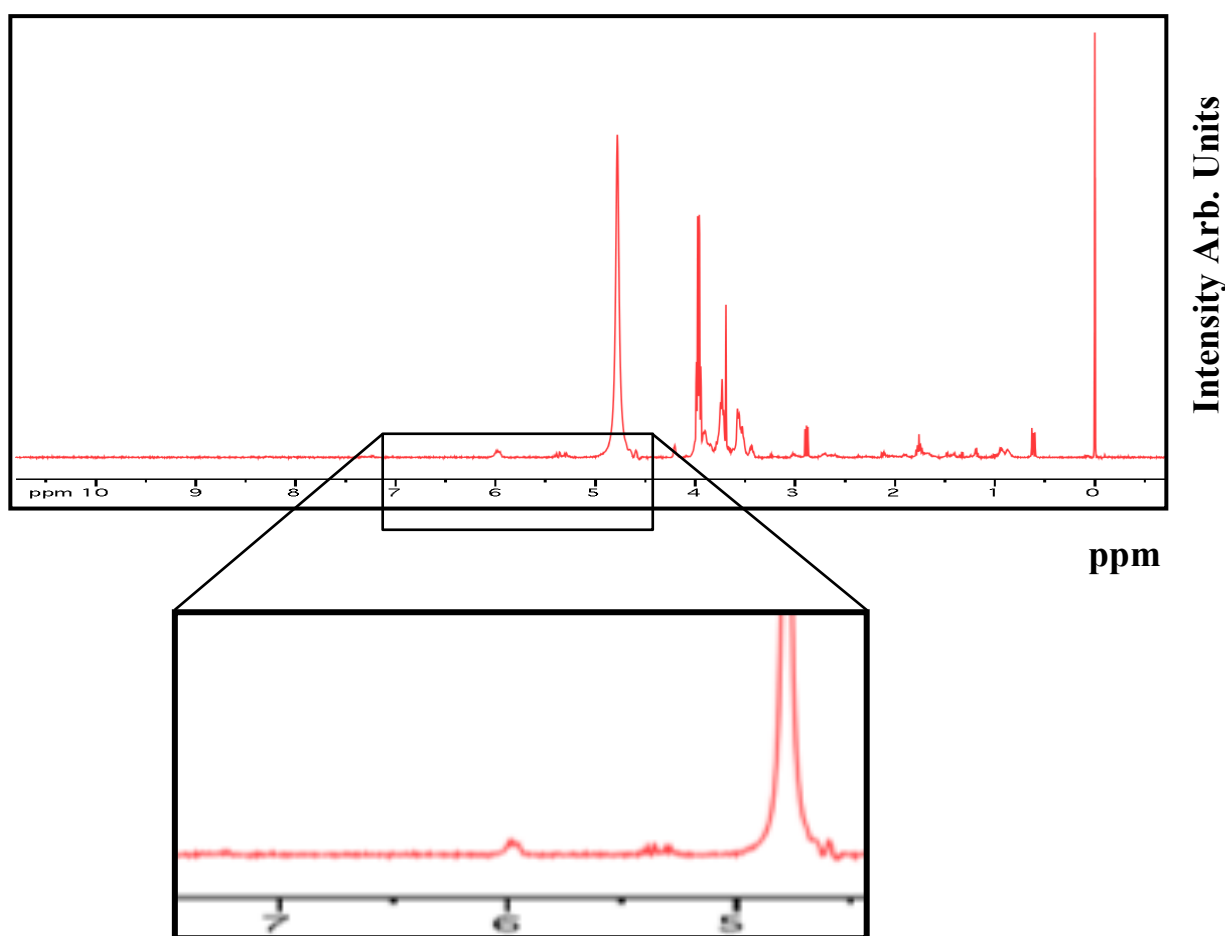
Figure 16 (cont)

B.
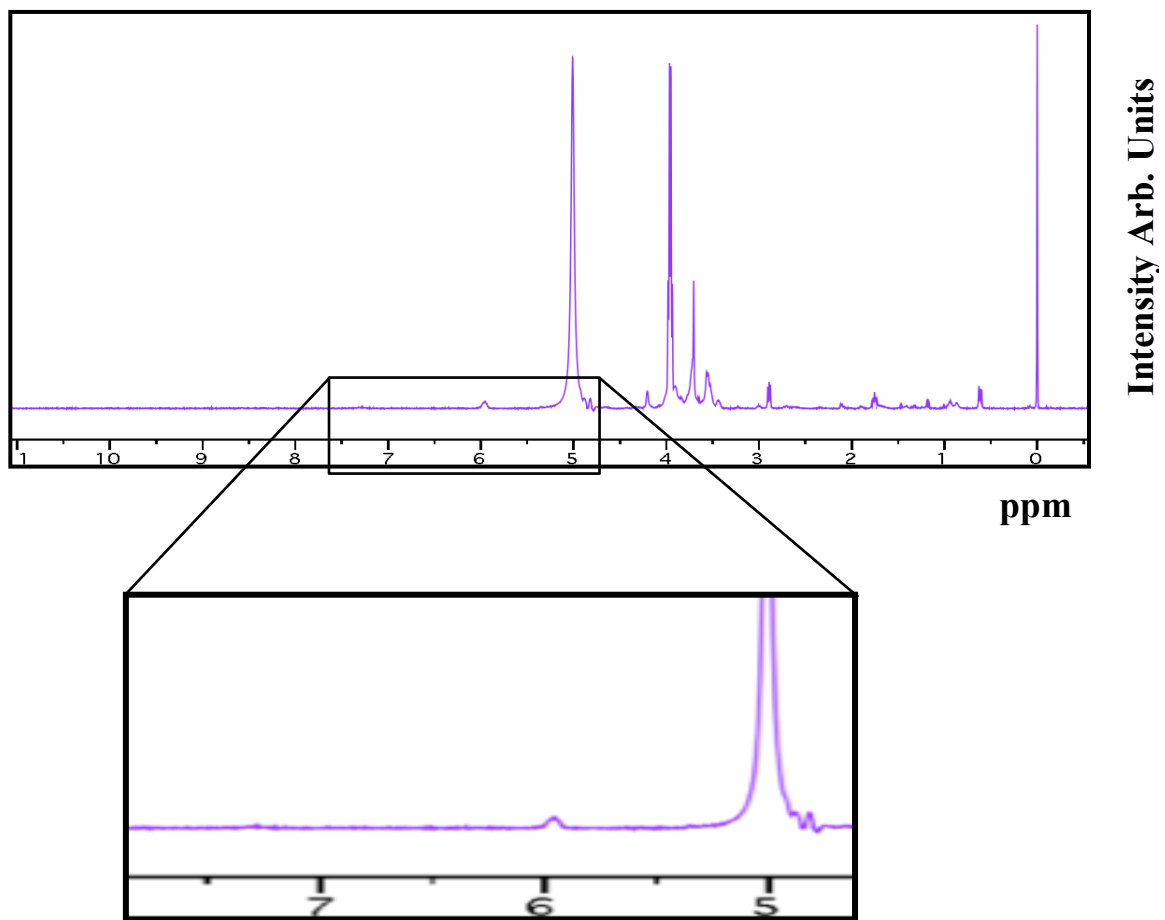
Figure 16 (cont)

C.
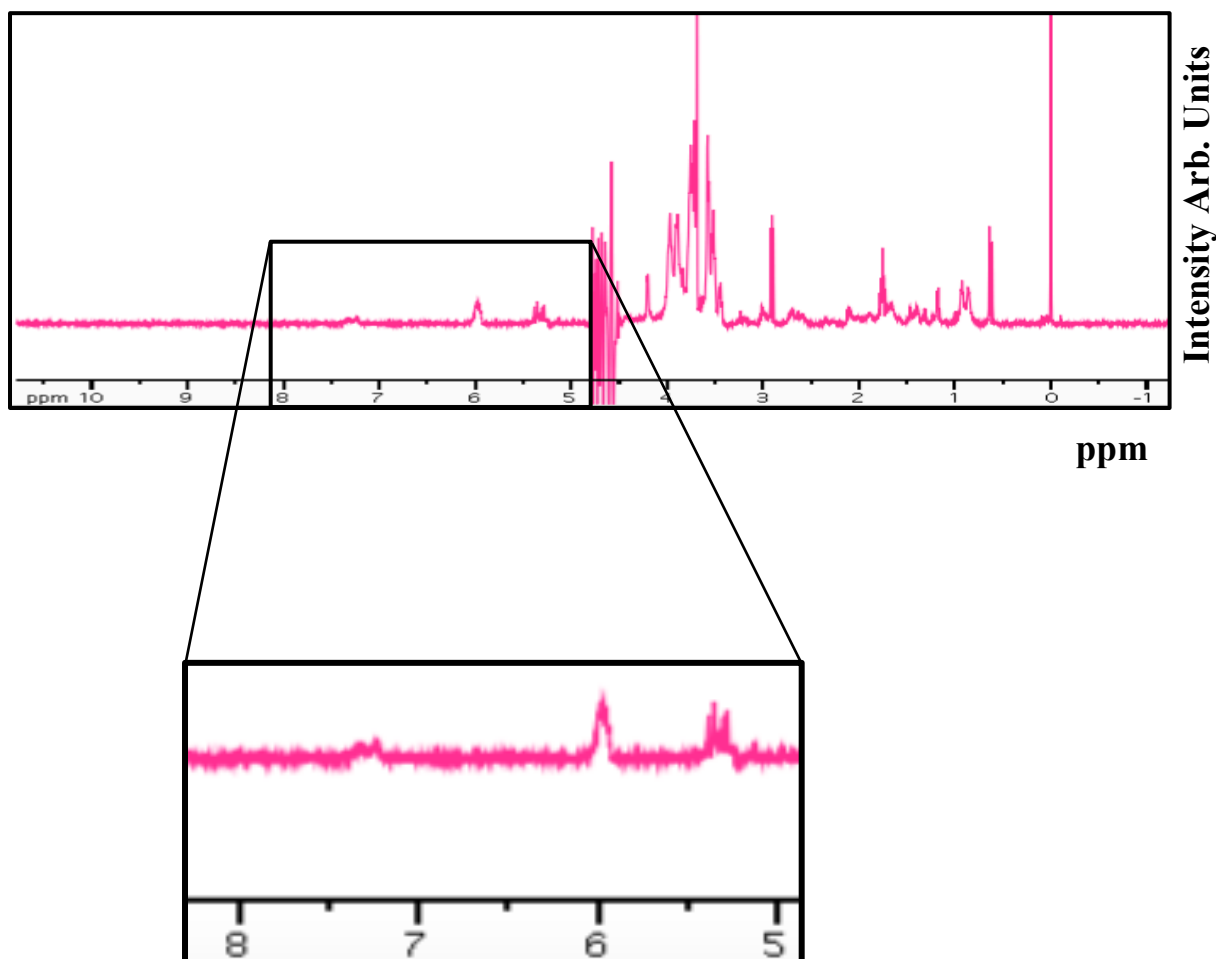
Figure 17: Determining structural components of the hHL$_{442\text{-}476}$ peptide using ^{1}H-NMR with 250 U of heparin

The hHL$_{442\text{-}476}$ peptide (1.5 mg) was reconstituted in 1 mL of 90% dH$_2$O and 10% D$_2$O. 1D water suppression was run for 250 scans at 25°C. Following the 250 scans, heparin was added to 250 U/mL and the sample was assessed for 250 scans at 25°C. The resulting spectra were Fourier transformed and phase corrected. The box highlights the H-N region, and "*" denotes the peaks that have changed upon the addition of heparin

Figure 17
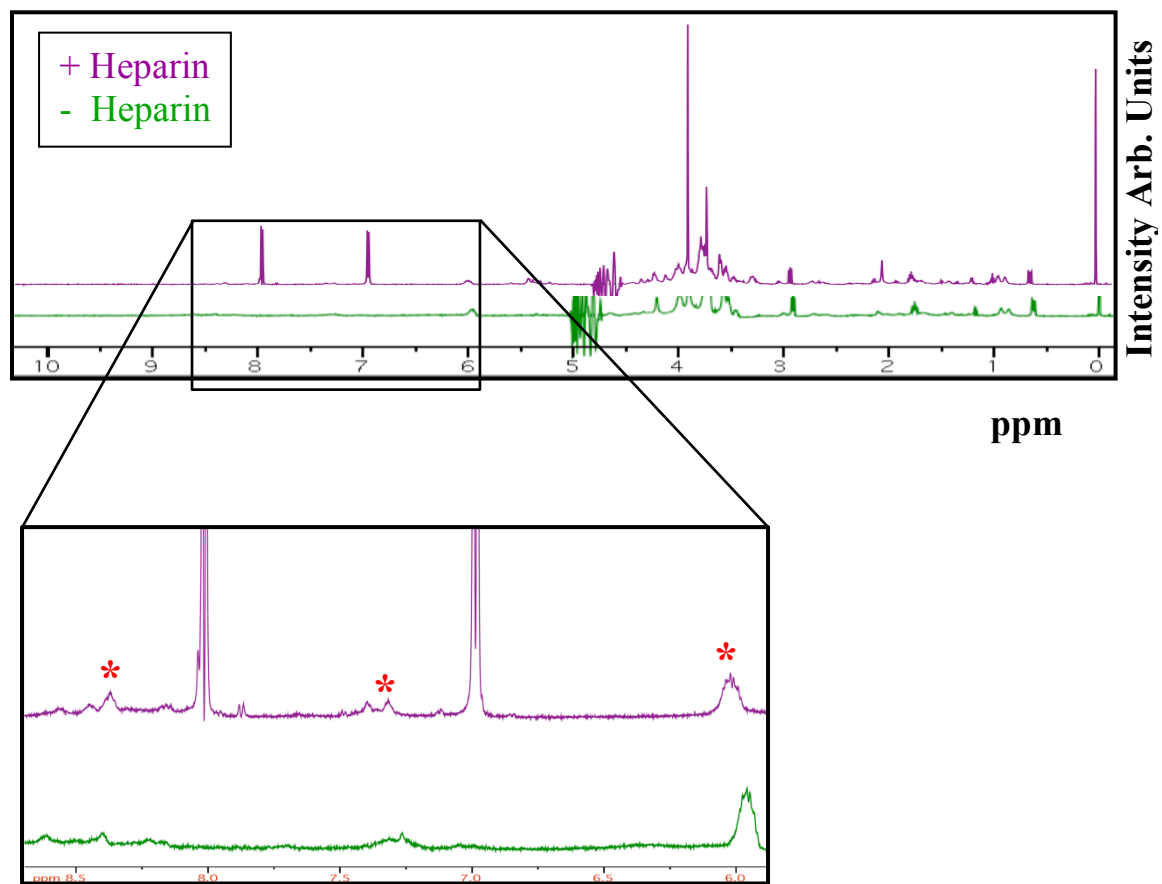
Table 4: Peaks from the H-N region of the ^{1}H-NMR of the hHL$_{442\text{-}476}$ peptide upon addition of 250 U heparin at 25°C

Molecule	Peaks (ppm)
hHL$_{442\text{-}476}$ peptide	6.00
	7.25
	8.40
Heparin	7.00
	8.00

Highlighted are the peaks that increased in both intensities and peak with upon the addition of 250 U of heparin within the H-N region of the spectrum. Also listed are the two prominent peaks due to heparin.

Figure 18: Determining structural components of the hHL$_{442-476}$ peptide using ^{1}H-NMR total correlation spectroscopy with 250 U of heparin

The hHL$_{442-476}$ peptide (1.5 mg) was reconstituted in 1 mL of 90% dH$_2$O and 10% D$_2$O. 2D TOCSY of the hHL$_{442-476}$ peptide with 250 U of heparin was run at 25°C. The resulting spectra were Fourier transformed and phase corrected. The circle highlights the peaks that are induced by heparin.

Figure 18
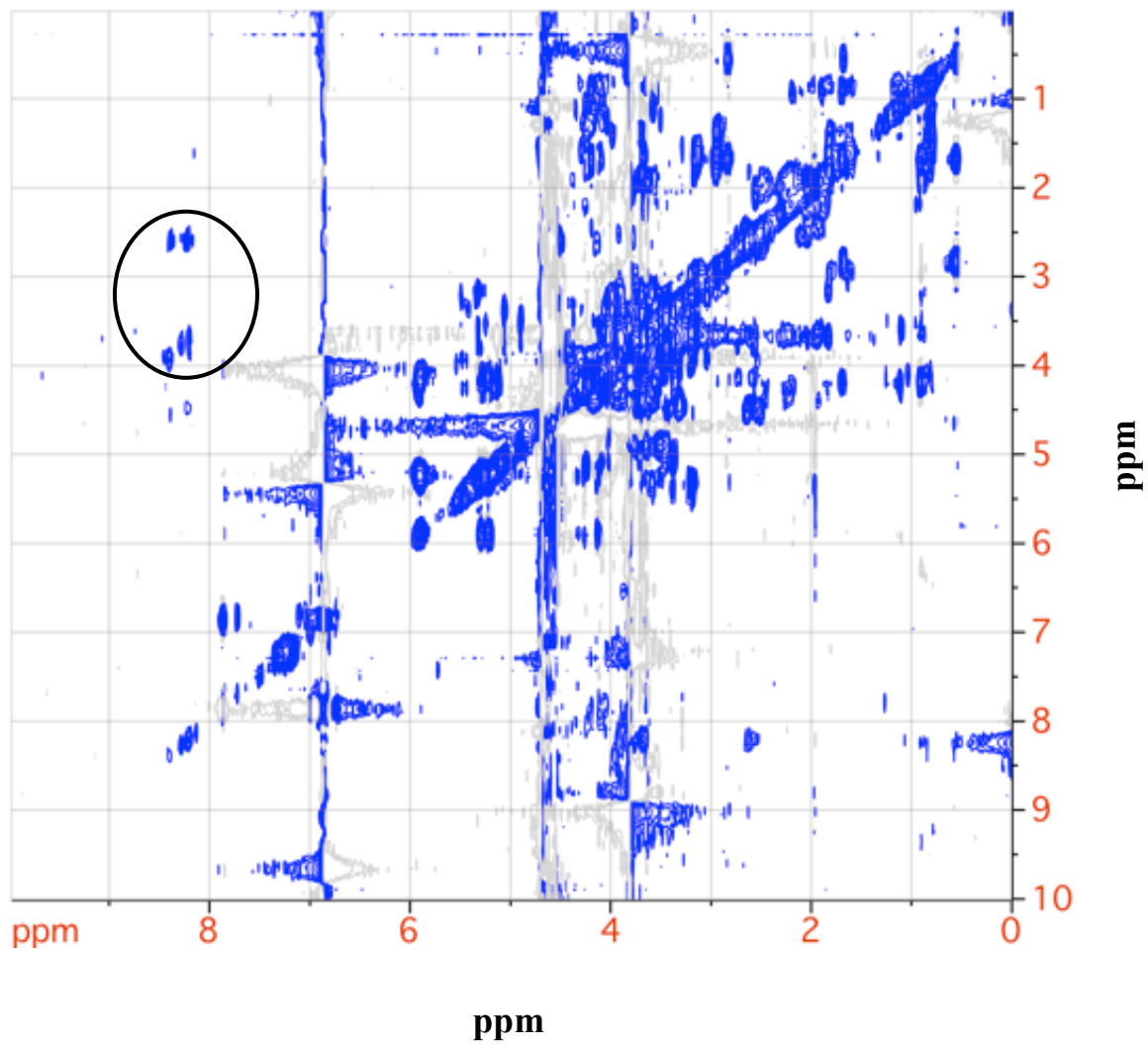
the diagonal line) in the TOCSY-NMR spectrum of the $hHL_{442-476}$ peptide indicate pairs of hydrogen nuclei within 3 covalent bonds of each other – i.e. within the same amino acid. The large line that runs down the left side of the spectrum at about 7 ppm belongs to heparin, very similar to what is observed in Figure 17. One plausible explanation for the correlation patterns highlighted within the circle is they derive from interactions that are not typical of the amino acids found in the peptide's sequence. However, arginine usually has an amide sidechain proton peak that is observed around 7.2 ppm. These highlighted peaks observed could be shifted up-field to roughly 8.2 ppm because they are interacting with heparin.

In addition to the TOSCY-NMR, an additional two-dimensional NMR method was used in an attempt to gain further information about the $hHL_{442-476}$ peptide. NOESY-NMR, which yields information about protons that are close in space although possibly distant in the amino acid sequence was used. Figure 19 shows the spectrum of the $hHL_{442-476}$ peptide in the presence of 250 U heparin. Identifying specific peaks from the spectrum is difficult due to a significant amount of background signal. However, the identification of unique peaks that are observed both in the TOCSY and in the NOESY spectra indicate that nuclei are close through bond and in space. This could represent the arginines present in the $hHL_{442-476}$ peptide, which are close through both bond and space that they may be associating with the heparin.

Lastly, a ^{15}N-labeled version of the $hHL_{442-476}$ peptide was generated for heteronuclear single quantum correlated spectroscopy (HSQC)-NMR (Figure 20), in order to obtain further structural data via correlation information between nitrogen and

Figure 19: Determining structural components of the hHL$_{442\text{-}476}$ peptide using ^{1}H-NMR nuclear Overhauser effect spectroscopy with 250 U of heparin

The hHL$_{442\text{-}476}$ peptide (1.5 mg) was reconstituted in 1 mL of 90% dH$_2$O and 10% D$_2$O. 2D NOESY of the hHL$_{442\text{-}476}$ peptide with 250 U of heparin was run at 25°C. The resulting spectra were Fourier transformed and phase corrected. The circle highlights the peaks that are induced by heparin.

Figure 19
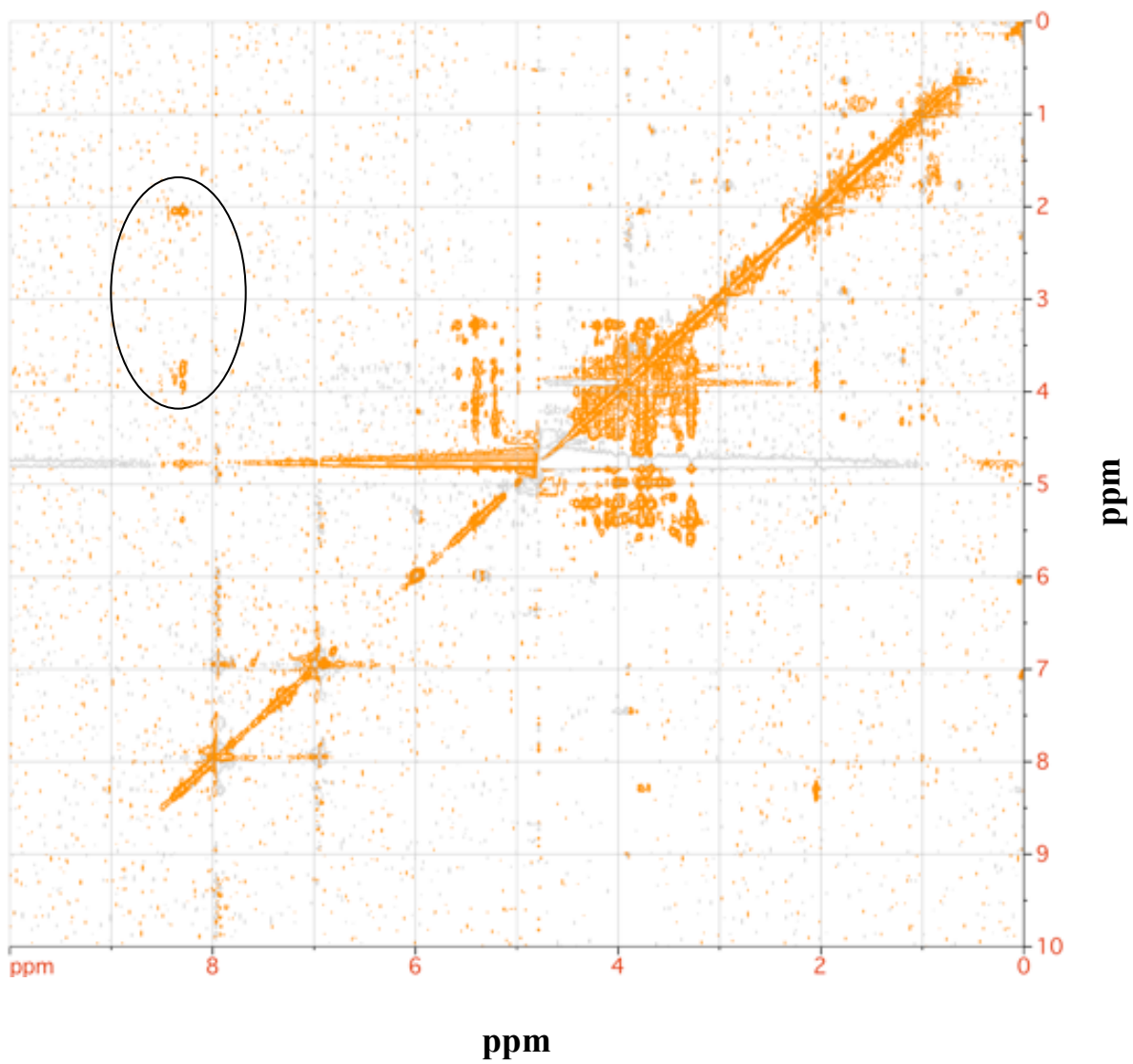
Figure 20: Determining structural components of the hHL$_{442-476}$ peptide using ^{1}H-^{15}N NMR heteronuclear single quantum correlation spectroscopy with and without heparin

The hHL$_{442-476}$ peptide (1.5 mg) was reconstituted in 1 mL of 90% dH$_2$O and 10% D$_2$O. The HSQC of the hHL$_{442-476}$ peptide was run at 25°C in the absence (blue) or presence (green) of 250 U of heparin. Highlighted is the chemical shift that occurred due to the addition of heparin.

Figure 20
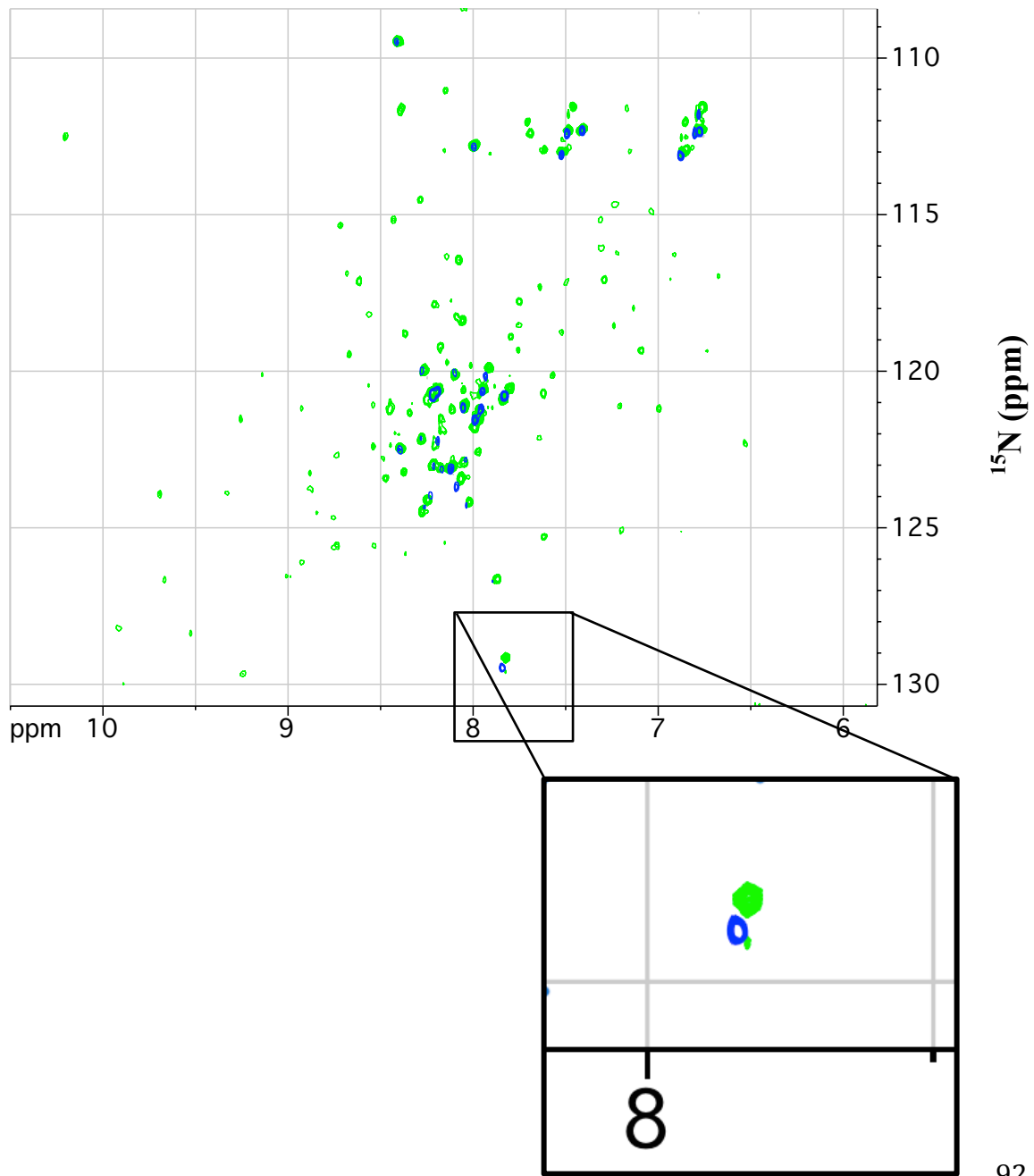
the amide protons. Figure 20 shows HSQC-NMR spectra for the $hHL_{442-476}$ peptide in the absence of the amide protons. The shows the HSQC-NMR spectra for the $hHL_{442-476}$ peptide in the absence of heparin (blue) and in the presence of 250 U heparin (green). In the absence of heparin, few peaks are observed and the backbone H-N peaks (everything except for the top, right hand side of the spectrum) are not very dispersed, indicative of an unstructured peptide. However, upon the addition of heparin, many more protein peaks are visible and they are well dispersed, representing a more structured peptide. Highlighted at the bottom of Figure 20 is a peak that is found both in the absence and presence of heparin and perhaps shifts slightly upon heparin binding. Overall, these NMR experiments indicate that in the absence of heparin the $hHL_{442-476}$ peptide does not assume a defined conformation. However, the addition of heparin appears to cause the $hHL_{442-476}$ peptide to undergo a conformational change, due to the appearance of unique chemical shifts (Table 4). Additionally, at least some of the chemical shift patterns do not correspond to what is typically observed and thus may indicate an unusual structure that the $hHL_{442-476}$ peptide uses to bind to heparin.

Chapter 4: Discussion

4.1 Functional Analysis of the hHL$_{442-476}$ Peptide

4.1.1 Optimal heparin-sepharose association of the hHL$_{442-476}$ peptide

The association of proteins to heparin-sepharose is used to characterize heparin binding proteins. The molarity of NaCl used to elute a protein from heparin-sepharose is generally proportional to the protein's dissociation constant.[95] The full-length dimer of hHL has been shown to elute from heparin-sepharose at 0.7 M NaCl.[73] In contrast, the full-length dimer of hLPL has a stronger association that requires 1.1 M NaCl for elution.[96] The biological significance of the differences in the heparin-sepharose association of the lipases remains unclear. The association of the hHL$_{442-476}$ peptide containing the major HBD[75] to heparin-sepharose was tested and was observed to be disrupted by 0.3 M NaCl, both under reducing and non-reducing conditions (Figure 10). This demonstrates that the hHL$_{442-476}$ peptide has a much lower association to heparin-sepharose compared to full-length hHL and that the putative disulfide bridge within the HL$_{442-476}$ peptide is not required for its association. Thus, the last 34 amino acids from hHL alone are not sufficient to reconstitute the heparin binding properties of full-length hHL. Although the hHL$_{442-476}$ peptide may contain the heparin binding motifs depicted in Figure 6B, the full-length hHL protein appears to require multiple HBDs to retain the optimal cell surface binding and heparin-sepharose association.

The current study is the first study to specifically investigate the last 34 amino acids of the C-terminal of hHL, although there have been other studies that have investigated the HBDs of hHL.[74,75] Brown *et al.* investigated a truncated hHL mutant, hHL_{471}, that was missing the last five amino acid residues of the C-terminal (KRKIR); they showed that it exhibited a decreased cell surface association, such that 40% of the extracellular hHL_{471} protein was released in the absence of heparin.[75] This suggests that the last 5 amino acids within the C-terminal 34 amino acids of hHL are critical for cell surface binding.

The weaker association of the $hHL_{442-476}$ peptide to heparin-sepharose could be a result of many different factors. Brown *et al*. observed that when the last 70 C-terminal amino acids from hHL were switched with the analogous sequence from mHL, the chimeric protein had a 20-fold decrease in cell surface association compared to wild-type hHL.[75] The 20-fold decrease in cell surface association indicates that the C-terminal of hHL contains a major HBD. However, Yu and Hill have also identified a HBD located in the N-terminal part of hHL.[74] This HBD might also be contributing to the optimal heparin-sepharose association observed with full-length hHL. When comparing the heparin-sepharose associations of the $hHL_{442-476}$ peptide to full-length hHL, it should be taken into consideration that active full-length hHL is understood to be in a head-to-tail homodimer conformation.[73] The head-to-tail homodimer conformation contains both the N- and C-terminal HBDs of hHL. This might account for full-length hHL having a greater association to heparin-sepharose compared to the $hHL_{442-476}$ peptide. In fact, the lower heparin-sepharose affinity is characteristic of lipase monomers. hLPL monomers

have been observed to have a lower affinity for heparin-sepharose compared to their full-length dimer, with their elution being characterized from 0.6-0.75 M NaCl.[97,98]

It is not just lipase monomers that have been observed to have lower heparin-sepharose affinities; some other species of HL also tend to have low heparin-sepharose affinities. When Breedveld *et al.* characterized the heparin binding of rat HL (rHL), they observed two protein peaks that eluted from heparin-sepharose, one at 0.3 M and 0.8 M NaCl, indicating that there are differences in the heparin binding abilities of rHL.[99] Interestingly, the NaCl molarity required for rHL is very comparable to what was observed for the $hHL_{442-476}$ peptide.

Other studies that have investigated the HBDs of hHL have also observed that small peptides encompassing putative HBDs elute from heparin-sepharose at lower NaCl concentrations.[74] When the peptide encompassing amino acids 304-323 of hHL was tested for heparin-sepharose binding ability, it was observed to elute at 0.42 M NaCl. The amino acids important for the association of this peptide are highlighted in the green box in Figure 4. Although the NaCl concentration is higher than observed for the $hHL_{442-476}$ peptide, it demonstrates that a single HBD is not sufficient to retain the association by the full-length dimer of hHL.

Additionally, the $hHL_{442-476}$ peptide has an analogous heparin-sepharose association compared to other smaller peptides that are also enriched with arginines and lysines.[100] Specifically, Caldwell *et al.* investigated the HBD of proteins using small (7-mer) peptides that were either enriched or non-enriched with arginines and lysines.[100] The enriched peptides were observed to have the highest heparin association, being eluted at

0.3 M NaCl compared to the non-enriched peptides, which were eluted with 0.15 M NaCl. This provides further evidence that the basic amino acids of the hHL$_{442-476}$ peptide do contribute to its association with heparin-sepharose.

4.1.2 Displacement of hHL from cell surfaces with the hHL$_{442-476}$ peptide

It is unclear whether hHL is active only within the circulation or when also bound to HSPGs on the cell surface. It was originally thought that lipases were only active when bound to the cell surface and that this enhanced their catalytic activity. However, recent studies have concluded that lipases are catalytically inactive when bound to the cell surface and only become active when displaced from the cell surface.[78,80] This is one reason why the ability of the hHL$_{442-476}$ peptide to displace hHL from cell surfaces was of interest (Figure 11).

The cell surface displacement studies for this thesis were conducted at 4°C. It has been previously shown that HEK-293T cells can be cultured at 4°C for up to nine days, while their cellular processes and cellular turnover dramatically slows.[101] This temperature was chosen in order to supress cell surface turnover and to get a true representation of hHL displacement without the influence of any newly synthesized protein. Figure 11 shows that the hHL$_{442-476}$ peptide does displace hHL from the cell surface into the media, and the hHL that was displaced by the hHL$_{442-476}$ peptide was catalytically active. However, the hHL$_{442-476}$ peptide did not displace as much hHL as heparin, as the amount activity was 57% lower. The lower activity and the decreased

amount of hHL displaced to the media by the hHL$_{442-476}$ peptide could be a result of many factors, including the peptide concentration, incubation time, and temperature.

The optimal amount of hHL$_{442-476}$ peptide for treatment remains to be determined. The 200 μg/mL of the hHL$_{442-476}$ peptide used may not be enough to optimally displace hHL from cell surfaces. It is known that hHL is displaced from cell surfaces by various proteins, such as HDL.[80] As a comparative control, it would be interesting to test the displacement of hHL by the hHL$_{442-476}$ peptide compared to HDL mediated displacement.

The optimal incubation time also needs to be determined for this displacement assay. For this thesis, the incubation time was 1 hour. However, to get a better representation of the ability of the hHL$_{442-476}$ peptide for displacing hHL from cell surfaces, various times points should be taken. Observing the amount of hHL displaced over time will help determine if the hHL$_{442-476}$ peptide is transiently displacing hHL from the cell surface.

Another parameter that needs to be optimized is the temperature. The 4°C temperature is good for slowing cellular turnover. However, it is not physiologically relevant. Once both the optimal hHL$_{442-476}$ peptide concentration and incubation time are determined, this experiment needs to be conducted at 37°C. Optimizing this experiment at 37°C is also important for future cholesterol efflux experiments.

In order to make better inference about the ability of the major HBD within the hHL$_{442-476}$ peptide, a scrambled peptide could have been employed. This would provide valuable information not only about the ability of the hHL$_{442-476}$ peptide but also about the significance of the arrangement of the positively charged amino acids located within the

HBD of hHL. This would serve as a more significant control than the plain DMEM media that was used in this experiment. A recombinantly expressed scrambled peptide would be ideal. However, it is possible that difficulty may arise with its purification, similar to that encountered with the $hHL_{442-476}$ peptide.

4.1.3 Displacement of hLPL from cell surfaces with $hHL_{442-476}$ peptide

To determine if the $hHL_{442-476}$ peptide specifically displaces hHL or if it displaces other cell surface associated lipases, the displacement assays were conducted with HEK-293T cells expressing myc-tagged hLPL. Figure 12 shows the activity data from the HEK-293T cells expressing myc-tagged hLPL treated with the $hHL_{442-476}$ peptide. From the activity data alone, it appears that the $hHL_{442-476}$ peptide does displace hLPL-myc from cell surfaces. The percent of total heparin releasable hLPL-myc and hHL activity by the $hHL_{442-476}$ peptide treatment are very similar – (36% and 43%, respectively), suggesting that the peptide displaces both lipases equally. However, both hLPL and hHL are not only associated with HSPGs on the cell surface, they can also be associated with the LDL receptor-related protein 1 (LRP1).[102,103] The lipases have a "bridging" function that allows for the capture of lipoproteins and brings them within close proximity of the LRP1. Once close enough, LRP1 can internalize the lipoproteins in a fashion similar to the LDL receptor.[104,105] hHL has been observed to aid in the uptake of remnant lipoproteins both via HSPG- and LRP-dependent pathways.[106] The C-termini of both hLPL and hHL are believed to contain the binding site for LRP1.[102,107] The putative

99

binding site within hHL is located within amino acids 378-448.[108] The hHL$_{442-476}$ peptide

retains seven of these amino acids, and thus it is possible that the hHL$_{442-476}$ peptide might

displace hLPL and hHL associated with LRP1 because HEK-293T cells are known to

express LRP1.[109]

4.2 Structural Analysis of hHL$_{442-476}$ Peptide

4.2.1 Secondary structural analysis of the hHL$_{442-476}$ peptide

Considering that the data suggest the hHL$_{442-476}$ peptide does displace both hHL

and myc-tagged hLPL, structural data could be useful, not only for identifying the HBD

of hHL, but also for designing peptides with improved binding affinity. To obtain

information about the secondary structure of the hHL$_{442-476}$ peptide, it was first subjected

to analysis by CD using the far-UV spectral region that includes 190-250 nm.[95,110] The

CD spectrum shown in Figure 13 (Blue) suggests that the hHL$_{442-476}$ peptide is in a

random coil in the absence of heparin. This is indicated by the minimum ellipticity

observed at 200 nm. However, this is not an uncommon observation when analyzing the

HBD of larger heparin binding proteins.[111,112] Tyler-Cross *et al*. observed that when

analyzing peptides of the heparin binding protein antithrombin III, a peptide

encompassing a low-affinity site for heparin binding (KSSKLVSANRLFG) has a random

coil secondary structure.[112] However, when the peptide having the high-affinity site for

heparin (KFAKLAARLYRKA) was tested, it did have the ability to adopt an α-helical

secondary structure in the presence of heparin. Heparin binding-induced α-helical

100

structuring was not observed in the CD data for the hHL$_{442-476}$ peptide, as its secondary structure remained as a random coil in the presence of heparin (Figure 13, Red). Mok *et al.* made a similar observation with the heparin binding protein amyloid precursor protein (APP), and peptides containing the APP HBDs.[111] They tested multiple peptides and the addition of heparin only changed the secondary structure of one of them (APP416-447), which adopted a more α-helical secondary structure.[111]

While heparin did not induce a change in the secondary structure of the hHL$_{442-476}$ peptide, the secondary structure inducing agent TFE induced an α-helical secondary structure, with the CD minimum, which was at 200 nm, shifting and changing to become two minima at 210 and 220 nm (Figure 14, Black). Caution must be used when making inferences about the hHL$_{442-476}$ peptide's propensity to adopt a different secondary structure in the presence of TFE. The mode of action of TFE is unknown. However, it is hypothesized that TFE enhances hydrogen bond formation in the protein and/or it lowers the dielectric value of water to allow for electrostatic interactions to occur.[113-115]

hPL has been shown to have a two domain structure with the N-terminal region having an α/β structure and a central β-sheet, and the C-terminal region consisting of a β-sandwich, made by two layers of β-sheets, with four antiparallel strands.[70] hHL is thought to have a structure similar to hPL. However, residues 442-476 of hHL cannot be aligned with the C-terminal residues of hPL. Thus, the secondary structure of hPL cannot be used to make secondary structure inferences for the hHL$_{442-476}$ peptide. However, there are bioinformatic tools that can predict the secondary structure of a protein based on its

amino acid sequence. PredictProtein was employed to elucidate secondary structure information about the hHL$_{442\text{-}476}$ peptide.[116] PredictProtein predicted that the hHL$_{442\text{-}476}$ peptide has no defined secondary structure (data not shown). Thus, further studies were employed to provide information about the interaction between the hHL$_{442\text{-}476}$ peptide and its association with heparin, as it is crucial for elucidating structural information about the hHL$_{442\text{-}476}$ peptide and thus, the C-terminal region of hHL.

4.2.2 Tertiary structural analysis of the hHL$_{442\text{-}476}$ peptide

After investigating the secondary structure of the hHL$_{442\text{-}476}$ peptide, ^{1}H-NMR was used to determine the overall structure of the hHL$_{442\text{-}476}$ peptide. As seen in Figure 15A, at 25°C the hHL$_{442\text{-}476}$ peptide has few peaks within the H-N region, most likely indicating that the hHL$_{442\text{-}476}$ peptide is switching between conformations.[117] Even when the temperature was lowered to 5°C, the ^{1}H-NMR spectrum did not reveal any tertiary configuration (Figure 15B). Based on the CD analyses, TFE induced an α-helical structure in the hHL$_{442\text{-}476}$ peptide, but this was not duplicated in the ^{1}H-NMR spectra obtained (Figure 16). Lastly, the combination of TFE and low temperature did not induce any observable structuring (Figure 16C). In agreement with my observation that TFE does not induce structural changes within the hHL$_{442\text{-}476}$ peptide, Yu and Hill obtained similar findings when they investigated the association of peptides containing the HBDs of hHL with heparin.[74] They observed that the (secondary structure inducer) TFE did not have any effect on the heparin association of the various hHL peptides tested. Thus, the

structural effect of TFE does not influence the association the HBDs of hHL to heparin-sepharose.

To further investigate the tertiary structure of the hHL$_{442-476}$ peptide, resonance data were collected for the hHL$_{442-476}$ peptide in the presence of heparin. The spectra in Figure 17 show that heparin did induce the appearance of more hHL$_{442-476}$ peptide peaks within the H-N region. The two large peaks at 7.0 and 8.0 ppm are likely heparin itself, due to their peak width and height. The signals are too narrow to be coming from a more ordered hHL$_{442-476}$ peptide. Considering that heparin is a highly sulfated molecule and that even its molecular mass is an estimate between 12-30 kDa, the published ¹H-NMR spectra for heparin are highly varied.[118-120] This variation depends upon the source, batch, and if there are any impurities present with the heparin. Table 3 lists the chemical shifts of the peaks induced by heparin. Judging from the correlation patterns observed in the TOCSY and NOESY spectra, the new peaks could possibly be from the association of basic amino acids such as arginines and lysines with heparin.[121]

There are various other mimetic peptides that have been synthesized for the purpose of raising levels of preβ-HDL in the circulation. However, they are designed to mimic apolipoproteins rather than to mimic hHL. The tertiary structures of several apolipoproteins are known.[23,122,123] The mimetic peptides based on apolipoproteins are designed to contain amphipathic α-helices that include various positively charged amino acids.[124,125]

The D-4F peptide, a mimetic of apoA-I, can reduce lesions in both apoE-deficient and LDLR-deficient mice.[126] In human trials, the D-4F peptide increased the anti-

inflammatory properties of HDL.[127] However, the D-4F peptide has low bioavailability and no recent studies have been published.

Perhaps the most recent mimetic peptides being tested for combating CVD are mimetic peptides for apoE. These peptides also have an amphipathic α-helical structure.[124,128] One of the peptides that showed great promise *in vitro* was ATI-5261, because it promoted preβ-HDL formation and RCT.[129] However, when the peptide was tested *in vivo*, it increased muscle toxicity in wild-type C57BL/6 mice, while also increasing TG levels.[130] These side effects were the consequence of aromatic phenylalanine residues on the polar face of the peptide, along with the large number of positively charged arginines. With this information in mind, a new non-toxic mimetic peptide (CS-6253) was designed.[131] This peptide has the ability to form preβ-HDL-CS-6253 particles that can accept cholesterol and deliver cholesterol to liver cells *in vitro*.[130] Even though these studies demonstrate the use of mimetic peptides for combating CVD, they do not come without their own pitfalls. These mimetic peptide therapies focus on the use of apolipoproteins as the vehicle for directly increasing preβ-HDL, unlike the hHL$_{442-476}$ peptide, which aims to increase hHL activity and possibly indirectly raising preβ-HDL. Nevertheless, the *in vivo* information gained from the apoE studies could be applied to the *in vivo* use of the hHL$_{442-476}$ peptide. Determining the structure of the hHL$_{442-476}$ peptide is not only important for elucidating the HBD of hHL, but also for improving the efficacy and reducing potential toxicity of the therapeutic hHL$_{442-476}$ peptide.

4.3 Troubleshooting the Purification of the hHL$_{442-76}$ Peptide

Although a minor portion of the results was the purification of the hHL$_{442-476}$ peptide, it still required just as much optimization as the functional assays. The expression of Trx fusion proteins commonly results in a high yield of functional protein.[131] Trx fusion proteins tend to adopt their proper tertiary conformation because of their ability to be expressed in *E. coli* in a soluble form that is not trafficked into inclusion bodies.[131] The Trx protein also provides proper disulfide bridge formation of the expressed protein.[132,133]

In attempts to separate the hHL$_{442-476}$ peptide from Trx and thrombin, size-exclusion chromatography was first used. In theory, the 7.9 kDa hHL$_{442-476}$ peptide should be easily separated from the 12.1 kDa Trx protein and the 37 kDa thrombin. However, the unsuccessful separation could be due to overloading of the Sephacryl-100 column, which would result in the column becoming saturated with proteins and the proteins eluting together. This could also be a consequence of the saturation of nickel-sepharose in the step prior to the size-exclusion. Nickel-sepharose chromatography is usually sufficient to purify a recombinately expressed protein from all of the non-specific bacterial proteins.[134] However, when overloaded with protein, nickel-sepharose fails to achieve proper separation. This would leave bacterial proteins present that could be affecting the separation of the hHL$_{442-476}$ peptide on size exclusion chromatography. To account for the overloading of both the nickel-sepharose and size-exclusion columns, the amount of bacterial culture used for protein purification was reduced. However, it did not result in the hHL$_{442-476}$ peptide being successfully purified by size-exclusion (Figure S5). This is

105

why heparin-sepharose was then employed for isolation of the $hHL_{442-476}$ peptide. When the $hHL_{442-476}$ peptide is used for *in vivo* studies, the best way to optimize its purification would be to use fast protein liquid chromatography. This would allow the $hHL_{442-476}$ peptide to be purified in an efficient manner that would decrease the time required to purify large amounts of $hHL_{442-476}$ peptide. This method would also cut down on the impurities that co-elute with the $hHL_{442-476}$ peptide. If the $hHL_{442-476}$ peptide can be purified via this method, it possibly could produce a concentrated sample that is required for structural analysis via NMR.

4.4 Perspectives and Future Directions

The role that hHL plays in the development of atherosclerosis still remains to be clarified. Numerous studies suggest hHL has a pro-atherogenic function,[62,65,135] while other studies suggest it has an anti-atherogenic function.[57,58,60,61] Considering these conflicting studies on whether hHL is pro- or anti-atherogenic appears to vary upon the model system used. The controversy of whether hHL is pro- or anti-atherogenic not only holds true for animal models, but conflicting results also exist from human studies. Some of these studies suggest that high levels of active hHL correlate to higher levels of smaller, denser LDL particles, which are considered to be pro-atherogenic in nature.[134,136] On the other hand, there have been studies suggesting that a deficiency of hHL leads to a pro-atherogenic phenotype, due to an abnormally high TG content of the LDL particles.[137,138] Subjects with a deficiency of hHL, together with genetically low levels of

106

CETP, have been observed to exhibit an increased the risk of CVD.[139] In addition, decreased hHL activity has been associated with buoyant LDL particles and higher HDL_2-C,[140] which is considered to represent an anti-atherogenic phenotype. With all of this in mind, hHL is very important in lipoprotein metabolism.[141-143] However, with the number of contradictory studies, much more needs to be clarified about its function in atherosclerosis.

The primary aim of this study was to generate a mimetic peptide for hHL with the goal of displacing active hHL from cell surfaces. The purpose of this aim was to generate a tool that could release active hHL from cell surfaces and one that might have the potential to generate more preβ-HDL within the circulation and improve RCT. The second aim was to reveal structural features of the $hHL_{442-476}$ peptide to provide novel information about the C-terminal structure of hHL, considering the lack of knowledge regarding its structure. Investigating the function and structure of the $hHL_{442-476}$ peptide has provided initial evidence that the use of mimetic peptides can displace cell surface associated hHL. The next step is to extensively test the $hHL_{442-476}$ peptide *in vivo* for its ability to displace cell surface associated hHL to improve cholesterol efflux, RCT, and CVD outcomes using animal models. Perhaps the most widely used atherosclerosis mouse models are the apoE knockout (apoE-/-) and the LDL receptor knockout mice. The apoE-/- mice spontaneously develop atherosclerosis even when fed a standard chow diet.[64] On the other hand, the LDL receptor knockout mice require dietary cholesterol to develop atherosclerosis.[59] This is not the only difference between the two models: the apoE-/- mice tend to have lower circulating HDL-C compared to wild-type mice.[64,144]

Conversely, LDL receptor knockout mice tend to have slightly elevated HDL-C compared to wild-type mice, and a lipoprotein profile that resembles that of humans, with cholesterol mainly confined to the LDL fraction.[59] This may be a good background model to study the hHL$_{442-476}$ peptide on hHL displacement and RCT *in vivo*. To appropriately test the hHL$_{442-476}$ peptide, the LDL receptor knockout mice must also be deficient in mHL but expressing hHL. This is due to the differences in the cell surface association between hHL and mHL.

The data obtained for elucidating the tertiary structure of the hHL$_{442-476}$ peptide at best showed that the peptide adopts conformational changes in the presence of heparin. HL exhibits a significant association to lipid emulsions (such as Intralipid);[78] however, the NMR studies for this thesis were conducted in aqueous environments. Thus, future NMR experiments could be conducted with the hHL$_{442-476}$ peptide in the presence of lipid micelles. If future structural experiments elucidate the tertiary structure of the hHL HBD, both in the absence and presence of heparin, it would provide useful information that can be used toward designing structural modifications to the peptide that may improve hHL displacement and possibly lead to better CVD therapies.

4.5 Overall Conclusion

This research has provided a foundation for the use of mimetic peptides for the displacement of lipases from cell surfaces. Through the functional analysis of the hHL$_{442-476}$ peptide, it can be concluded that it has a weak association to heparin-sepharose but it

exhibits the ability to displace cell surface associated lipases. The weak heparin-sepharose association could be a desirable property of the hHL$_{442-476}$ peptide, such that it may only displace some (but not all) of cell surface bound lipases, thus leaving some lipase to carry out bridging functions and associations with LRP1. In conjunction with the structural analysis, it can be concluded that the hHL$_{442-476}$ peptide is relatively unstructured but specific amino acids appear to interact with heparin. Further analysis of the structure of the hHL$_{442-4476}$ peptide needs to be conducted in order to draw any conclusion about the potential tertiary structure of the major HBD of hHL.

Chapter 5: References

1.   Alwan, A., Armstrong, T., Bettcher, D., Branca, F., Chisholm, D., Ezzati, M., Garfield, R., MacLean, D., Mathers, C., Mendis, S., Poznyak, V., Riley, L., Tang, K C., Wild, C. (2011) Global status report on noncommunicable diseases 2010. Geneva, Switzerland: World Health Organization

2.   Health Canada. (2002) Economic burden of illness in Canada, 1998. Ottawa, Canada: Health Canada

3.   Tarride, J.-E., Lim, M., DesMeules, M., Luo, W., Burke, N., O'Reilly, D., Bowen, J., Goeree, R. A review of the cost of cardiovascular disease. *Canadian Journal of Cardiology* **25,** e195–e202 (2009).

4.   de Oliveira, C., Ngyuen, V. H., Wijeysundera, H. C., Wong, W.W.L., Woo, G., Liu, P. P., Krahn, M D. How much are we spending? The estimation of research expenditures on cardiovascular disease in Canada. *BioMed Central Health Services Research* **12,** 1–8 (2012).

5.   Glomset, J. A. The plasma lecithin:cholesterol acyltransferase reaction. *The Journal of Lipid Research* **9,** 155–167 (1968).

6.   Cuchel, M., Rader, D. J. Macrophage reverse cholesterol transport: key to the regression of atherosclerosis? *Circulation* **113,** 2548–2555 (2006).

7.   Ohashi, R., Mu, H., Wang, X., Yao, Q., Chen, C. Reverse cholesterol transport and cholesterol efflux in atherosclerosis. *QJM: An International Journal of Medicine* **98,** 845–856 (2005).

8.   Libby, P. Inflammation and cardiovascular disease mechanisms. *The American Journal of Clinical Nutrition* **83,** 456s–460s (2006).

9.   Gordon, T., Kannel, W. B., Castelli, W. P., Dawber, T. R. Lipoproteins, cardiovascular disease, and death. The Framingham Study. *Archives of Internal Medicine* **114,** 1129–1131 (1981).

10.   Gerrity, R. G. The role of the monocyte in atherogenesis I. transition of blood-borne monocyte into foam cells in fatty lesions. *American Journal of Pathology* **103,** 181–190 (1981).

11.   Jonas, A., Phillips, M. C. in *Biochemistry of lipids, lipoproteins and membranes (Fifth Edition)* (eds. Vance, D. E. & Vance, J. E.) 485–506 (Elsevier, 2008).

12.   Jairam, V., Uchida, K., Narayanaswami, V. in *Lipoproteins - role in health and diseases* (eds. Frank, S. & Kostner, G.) 383–408 (InTech, 2012).

13.   Hofmann, A. F., Borgström, B. The intraluminal phase of fat digestion in man: the lipid content of the micellar and oil phases of intestinal content obtained during fat digestion and absorption. *The Journal of Clinical Investigation.* **43,** 247–257 (1964).

14.   Westergaard, H., Dietschy, J. M. The mechanism whereby bile acid micelles increase the rate of fatty acid and cholesterol uptake into the intestinal mucosal cell. *The Journal of Clinical Investigation.* **58,** 97–108 (1976).

15.   Milger, K., Herrmann, T., Becker, C., Gotthardt, D., Zickwolf, J., Ehehalt, R., Watkins, P. A., Stremmel, W., Füllekrug, J. Cellular uptake of fatty acids driven by the ER-localized acyl-CoA synthetase FATP4. *The Journal of Cell Science* **119,** 4678–4688 (2006).

16.   Vance, J. E., Adeli, K. in *Biochemistry of Lipids, Lipoproteins and Membranes (Fifth Edition)* (eds. Vance, D. E. & Vance, J. E.) 507–531 (Elsevier, 2008).

17.   Zannis, V., Cole, S., Jackson, C., Kurnit, D., Karathanasis, S. Distribution of apolipoprotein A-I, C-II, and E mRNA in fetal human tissues. Time-dependent induction of apolipoprotein E mRNA by culture human monocyte-macrophages. *Biochemistry* **24,** 4450–4455 (1985).

18.   Zannis, V., Kurnit, D. M., Breslow, J. L. Hepatic apo-A-I and apo-E and intestinal apo-A-I are synthesized in precursor isoprotein forms by organ cultures of human fetal tissues. *The Journal of Biological Chemistry* **257,** 536–544 (1982).

19.   Davidson, S. W., Sparks, D. L., Lund-Katz, S., Phillips, M.C. The molecular basis for the difference in charge between pre-β and α-migrating high density lipoproteins. *The Journal of Biological Chemistry* **269,** 8959–8965 (1994).

20.   Fielding, C. J., Fielding, P. E. Cellular cholesterol efflux. *Biochimica et Biophysica Acta - Molecular and Cell Biology of Lipids* **1533,** 175–189 (2001).

21.   Rosenson, R. S., Brewer, B. H., Davidson, S. W., Fayad, Z. A., Fuster, V., Goldstein, J., Hellerstein, M., Jiang, X., Phillips, M. C., Rader, D. J., Remaley, A. T., Rothblat, G. H., Tall, A. R., Yvan-Charvet, L. Cholesterol efflux and atheroprotection: advancing the concept of reverse cholesterol

transport. *Circulation* **125,** 1905–1919 (2012).

22.   Phillips, J. C., Wriggers, W., Li, Z., Jonas, A., Schulten, K. Predicting the structure of apolipoprotein A-I in reconstituted high-density lipoprotein disks. *Biophysical Journal* **73,** 2337–2346 (1997).

23.   Pollard, R. D., Fulp, B., Samuel, M. P., Sorci-Thomas, M. G., Thomas, M. J. The conformation of lipid-free human apolipoprotein A-I in solution. *Biochemistry* **52,** 9470–9481 (2013).

24.   Barter, P. J. Hugh Sinclair Lecture: The regulation and remodelling of HDL by plasma factors. *Atherosclerosis Supplementals* **3,** 39–47 (2002).

25.   Vedhachalam, C., Duong, P. T., Nickel, M., Nguyen, D., Dhanasekaran, P., Saito, H., Rothblat, G. H., Lund-Katz, S., Phillips, M.C. Mechanism of ATP-binding cassette transporter A1-mediated cellular lipid efflux to apolipoprotein A-I and formation of high density lipoprotein particles. *The Journal of Biological Chemistry* **282,** 25123–25130 (2007).

26.   Norata, G. D., Catapano, A. L. Molecular mechanisms responsible for the antiinflammatory and protective effect of HDL on the endothelium. *Vascular Health and Risk Management* **1,** 119–129 (2005).

27.   Nicholls, S. J., Cutri, B., Worthley, S., Kee, P., Rye, K-A., Bao, S., Barter, P. J. Impact of short-term administration of high-density lipoproteins and atorvastatin on atherosclerosis in rabbits. *Arteriosclerosis, Thrombosis, and Vascular Biology* **25,** 2416–2421 (2005).

28.   Badimon, J. J., Badimon, L., Fuster, V. Regression of atherosclerosis lesions by high density lipoprotein plasma fraction in the cholesterol-fed rabbit. *Journal of Clinical Investigation* **85,** 1234-1241 (1990).

29.   Connelly, P. W. The role of hepatic lipase in lipoprotein metabolism. *Clinica Chimica Acta* **286,** 243–255 (1999).

30.   Barrans, A., Collet, X., Barbaras, R., Jaspard, B., Manent, J., Vieu, C., Chap, H., Perret, B. Hepatic lipase induces the formation of pre-β_1 high density lipoprotein (HDL) from triacylglycerol-rich HDL$_2$. *The Journal of Biological Chemistry* **269,** 11572–11577 (1994).

31.   Tall, A. R. Plasma high density lipoproteins. Metabolism and relationship to atherogenesis. *The Journal of Clinical Investigation.* **86,** 379–384 (1990).

32.   Rye, K. A., Clay, M. A., Barter, P. J. Remodelling of high density

lipoproteins by plasma factors. *Atherosclerosis* **145,** 227–238 (1999).

33.   de la Llera-Moya, M. Drazul-Schrader, D., Asztalos, B. F., Cuchel, M., Rader, D. J., Rothblat, G. H. The ability to promote efflux via ABCA1 determines the capacity of serum specimens with similar high-density lipoprotein cholesterol to remove cholesterol from macrophages. *Arteriosclerosis, Thrombosis, and Vascular Biology* **30,** 796–801 (2010).

34.   Nanjee, M. N., Cooke, C. J., Garvin, R., Semeria, F., Lewis, G., Olszewski, W. L., Miller, N. E. Intravenous apoA-I/lecithin discs increase pre-β-HDL concentration in tissue fluid and stimulates reverse cholesterol transport in humans. *The Journal of Lipid Research* **42,** 1586–1593 (2001).

35.   Nakamura, Y., Kotite, L., Gan, Y., Spencer, T. A., Fielding, C. J., Fielding, P. E. Molecular mechanism of reverse cholesterol transport: reaction of pre-β-migrating high-density lipoprotein with plasma lecithin/cholesterol acyltransferase. *Biochemistry* **43,** 14811–14820 (2004).

36.   Zannis, V., Chroni, A., Krieger, M. Role of apoA-I, ABCA1, LCAT, and SR-BI in the biogenesis of HDL. *Journal of Molecular Medicine* **84,** 276–294 (2006).

37.   Lund-Katz, S., Phillips, M. C. High density lipoprotein structure-function and role in reverse cholesterol transport. *Subcellular Biochemistry* **51,** 183–227 (2010).

38.   Duong, P. T., Weibel, G. L., Lund-Katz, S., Rothblat, G. H., Phillips, M. C. Characterization and properties of preβ-HDL particles formed by ABCA1-mediated cellular lipid efflux to apoA-I. *The Journal of Lipid Research* **49,** 1006–1014 (2008).

39.   Clay, M. A., Newnham, H. H., Barter, P. J. Hepatic lipase promotes a loss of apolipoprotein A-I from triglyceride- enriched human high density lipoproteins during incubation in vitro. *Arteriosclerosis and Thrombosis* **11,** 415–422 (1991).

40.   Wang, N., Lan, D., Chen, W., Matsuura, F., Tall, A. R. ATP-binding cassette transporters G1 and G4 mediate cellular cholesterol efflux to high-density lipoproteins. *Proceedings of the National Academy of Sciences of the United States of America* **101**, 9774-9779 (2004).

41.   Laffitte, B. A., Repa, J. J., Joseph, S. B., Wilpitz, D. C., Kast, H. R., Mangelsdorf, D. J., Tontonoz, P. LXRs control lipid-inducible expression of the apolipoprotein E gene in macrophages and adipocytes. *Proceedings of the*

National Academy of Sciences of the United States of America **98** 507-512 (2001).

42.   Kennedy, M. A., Venkateswaran, A., Tarr, P. T., Xenarios, I., Kudoh, J., Shimizu, N., Edwards, P. E. Characterization of the human ABCG1 gene: liver X receptor activates an internal promoter that produces a novel transcript encoding an alternative form of the protein. *The Journal of Biological Chemistry* **276,** 39438–39447 (2001).

43.   Chawla, A., Boisvert, W. A., Lee, C-H., Laffitte, B. A., Barak, Y., Joseph, S. B., Liao, D., Nagy, L., Edwards, P. A., Curtiss, L. K., Evans, R. M., Tontonoz, P. A PPARɣ-LXR-ABCA1 pathway in macrophages is involved in cholesterol efflux and atherogenesis. *Molecular Cell* **7,** 161–171 (2001).

44.   Out, R., Hoekstra, M., Habets, K., Meurs, I., de Waard, V., Hildebrand, R. B., Wang, Y., Chimini, G., Kuiper, J., Van Berkel, T. J. C., Van Eck, M. Combined deletion of macrophage ABCA1 and ABCG1 leads to massive lipid accumulation in tissue macrophages and distinct atherosclerosis at relatively low plasma cholesterol levels. *Arteriosclerosis, Thrombosis, and Vascular Biology* **28,** 258–264 (2008).

45.   Gordon, T., Castelli, W. P., Hjortland, M. C., Kannel, W. B., Dawber, T. R. High density lipoprotein as a protective factor against coronary heart disease. The Framingham Study. *The American Journal of Medicine* **62,** 707–714 (1977).

46.   Rader, D. J., Tall, A. R. The not-so-simple HDL story: Is it time to revise the HDL cholesterol hypothesis? *Nature Medicine* **18,** 1344–1345 (2012).

47.   Naik, S. U., Wang, X., Da Silva, J. S., Jaye, M., Macphee, C. H., Reilly, M. P., Billheimer, J. T., Rothblat, G. H., Rader, D. J. Pharmacological activation of liver X receptors promotes reverse cholesterol transport in vivo. *Circulation* **113,** 90–97 (2006).

48.   Mckenney, J. M., Proctor, J. D., Harris, S., Chinchili, V. M. A comparison of the efficacy and toxic effects of sustained- vs immediate-release niacin in hypercholesterolemic patients. *Journal of American Medical Association* **271,** 672–677 (1994).

49.   Albers, J., Slee, A., O'Brien, K., Robinson, J., Kashyap, M, Kwiterovich, P., Ping, X., Marcovina, S. M. Relationship of apolipoproteins A-1 and B, and lipoprotein(a) to cardiovascular outcomes The AIM-HIGH trial (atherothrombosis intervention in metabolic syndrome with low HDL/high triglyceride and impact on global health outcomes). *Journal of the American*

College of Cardiology **62,** 1575–1579 (2013).

50. Marotti, K. R., Castle, C. K., Boyle, T. P., Lin, A. H., Murray, R. W., Melchlor, G. W. Severe atherosclerosis in transgenic mice expressing simian cholesteryl ester transfer protein. *Nature* **364,** 73–75 (1993).

51. Barter, P. J., Caulfield, M., Eriksson, M, Grundy, S. M., Kastelein, J. J. P., Kornajda, M., Lopez-Sendon, J., Mosca, L., Tardif, J-C., Waters, D. D., Shear, C. L., Revkin, J. H., Buhr, K. A., Fisher, M. R., Tall, A. R., Brewer, B. Effects of torcetrapib in patients at high risk for coronary events. *The New England Journal of Medicine* **357,** 2109–2122 (2007).

52. Easton, R., Gille, A., D'Andrea, D., Davis, R., Wright, S. D., Shear, C. A multiple ascending dose study of CSL112, an infused formulation of apoA-I. *The Journal of Clinical Pharmacology* **54,** 301–310 (2013).

53. Zhang, Y., Zanotti, I., Reilly, M. P., Glick, J. M., Rothblat, G. H., Rader, D. J. Overexpression of apolipoprotein A-I promotes reverse transport of cholesterol from macrophages to feces in vivo. *Circulation* **108,** 661–663 (2003).

54. Reddy, S. T., Navab, M., Anantharamaiah, G. M., Fogelman, A. M. Apolipoprotein A-I mimetics. *Current Opinion in Lipidology* **25,** 304–308 (2014).

55. Jansen, H., van Berkel, T. J. C., Hulsmann, W. C. Binding of liver lipase to parenchymal and non-parenchymal rat liver cells. *Biochemical and Biophysical Research Communications* **85,** 148–152 (1978).

56. Demant, T., Carlson, L. A., Holmquist, L., Karpe, F., Nilsson-Ehle, P., Packard, C. J., Shepherd, J. Lipoprotein metabolism in hepatic lipase deficiency: studies on the turnover of apolipoprotein B and on the effect of hepatic lipase on high density lipoprotein. *The Journal of Lipid Research* **29,** 1603–1611 (1988).

57. Ruel, I. L., Couture, P., Cohn, J. S., Bensadoun, A., Marcil, M., Lamarche, B. Evidence that hepatic lipase deficiency in humans is not associated with proatherogenic changes in HDL composition and metabolism. *The Journal of Lipid Research* **45,** 1528–1537 (2004).

58. Barcat, D., Amadio, A., Palos-Pinot, A., Daret, D., Benlian, P., Darmon, M., Bérard, A. M. Combined hyperlipidemia/hyperalphalipoproteinemia associated with premature spontaneous atherosclerosis in mice lacking hepatic lipase and low density lipoprotein receptor. *Atherosclerosis* **188,**

347–355 (2006).

59.   Ishibashi, S., Brown, M. S., Goldstein, J. L., Gerard, R. D., Hammer, R. E., Herz, J. Hypercholesterolemia in low density lipoprotein receptor knockout mice and its reversal by adenovirus-mediated gene delivery. *The Journal of Clinical Investiagtion* **92,** 883–893 (1993).

60.   Fan, J., Wang, J., Bensadoun, A., Lauer, S. J., Dang, Q., Mahley, R. W., Taylor, J. M. Overexpression of hepatic lipase in transgenic rabbits leads to marked reduction of plasma high density lipoproteins and intermediate density lipoproteins. *Proceedings of the National Academy of Sciences of the United States of America* **91,** 8724–8728 (1994).

61.   Busch, S. J., Barnhart, R. L., Martin, G. A., Fitzgerald, M. C., Yates, M. T., Mao, S. J.T., Thomas, C.E., Jackson, R. L. Human hepatic triglyceride lipase expression reduces high density lipoprotein and aortic cholesterol in cholesterol-fed transgenic mice. *The Journal of Biological Chemistry* **269,** 16376–16382 (1994).

62.   Nong, Z., Gonzalez-Navarro, H., Amar, M., Freeman, L., Knapper, C., Neufeld, E. B., Paigen, B. J., Hoyt, R. F., Fruhart-Najib, J., Santamarina-Fojo, S. Hepatic lipase expression in macrophages contributes to atherosclerosis in apoE-deficient and LCAT-transgenic mice. *The Journal of Clinical Investigation* **112,** 367–378 (2003).

63.   Vaisman, B. L., Klein, H-G., Rouis, M., Bérard, A. M., Kindt, M. R., Talley, G. D., Meyn, S. M., Hoyt, R. F, Marcovina, S. M., Albers, J. J., Hoeg, J., Brewer, B., Santamarina-Fojo, S. Overexpression of human lecithin cholesterol acyltransferase leads to hyperalphalipoproteinemia in transgenic mice. *The Journal of Biological Chemistry* **270,** 12269–12275 (1995).

64.   Zhang, S. H, Reddick, R. L., Piedrahita, J. A., Maeda, N. Spontaneous hypercholesterolemia and arterial lesions in mice lacking apolipoprotein E. *Science* **258,** 468–471 (1992).

65.   Mezdour, H., Jones, R., Dengremont, C., Castro, G., Maeda, N. Hepatic lipase deficiency increases plasma cholesterol but reduces susceptibility to atherosclerosis in apolipoprotein E-deficient mice. *The Journal of Biological Chemistry* **272,** 13570–13575 (1997).

66.   Martin, G. A., Busch, S. J., Meredith, G. D., Cardin, A. D., Blankenship, D. J.T., Mao, S., Rechtin, A. E., Woods, C. W., Racke, M. M., Schafer, M. P., Fitzgerald, M. C., Burke, D. M., Flanagan, M. A., Jackson, R. L. Isolation and cDNA sequence of human postheparin plasma hepatic triglyceride lipase.

The Journal of Biological Chemistry **263,** 10907–10914 (1988).

67.   Wölle, J., Jansen, H., Smith, L. C., Chan, L. Functional role of N-linked glycosylation in human hepatic lipase: asparagine-56 is important for both enzyme activity and secretion. *The Journal of Lipid Research* **34,** 2169–2176 (2002).

68.   Hide, W. A., Chan, L., Li, W-H. Structure and evolution of the lipase superfamily. *The Journal of Lipid Research* **33** 167–178 (1992).

69.   McWilliam, H., Li, W., Uludag, M., Squizzto, S., Park, Y. M., Buso, N., Cowley, AP., Lopez, R. Analysis tool web services from the EMBL-EBI. *Nucleic Acids Research* **41** W597-W600 (2013).

70.   Winkler, F. K., D'Arcy, A., Hunziker, W. Structure of human pancreatic lipase. *Nature* **343,** 771–774 (1990).

71.   Dichek, H. L., Qian, K., Agrawal, N. The bridging function of hepatic lipase clears plasma cholesterol in LDL receptor-deficient "apoB-48-only" and "apoB-100-only" mice. *The Journal of Lipid Research* **45,** 551–560 (2004).

72.   Dichek, H. L., Parrott, C., Ronan, R., Brunzell, J. D., Brewer, B. H., Santamarina-Fojo, S. Functional characterization of a chimeric lipase genetically engineered from human lipoprotein lipase and human hepatic lipase. *The Journal of Lipid Research* **34,** 1393–1401 (1993).

73.   Hill, J. S., Davis, R. C., Yang, D., Wen, J., Philo, J. S., Poon, P. H., Phillips, M. L., Kempner, E. S., Wong, H. Human hepatic lipase subunit structure determination. *The Journal of Biological Chemistry* **271,** 22931–22936 (1996).

74.   Yu, W., Hill, J. S. Mapping the heparin-binding domain of human hepatic lipase. *Biochemical and Biophysical Research Communications* **343,** 659–665 (2006).

75.   Brown, R. J., Schultz, J. R., Ko, K. W. S., Hill, J. S., Ramsamy, T. A, White, A. L., Sparks, D. L., Yao, Z. The amino acid sequences of the carboxyl termini of human and mouse hepatic lipase influence cell surface association. *The Journal of Lipid Research* **44,** 1306–1314 (2003).

76.   Watson, T. D. G., Tan, C-E., McConnell, M., Clegg, S. K., Squires, L. F., Packard, C. J. Measurement and physiological significance of lipoprotein and hepatic lipase activities in preheparin plasma. *Lipids and Lipoproteins* **41,** 405–412 (1995).

77.   Chatterjee, C., Young, E. K., Pussegoda, K. E., Twomey, E., Pandey, N. R., Sparks, D. L. Hepatic high-density lipoprotein secretion regulates the mobilization of cell-surface hepatic lipase. *Biochemistry* **48,** 5994–6001 (2009).

78.   Ramsamy, T. A., Neville, T. A-M., Chauhan, B. M., Aggarwal, D., Sparks, D. L. Apolipoprotein A-I regulates lipid hydrolysis by hepatic lipase. *The Journal of Biological Chemistry* **275,** 33480–33486 (2000).

79.   Goldberg, I. J. Lipoprotein lipase and lipolysis: central roles in lipoprotein metabolism and atherogenesis. *The Journal of Lipid Research* **37,** 693–707 (1996).

80.   Ramsamy, T. A., Boucher, J., Brown, R. J., Yao, Z., Sparks, D. L., HDL regulates the displacement of hepatic lipase from cell surface proteoglycans and the hydrolysis of VLDL triacylglycerol. *The Journal of Lipid Research* **44,** 733–741 (2003).

81.   Boucher, J., Ramsamy, T. A, Braschi, S., Sahoo, D., Neville, T. A-M., Sparks, D. L. Apolipoprotein A-II regulates HDL stability and affects hepatic lipase association and activity. *The Journal of Lipid Research* **45,** 849–858 (2004).

82.   Toth, P. P.*,* Barylski, M.*,* Nikolic, D., Rizzo, M., Montalto, G., Banach, M. Should low high-density lipoprotein cholesterol (HDL-C) be treated? *Best Practice & Research Clinical Endocrinology & Metabolism* **28,** 353–368 (2014).

83.   Beaglehole, R., Bonita, R. Global public health: a scorecard. *Lancet* **372** 1988–96 (2008).

84.   Cardin, A., Weintraub, H. J. R. Molecular modeling of protein-glycosaminoglycan interactions. *Atherosclerosis* **9,** 21–32 (1989).

85.   Margalit, H., Fischer, N., Ben-Sasson, S. A. Comparative analysis of structurally defined heparin binding sequences reveals a distinct spatial distribution of basic residues. *The Journal of Biological Chemistry* **268,** 19228–19231 (1993).

86.   Hefti, M. H., Van Vugt-Van der Toorn, C. J. G., Dixon, R., Vervoort, J. A novel purification method for histidine-tagged proteins containing a thrombin cleavage site. *Analytical Biochemistry* **295,** 180–185 (2001).

87.   Brown, R. J., Miller, G. C., Griffon, N., Long, C. J., Rader, D. J. Glycosylation of endothelial lipase at asparagine-116 reduces activity and the hydrolysis of native lipoproteins in vitro and in vivo. *The Journal of Lipid Research* **48,** 1132–1139 (2007).

88.   Lui, J., Afroza, H., Rader, D. J., Jin, W. Angiopoietin-like protein 3 inhibits lipoprotein lipase activity through enhancing its cleavage by proprotein convertases. *The Journal of Biological Chemistry* **285,** 27561–27570 (2010).

89.   Lehner, R., Verger, R. Purification and characterization of a porcine liver microsomal triacylglycerol hydrolase. *Biochemistry* **36,** 1861–1868 (1997).

90.   Hames, B. D. *Gel Electrophoresis of Proteins (Third edition).* 1–373 (Oxford University Press, 1998).

91.   Ylä-Herttuala, S., Lipton, B. A., Rosenfeld, M. E., Gildberg, I. J., Steinberg, D., Witztum, J. L. Macrophages and smooth muscle cells express lipoprotein lipase in human and rabbit atherosclerotic lesions. *Proceedings of the National Academy of Sciences of the United States of America* **88,** 10143–10147 (1991).

92.   Zilversmit, D. B. A proposal linking atherogenesis to the interaction of endothelial lipoprotein lipase with triglyceride-rich lipoprotiens. *Circulation Research* **33,** 633–638 (1973).

93.   Renier, G., Skamene, E., Desantis, J. B., Radzioch, D. High macrophage lipoprotein lipase expression and secretion are associated in inbred murine strains with susceptibility to atherosclerosis. *Arteriosclerosis and. Thrombosis.* **13,** 190–196 (1993).

94.   Greenfield, N. J. Using circular dichroism spectra to estimate protein secondary structure. *Nature Protocols* **1,** 2876–2890 (2006).

95.   Esko, J., Linhardt, R. (2009) *Proteins that Bind Sulfated Glycosaminoglycans - Essentials of Glycobiology - Chapter 35.* Cold Spring Harbor, New York: Cold Spring Harbor Laboratory Press.

96.   Davis, R. C.*,* Wong, H., Nikazy, J., Wang, K., Han, Q., Schotz, M. C. Chimeras of hepatic lipase and lipoprotein lipase. Domain localization of enzyme-specific properties. *The Journal of Biological Chemistry* **267,** 21499–21504 (1992).

97.   Peterson, J., Fujimoto, W. Y., Brunzell, J. D. Human lipoprotein lipase: relationship of activity, heparin affinity, and conformation as studied with

monoclonal antibodies. *The Journal of Lipid Research* **33,** 1165–1170 (1992).

98.   Olivecrona, G., Lookene, A. Noncatalytic functions of lipoprotein lipase. *Methods in Enzymology* **286,** 102–116 (1997).

99.   Breedveld, B., Schoonderwoerd, K., Jansen, H. Identification of a heparin-releasable hepatic lipase binding protein from rat liver. *Biochemical Journal* **330,** 785–789 (1998).

100.   Caldwell, E. E. O., Nadkarni, V. D., Fromm, J. R., Linhardt, R. J., Weiler, J. M. Importance of specific amino acids in protein binding sites for heparin and heparan sulfate. *International Journal Biochemistry and Cell Biology* **28,** 203–216 (1996).

101.   Hunt, L., Hacker, D. L., Grosjean, F., Jesus, M., Uebersax, L., Jordan, M., Wurnm, F. M. Low-temperature pausing of cultivated mammalian cells. *Biotechnology and Bioengineering* **89,** 157–163 (2004).

102.   Nykær, A., Bengtsson-Olivecrona, G., Lookene, A., Moestrup, S. K., Peterson, C. M., Weber, W., Beisiegell, U., Gliemann, J. The α$_2$-macroglobulin receptor/low density lipoprotein receptor- related protein binds lipoprotein lipase and β-migrating very low density lipoprotein dssociated with the lipase. *The Journal of Biological Chemistry* **268,** 15048–15055 (1993).

103.   Kounnas, M. Z., Chappell, D. A., Wong, H., Argraves, S. W., Strickland, D. K. The cellular internalization and degradation of hepatic lipase is mediated by low density lipoprotein-related protein and requires cell surface proteoglycans. *The Journal of Biological Chemistry* **270,** 9307–9312 (1995).

104.   Krapp, A., Ahle, S., Kersting, S., Hua, Y., Kneser, K., Nielsen, M, Gliemann, J., Beisiegel, U. Hepatic lipase mediates the uptake of chylomicrons and β-VLDL into cells via the LDL receptor-related protein (LRP). *The Journal of Lipid Research* **37,** 926–936 (1996).

105.   Chappell, D., Fry, G. L., Waknitz, M. A., Iverius, P-H., Williams, S. E., Strickland, D. K. The low density lipoprotein receptor-related protein/α$_2$-macroglobulin receptor binds and mediates catabolism of bovine milk lipoprotein lipase. *The Journal of Biological Chemistry* **267,** 25764–25767 (1992).

106.   Ji, Z., Dichek, H. L., Miranda, D. R., Mahley, R. W. Heparan sulfate proteoglycans participate in hepatic lipase- and apolipoprotein E-mediated

binding and uptake of plasma lipoproteins, including high density lipoproteins. *The Journal of Biological Chemistry* **272,** 31285–31292 (1997).

107.   Williams, S. E., Inoue, I., Tran, H., Fry, G. L., Pladet, M. W., Iverius, P-H., Lalouel, J-M., Chappell, D. A., Strickland, D. K. The carboxyl-terminal domain of lipoprotein lipase binds to the low density lipoprotein receptor-related protein/α_2-macroglobulin receptor (LRP) and mediates binding of normal very low density lipoproteins to LRP. *The Journal of Biological Chemistry* **269,** 8653–8658 (1994).

108.   Nykær, A.*,* Nielsen, M., Lookene, A., Meyer, N., Røigaard, H., Etzerodt, M., Beisiegel, U., Olivecrona, G., Gliemann, J. Carboxyl-terminal fragment of lipoprotein lipase binds to the low density lipoprotein receptor-related protein and inhibits lipase-mediate uptake of lipoproteins in cells. *The Journal of Biological Chemistry* **269,** 31747–31755 (1994).

109.   Canuel, M., Sun, X., Asselin, M-C., Paramithiotis, E., Prat, S., Seidah, N. G. Proprotein convertase subtilisin/kexin type 9 (PCSK9) can mediate degradation of the low density lipoprotein receptor-related rrotein 1 (LRP-1). *PLoS One* **8,** e64145 (2013).

110.   Woody, R. Circular dichroism. *Methods in Enzymology* **246,** 34–71 (1995).

111.   Mok, S., Sberna, G., Heffernan, D, Cappai, R., Galatis, D., Clarris, H. J., Sawyer, W. H., Beyreuther, K., Masters, C. L., Small, D. H. Expression and analysis of heparin-binding regions of the amyloid precursor protein of Alzheimer's disease. *Federation of European Biochemical Societies Letters* **415,** 303–307 (1997).

112.   Tyler-Cross, R., Sobel, M., Marques, D., Harris, R. B. Heparin binding domain peptides of antithrombin III: Analysis by isothermal titration calorimetry and circular dichrosim spectroscopy. *Protein Science* **3,** 620–627 (1994).

113.   Main, E. R. G., Jackson, S. E. Does trifluoroethanol affect folding pathways and can it be used as a probe of structure in transition states? *Nature Structural Biology* **6,** 831–835 (1999).

114.   Ionescu, R. M., Mattews, C. R.. Folding under the influence. *Nature Structural Biology* **6** 304–307 (1999).

115.   Chiti, F. Taddei, N., Paul, W., Hamada, D., Fiaschi, T., Ramponi, G., Dobson, C. M. Acceleration of the folding of acylphosphatase by stabilization of local secondary structure. *Nature Structural Biology* **6,** 380–

387 (1999).

116.   Yachdav, G., Kloppmann, E., Kajan, L., Hect, M., Golberg, T., Hamp, T., Hönigschmid, P., Scafferans, A., Roos, M., Bernhofer, M., Richter, L., Ashkenazy, H. Punta, M., Schlessinger, A., Bromberg, Y., Schneider, R., Vriend, G., Sander, C., Ben-Tal, N., Rost, B. PredictProtein--an open resource for online prediction of protein structural and functional features. *Nucleic Acids Research,* **42** W337-W343 (2014).

117   Yang, T-C., Rendell, J., Gulliver, W., Booth, V. Peptide T exhibits a well-defined structure in fluorinated solvent at low temperature. *Journal of Peptide Science* **15,** 818–823 (2009).

118.   Perlin, S. A., Casu, B., Sanderson, G. R., Johnson, L. F. 220 MHz spectra of heparin, chondroitins, and other mucopolysaccharides. *Canadian Journal of Chemistry* **48,** 2260–2268 (1970).

119.   Pan, J., Qian, Y., Zhou, X., Pazandak, A., Frazier, S. B., Weiser, P., Lu, H., Zhang, L. Oversulfated chondroitin sulfate is not the sole contaminant in heparin. *Nature Biotechnology* **28,** 203–207 (2010).

120.   Guerrini, M. Over, Beccati, D., Shriver, Z., Naggi, A., Viswanathan, K., Bisio, A., Capila, I., Lansing, J., Guglieri, S., Fraser, B., Al-Hakim, A., Gunay, N., Zhang, Z., Robinson, L., Bushe, L., Nasr, M, Woodcock, J., Langer, R., Venkataraman, G., Lindthardt, R. J., Casu, B., Torri, G., Sassisekharan, R. Oversulfated chondroitin sulfate is a contaminant in heparin associated with adverse clinical events. *Nature Biotechnology* **26,** 669–675 (2008).

121.   Wuthrich, K. Protein structure determination in solution by nuclear magnetic resonance spectroscopy. *Science* **243,** 45–50 (1989).

122.   Yang, C., Gu, Z., Weng, S., Kim, T. W., Chen, S., Pownall, H. J., Pownall, P. M., Sharp, Liu, S., Li, W., Gotto, A. M., Chan, L. Structure of apolipoprotein B-100 of human low density lipoproteins. *Arteriosclerosis* **9,** 96–108 (1989).

123.   Wilson, C., Wardell, M. R., Weisgraber, K. H., Mahley, R. W., Agard, D. A. Three-dimensional structure of the LDL receptor-binding domain of Human apolipoprotein E. *Science* **252,** 1817–1822 (1991).

124.   Epand, R. M., Epand, R. F., Sayer, B. G., Melacini, G., Palgulachari, M. N., Segrest, J. P., Anantharamaiah, G. M. An apolipoprotein AI mimetic peptide: membrane interactions and the role of cholesterol. *Biochemistry* **43,** 5073–5083 (2004).

125.   Christensen, D. J., Ohkubo, N., Oddo, J., Van Kanegan, M. J., Neil, J., Li, F., Colton, C. A., Vitek, M. P. Apolipoprotein E and peptide mimetics modulate inflammation by binding the SET protein and activating protein phosphatase 2A. *The Journal of Immunology* **186,** 2535–2542 (2011).

126.   Navab, M., Anantharamaiah, G. M., Hama, S., Garber, D. W., Chaddha, M., Hough, G., Lallone, R., Fogelman, A. M. Oral administration of an apo A-I mimetic peptide synthesized from D-amino acids dramatically reduces atherosclerosis in mice independent of plasma cholesterol. *Circulation* **105,** 290–292 (2002).

127.   Bloedon, L. T., Dunbar, R., Duffy, D., Pinell-Salles, P., Norris, R., DeGroot, B. J., Movva, R., Navab, M., Fogelman, A. M., Rader, D. J. Safety, pharmacokinetics, and pharmacodynamics of oral apoA-I mimetic peptide D-4F in high-risk cardiovascular patients. *The Journal of Lipid Research* **49,** 1344–1352 (2008).

128.   Saito, H., Dhanasekaran, P., Nguyen, D., Baldwin, F., Weisgraber, K. H., Wehrl, S., Phillips, M. C., Lund-Katz, S. Characterization of the heparin binding sites in human apolipoprotein E. *The Journal of Biological Chemistry* **278,** 14782–14787 (2003).

129.   Hafiane, A., Bielicki, J. K., Johansson, J. O., Genest, J. Apolipoprotein E derived HDL mimetic peptide ATI-5261 promotes nascent HDL formation and reverse cholesterol transport in vitro. *Biochimica et Biophysica Acta-Molecular and Cell Biology of Lipids* **1842,** 1498–1512 (2014).

130.   Hafiane, A., Bielicki, J., Johansson, J. O., Genest, J. Novel Apo E-derived ABCA1 agonist peptide (CS-6253) promotes reverse cholesterol transport and induces formation of preβ-1 HDL *in vitro*. *PLoS One* **10,** e0131997 (2015).

131.   LaVallie, E. R., DiBlasio, E. A., Kovacic, S., Grant, K. L., Schendel, P. F., McCoy, J. M. A thioredoxin gene fusion expression system that circumvents inclusion body formation in the E. coli cytoplasm. *Biotechnology* **11,** 187–193 (1993).

132.   Holmgren, A. Thioredoxin. *Annual Reviews in Biochemistry* **54,** 237–271 (1985).

133.   Porath, J. Immobilized metal ion affinity chromatography. *Protein Expression and Purification* **3,** 263–281 (1992).

134.   Carr, M. C., Hokanson, J. E., Zambon, A., Deeb, S. S., Barrett, H. R., Purnell, J. Q., Brunzell, J. D. The contribution of intraabdominal fat to gender differences in hepatic lipase activity and low/high density lipoprotein heterogeneity. *Journal of Clinical Endocrinology Metabolism* **86,** 2831–2837 (2001).

135.   Bamji-Mirza, M., Sundaram, M., Zhong, S., Yao, E. F., Parks, R. J., Yao, Z. Secretion of triacylglycerol-poor VLDL particles from McA-RH7777 cells expressing human hepatic lipase. *The Journal of Lipid Research* **52,** 540–548 (2011).

136.   Allayee, H., Dominquez, K. M., Aouizerat, B. E., Krauss, R. M., Rotter, J. I, Lu, J., Cantor, R. M., de Bruin, T. W. A., Lusis, A. J. Contribution of the hepatic lipase gene to the atherogenic lipoprotein phenotype in familial combined hyperlipidemia. *The Journal of Lipid Research* **41,** 245–252 (2000).

137.   Breckenridge, W. C., Little, J. A., Alaupovic, P., Wang, C. S., Kuksis, A., Kakis, G., Lindgren, F., Gardiner, G., Lipoprotein abnormalities associated with a familial deficiency of hepatic lipase. *Atherosclerosis* **45,** 161–179 (1982).

138.   Hegele, R. A., Little, J. A.., Vezina, C., Maguire, G. F., Tu, L., Wolever, T. S., Jenkins, D. J. A., Connelly, P. W. Hepatic lipase deficiency. clinical, biochemical, and molecular genetic characteristics. *Arteriosclerosis and Thrombosis.* **13,** 720–728 (1993).

139.   Hirano, K., Yamashitu, S., Kuga, Y., Sakai, N., Nozaki, S., Kihara, S., Arai, T., Yangai, K., Takami, S., Merju, M., Ishigami, M. Atherosclerotic disease in marked hyperalphalipoproteinemia combined reduction of cholesteryl ester transfer protein and hepatic triglyceride lipase. *Arteriosclerosis, Thrombosis, and Vascular Biology* **15,** 1849–1856 (1995).

140.   Jansen, H., Verhoeven, Week, L., Kastelein, J., Hailey, D., Ouweland, A., Jukema, W., Seidall, J., Birkenhager, J. Common C-to-T substitution at position -480 of the hepatic lipase promoter asscoiated with a lower lipase activity in coronary artery disease patients. *Arteriosclerosis, Thrombosis, and Vascular Biology* **17,** 2837–2842 (1997).

141.   Ehnholm, C., Shaw, W., Greten, H., Brown, W. V. Purification from human plasma of a heparin-released lipase with activity against triglyceride and phospholipids. *The Journal of Biological Chemistry* **250,** 6756–6761 (1975).
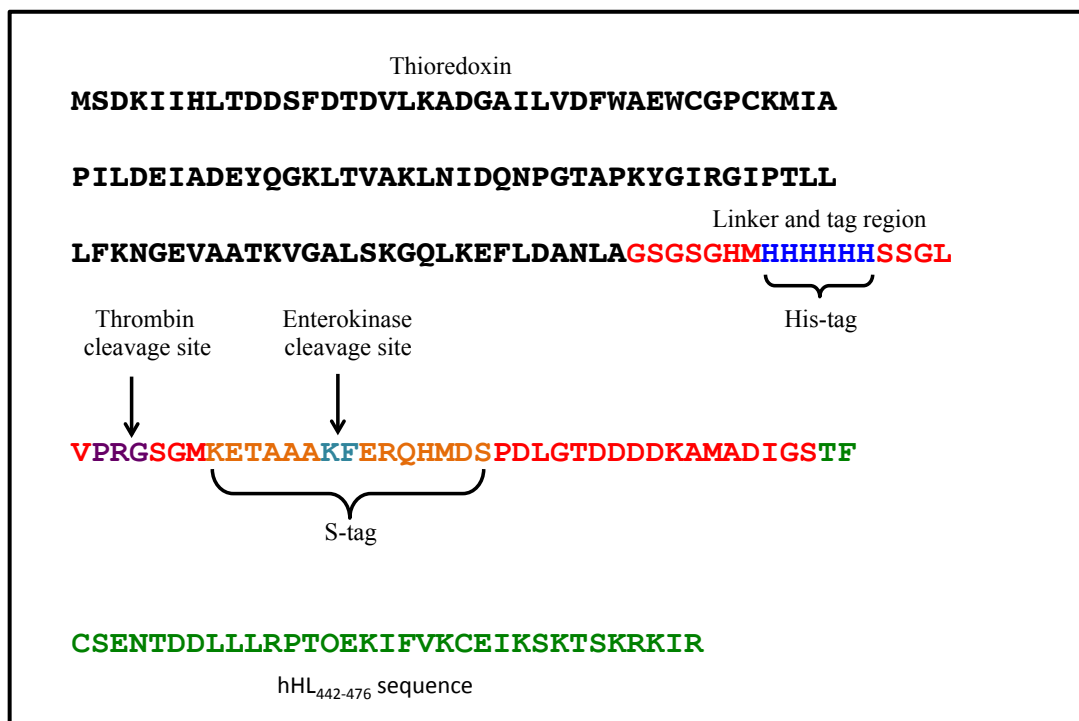
142.   Shafi, S., Brady, S. E., Bensadoun, A., Havel, R. J., Role of hepatic lipase in the uptake and processing of chylomicron remnants in rat liver. *The Journal of Lipid Research* **35,** 709–720 (1994).

143.   Homanics, G. E., de Dilva, H. V., Osada, J., Zhang, S. H., Wong, H., Borensztajn, J., Maeda, N. Mild dyslipidemia in mice following targeted inactivation of the hepatic lipase gene. *The Journal of Biological Chemistry* **270,** 2974–2880 (1995).

144.   Plump, A. S., Smith, J. D., Hayek, T., Aalto-Setälä, K., Walsh, A., Verstuyft, J. G., Rubin, E. M., Breslow, J. L. Severe hypercholesterolemia and atherosclerosis in apolipoprotein E-deficient mice created by homologous recombination in ES cells. *Cell* **71,** 343–353 (1992).

Appendix I: Supplemental Figures

Figure S1: Amino acid sequence of the hHL$_{442-476}$-Trx protein
Highlighted in black is the partial sequence of Trx with the link region highlighted in red. The hHL 442-476 sequence is highlighted in green. The cleavage site for thrombin is highlighted in purple and the enterokinase cleavage site is highlighted in light blue. The 6xhis tag is highlighted in blue and the S-tag is highlighted in orange.

Thioredoxin
MSDKIIHLTDDSFDTDVLKADGAILVDFWAEWCGPCKMIA

PILDEIADEYQGKLTVAKLNIDQNPGTAPKYGIRGIPTLL

Linker and tag region
LFKNGEVAATKVGALSKGQLKEFLDANLAGSGSGHMHHHHHHSSGL

His-tag

Thrombin
cleavage site

Enterokinase
cleavage site

VPRGSGMKETAAAKFERQHMDSPDLGTDDDDKAMADIGSTF

S-tag

CSENTDDLLLRPTOEKIFVKCEIKSKTSKRKIR

hHL$_{442-476}$ sequence

Figure S2: Activity of wild-type LPL compared to myc-tagged LPL using a resorufin ester hydrolysis assay

HEK-293T cells in 100-mm dishes were transfected with 6.5 µg of either wild-type hLPL cDNA (in pcDNA$_3$ plasmid), myc-tagged hLPL, or pcDNA$_3$ vector using Lipofectamine™. After 23.5 hours post transfection, media were replaced with DMEM containing 100 U/mL heparin. After 0.5 hours, media were collected and analyzed using a resorufin ester hydrolysis assay. *n*=3, technical replicates.
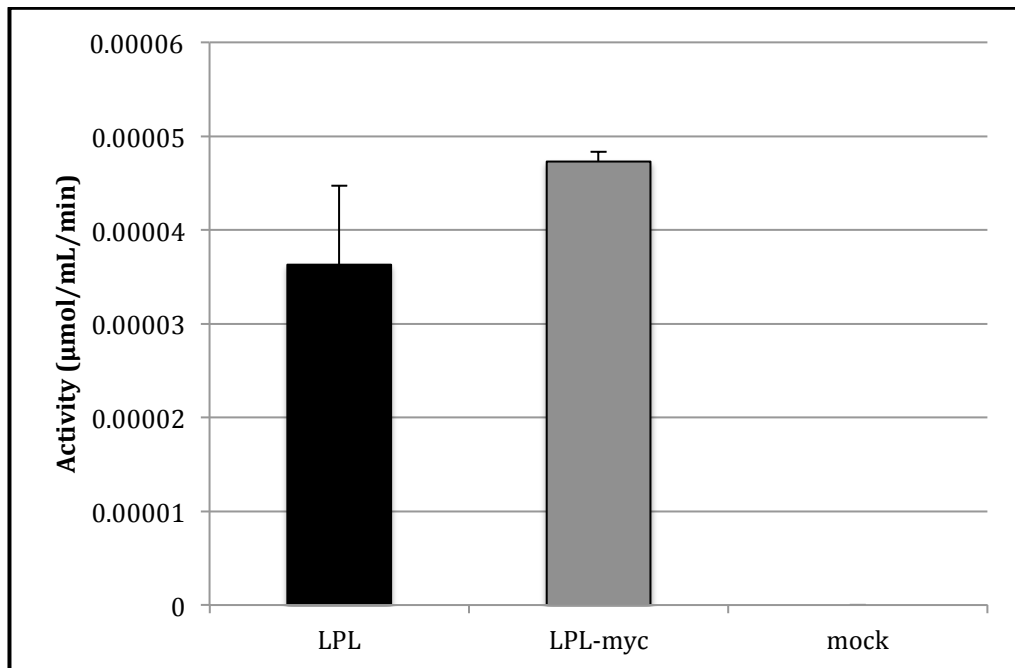
Figure S3: Immunoblot of the displacement of LPL by the hHL$_{442\text{-}476}$ peptide using polyclonal LPL antibody

Immunoblot of hLPL displaced from HEK-293T cells expressing myc-tagged hLPL with DMEM, 100 U heparin, or 200 µg/mL hHL$_{442\text{-}476}$ peptide. Cells in 6-well plates received one of the following treatments for 1 hour at 4°C: DMEM containing 100 U heparin (positive control), plain DMEM (negative control), or DMEM containing 200 µg/mL hHL$_{442\text{-}476}$ peptide. Following the hour incubation, the media were collected and the cells were washed with ice cold plain DMEM. The media were analyzed for the presence of LPL by immunoblot with the polyclonal LPL (H-53) antibody. No immunoreactivity was observed for the expected molecular mass for hLPL (58 kDa).
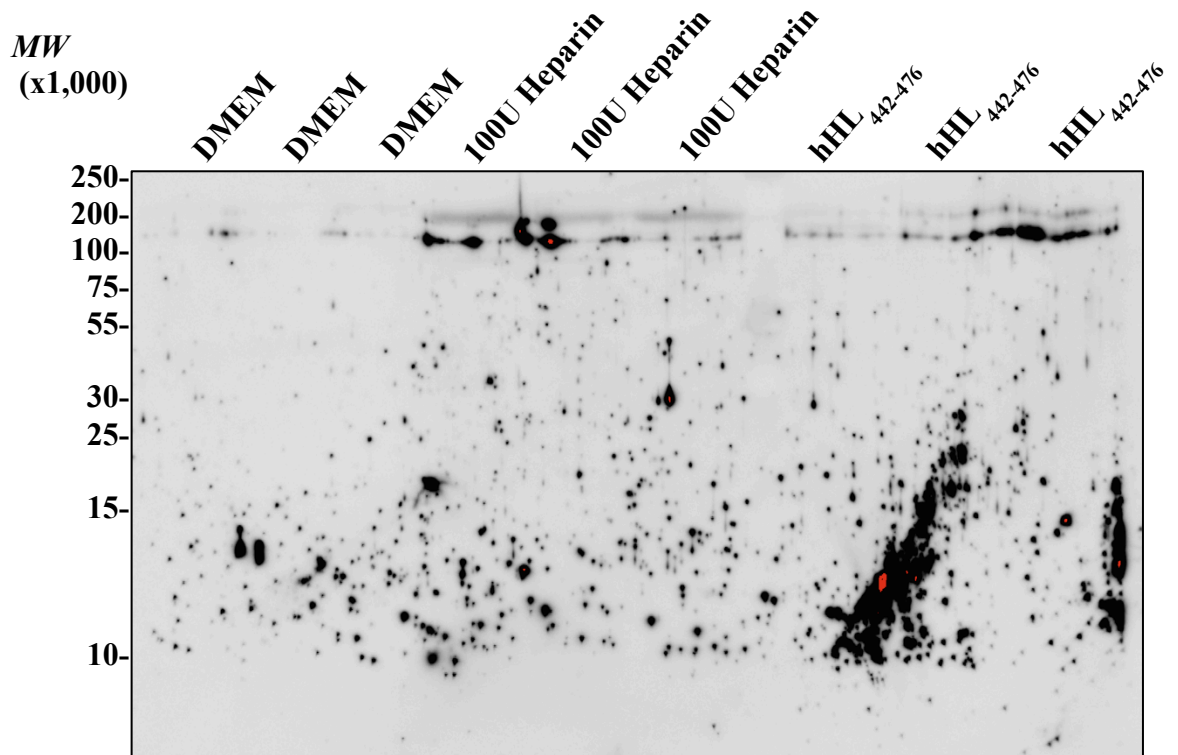
Figure S4: Immunoblot of hLPL using the F-1 monoclonal hLPL antibody
HEK-293T cells in 100-mm dishes were transfected with 6.5 µg of either wild-type
hLPL cDNA in pcDNA$_3$ plasmid or pcDNA$_3$ vector using Lipofectamine™. After 23.5
hours, media was replaced with DMEM containing 100 U/mL heparin. After 0.5
hours, media and cell lysates were collected and analyzed via immunoblot analysis. No
immunoreactivity was observed for the expected molecular mass for hLPL at 58 kDa.

MW (x1,000)   Mock cell lysates   Mock Media   LPL Media   LPL cell lysates

250-
200-
100-
75-
55-

30-
25-

15-

10-
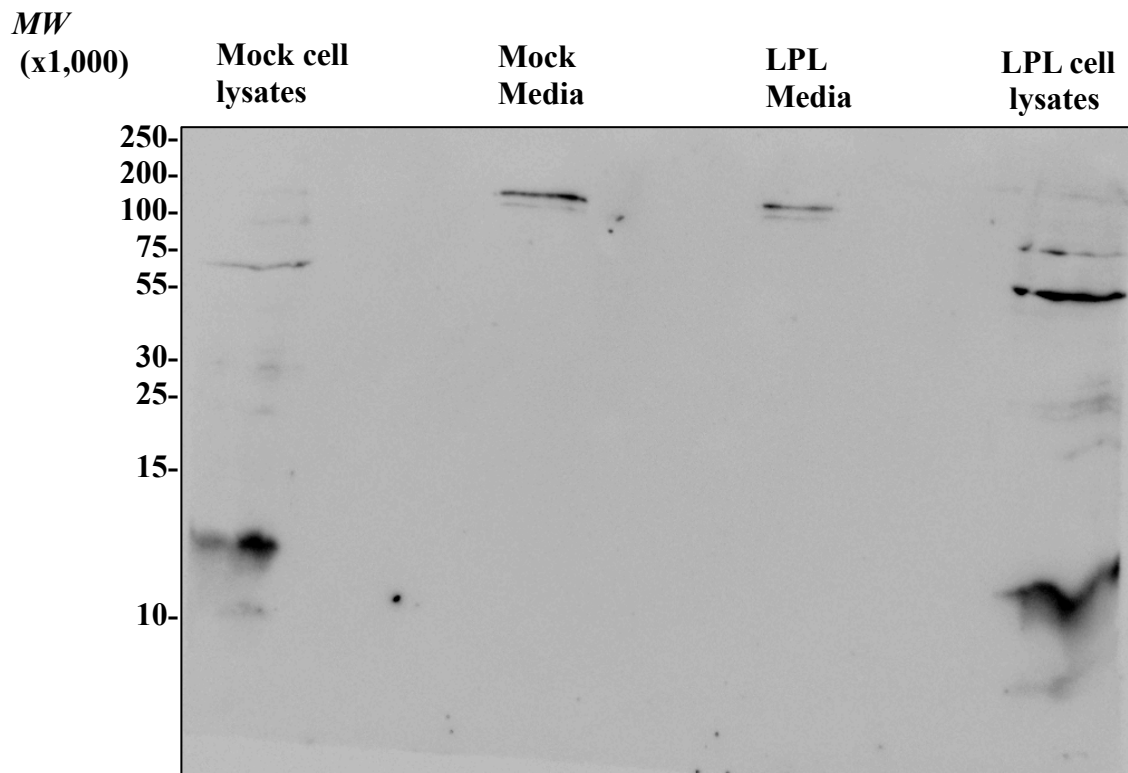
Figure S5: Isolation of hHL$_{442-476}$ peptide from Trx protein by size-exclusion chromatography

Approximately 15 mL of the hHL$_{442-476}$ peptide, Trx and thrombin was lyophilized and resuspended in 2 mL of 1X TBS (pH 7.0) and loaded onto a Sephacryl S-100 size-exclusion column that was pre-equilibrated with 1X TBS (pH 7.0). One mL fractions were collected from the column and the presence of the hHL$_{442-476}$ peptide was analyzed by SDS-PAGE using a Tris-tricine gradient gel (4-16%) stained with Coomassie blue. The contaminated hHL$_{442-476}$ peptide was observed in fractions (F) 50-75, denoted by *. However, the hHL$_{442-476}$ peptide was not isolated to purity.